

# **APPLICATION OF MATHEMATICAL MODELLING IN INVESTIGATING COASTAL PHENOMENA**

By

G. N. Wijesekara

A Thesis submitted to University of Moratuwa  
for the Degree in Master of Engineering



University of Moratuwa, Sri Lanka.  
Electronic Theses & Dissertations  
[www.lib.moratuwa.lk](http://www.lib.moratuwa.lk)



Research supervised

By

Dr. S. P. Samarawickrama

Professor S. S. L. Hettiarachchi

**DEPARTMENT OF CIVIL ENGINEERING  
UNIVERSITY OF MORATUWA  
MORATUWA  
SRI LANKA**

## ABSTRACT

With the evolvement of Information Technology, the simulation of physical theories on real matter in order to envisage the behavior of man-made structures and its impact on earth resources have “spread its wings” from scaled models to highly sophisticated virtual reality computer models where all elements can be viewed in 2D/3D in graphic user interfaces.

Particularly the study in Coastal wave mechanics and simulation of such uncertainty with man-made structures, have proven the value of technology and it has been much effective with cost and time.

With the current research that had been carried so far, commercially used in-house wave models were studied and a whole new design and analysis of a computer simulated numerical model for Sediment Transport Modelling was carried out.

Case study on Hambanthota describes the coastal processes that has been undertaken in order to investigate the wave climate, wave induced currents and sediment movement for the proposed fishery harbour at Hambathota in Sri Lanka.

Various components of an available wave modelling suite (“Halcrow”) were applied to evaluate the nearshore wave climate for design purposes, for optimization of the harbour configuration, for examination of wave penetration and for the input to the beach evolution model. The wave modelling shows that there is no significance wave penetration for the proposed fishery harbour. In addition, Wave-induced current modelling and investigation of beach evolution of the existing bay has been undertaken.

The proceedings of a final year project discussed on environmental impact on ecological and social environment with several proposed alternatives for a fishery harbour in Negombo Lagoon were considered for a case study using a commercial wave model to examine the significance impact of the wave climate for the nearshore region and structures proposed to be located in Negombo Bay. Several components of “Halcrow” wave model are used in order to validate the first alternative and modifications required are suggested herewith.

Most important of all, a sophisticated numerical model is designed and analyzed with the use of paradigms of software engineering for the simulation of Alongshore

Sediment Transport. Equations by Kamphuis (1992) based on empirical co-relations and dimensional analysis of properties have been used and followed through the whole design. Theories and equations integrated from research carried out by Dr. Saman Samarawickrama were used in deriving solutions for the numerical model of which the design is based on many GIS (*Geographical Information System*) functionalities.



University of Moratuwa, Sri Lanka.  
Electronic Theses & Dissertations  
[www.lib.mrt.ac.lk](http://www.lib.mrt.ac.lk)

## ACKNOWLEDGMENT

I offer my most heartfelt gratitude to Prof. Samantha Hettiarachchi and Dr. Saman Samarawickrama for the extravagant assistance and perfect guidance held upon my research. The inspiring work on several government projects funded by international funding organizations was possible with their precious directions and absolute collaboration and involvement towards guiding my research.

I was privileged to conquer this opportunity with the absolute co-operation of National Science Foundation with their funding during my course of research, and I warmly appreciate their efforts to do so, without them this research would not be a possibility. I would also like to thank the Vice Chancellor, Dean of Engineering Faculty and the Senate Research committee, Head, Department of Civil Engineering, Director, Postgraduate Studies of University of Moratuwa for their favorable arrangements.

I'm grateful to consultants/engineers of Halcrow's Group of companies and Applied Science Association Inc. for the collaboration with their expensive resources and guidance.

My sincere gratitude is also offered to Dr. Ranjith Galappaththi and the rest of the staff at Lanka Hydraulic Institute for their wonderful collaboration towards my research work.

My warm gratitude is for my parents and my sister who always stood by me during difficult moments and for nourishing my mind with hope.

## DECLARATION

This thesis is a report of research carried out in the Department of Civil Engineering, University of Moratuwa, between August 2001 and December 2003. Except where references are made to other work, the contents of this thesis are original and have been carried out by the undersigned. The work has not been submitted in part or whole to any other university. This thesis contains 173 pages.

---

G. N. Wijesekara  
Department of Civil Engineering  
University of Moratuwa  
Sri Lanka



University of Moratuwa, Sri Lanka.  
Electronic Theses & Dissertations  
[www.lib.mrt.ac.lk](http://www.lib.mrt.ac.lk)

---

Supervisor  
Prof. S.S.L. Hettiarachchi  
Department of Civil Engineering  
University of Moratuwa  
Sri Lanka

---

Supervisor  
Dr. S. P. Samarawickrama  
Department of Civil Engineering  
University of Moratuwa  
Sri Lanka

## CONTENTS

<b>1.0 Introduction</b>	01
<b>2.0 Literature Review</b>	03
2.1 Hydrodynamics and Sediment Transport Modeling	04
2.1.1 Hydrodynamics	04
2.1.2 Sediment Transportation	06
<b>3.0 Coastal Sediment Transport Modelling</b>	08
3.1 Introduction	09
3.2 Literature Review	12
3.2.1 Alongshore transport formulae	12
3.2.2 Wave Breaking	15
3.2.3 One-line models	16
3.2.4 The cross-shore distribution of alongshore transport	17
3.2.5 Multi-Line (N-Line) models	21
3.3 Sediment Transport Model Development	22
3.3.1 Calculation of Wave Heights for the solution domain	22
3.3.2 Calculation of Wave angles for the solution domain	26
3.3.3 Calculation of Wave Height ( $H_{sb}$ ) and Wave Angle ( $\alpha_b$ ) at breaking	26
3.3.4 Correction for Combined refraction and diffraction behind a structure	26

3.3.5	Groyne By-passing and Permeability	27
3.3.6	Alongshore Sediment Transport Rate	29
3.3.7	Alongshore Sediment Transport Rate - Kamphuis, 1991a	29
3.3.8	Distribution of the Alongshore Sediment Transport Rate Across the Surf Zone	32
3.3.9	The Cross- Shore Distribution of Alongshore Sediment Transport Rate, Perlin & Dean, 1983	32
3.4	Design of Along Shore Transport Model ( <i>SandPro</i> ) – Design and Details	35
3.4.1	Wave Climate Transformation	38
3.4.2	Calculation of wave-directional gradient	46
3.4.3	Correction for combined refraction and diffraction behind a structure	51
3.4.4	Implementing the Sediment Balance	53
3.4.5	Implementing the flow distribution	55
3.4.6	Main Algorithm	63
3.4.7	Technical guidelines for the development of <i>SanPro</i>	65
<b>4.0</b>	<b>Numerical Modelling –Case Study – Proposed Harbour at the Negombo Lagoon</b>	<b>69</b>
4.1	Introduction	70
4.1.1	Need for Development	70
4.1.2	Introduction to Alternatives	72
4.1.3	Alternative: Construction of Breakwaters and Associated Facilities at Morawala	72
4.2	Data Review and Analysis	73
4.2.1	Data collection	73

---

4.3 Model Basis	83
4.4 Regional Wave Modelling	83
4.4.1 Wave Penetration Modelling	87
4.4.2 Wave Model Setup for Regional Model	89
4.5 Local Wave Modelling	95
4.5.1 Wave Model Setup for Local Model	95
<b>5.0 Application of Mathematical Modeling in the Design of Proposed Hambanthota Fishery Harbour.</b>	100
5.1 Data Review and Analysis	101
5.1.1 Data collection	101
5.2 Wave Modelling	113
5.2.1 Model Basis	113
5.2.2 Local Wave Modelling	118
5.2.3 Wave- Induced Current Modelling	122
5.3 Modelling of Sediment Movements	124
5.3.1 General	124
5.3.2 Alongshore Drift	124
5.3.3 Cross-shore Modelling	126
<b>6.0 Conclusions</b>	133
6.1 Design of Sediment Transport Model	134
6.2 Proposed Fishery Harbour at Hambantota Bay	136
6.3 Proposed Fishery Harbour at Negombo	138
<b>Bibliography</b>	139



<b>References</b>	161
<b>Appendix</b>	164



University of Moratuwa, Sri Lanka.  
Electronic Theses & Dissertations  
[www.lib.mrt.ac.lk](http://www.lib.mrt.ac.lk)

## LIST OF FIGURES

<b>Figure</b>	<b>Description</b>	<b>Page No.</b>
<b>2.1</b>	<i>Schematization of range of application of Tidal Modelling, showing relations to other areas of modelling activity</i>	06
<b>3.1</b>	<i>Classification of beach change prediction models - after Kraus (1983)</i>	11
<b>3.2</b>	<i>Diffraction approximation near groyne - after Kamphuis (1992)</i>	25
<b>3.3</b>	<i>Refraction-diffraction approximation near groyne - after Kamphuis (1992)</i>	27
<b>3.4</b>	<i>Grid space for bathymetry</i>	35
<b>3.5</b>	<i>Structures defined alongshore</i>	36
<b>3.6</b>	<i>Bathymetry Space with the Grid with structures defined with the shoreline</i>	37
<b>3.7</b>	<i>Grid formats for beach slope calculation and to identify shoreline</i>	39
<b>3.8</b>	<i>Diffraction approximation near groyne - after Kamphuis (1992)</i>	45
<b>3.9</b>	<i>Identifying points of diffraction</i>	45
<b>3.10</b>	<i>Considered Angle for Calculations</i>	46
<b>3.11</b>	<i>Calculating shoreline gradient</i>	47
<b>3.12</b>	<i>Calculating gradient at middle points along shoreline</i>	47

---

<b>3.13</b>	<i>Influence zone under diffraction</i>	48
<b>3.14</b>	<i>Considered Angle from Incident Angle for Diffraction Calculations</i>	48
<b>3.15</b>	<i>Angles derived for Diffraction Calculations</i>	48
<b>3.16</b>	<i>Two cases for the correction of combined refraction and diffraction</i>	51
<b>3.17</b>	<i>Calculating sediment flow for intermediate cells of the grid</i>	53
<b>3.18</b>	<i>General Case</i>	56
<b>3.19</b>	<i>Corner starting middle cell</i>	56
<b>3.20</b>	<i>Corner Starting Lower Cell</i>	56
<b>3.21</b>	<i>Corner Middle Lower Cell</i>	57
<b>3.22</b>	<i>Structure for Flow_Distributig_Array</i>	57
<b>3.23</b>	<i>Specifications and Grid Layout Considered for development of SandPro</i>	67
<b>4.1</b>	<i>Proposed Fisheries Harbour at Morawala</i>	72
<b>4.2</b>	<i>Wave rose produced from Galle 70m offshore wave data.</i>	85
<b>4.3</b>	<i>Bathymetry for Regional wave modeling and wave climate transformation</i>	86
<b>4.4</b>	<i>Regional Model Setup</i>	89

---

<b>4.5</b>	<i>Wave Rose for Negombo-Inshore wave data after transformation</i>	92
<b>4.6</b>	<i>Local Model Setup</i>	95
<b>4.7</b>	<i>Local Model Critical Cases Run no 1</i>	96
<b>4.8</b>	<i>Local Model Critical Cases Run no 2</i>	97
<b>4.9</b>	<i>Local Model Critical Cases Run no 3</i>	98
<b>4.10</b>	<i>Local Model Critical Cases Run no 4</i>	99
<b>5.1</b>	<i>Regional Wave Model Bathymetry for Southern Coast of Sri Lanka</i>	114
<b>5.2</b>	<i>Layout Options</i>	118
<b>5.3</b>	<i>Typical wave penetration model result</i>	121
<b>5.4</b>	<i>Typical wave-induced current pattern</i>	123
<b>5.5</b>	<i>Typical alongshore model result</i>	126
<b>5.6</b>	<i>Hambatota Harbour Optimization Modelling Existing Bay – SW Monsoon</i>	128
<b>5.7</b>	<i>Hambatota Harbour Optimization Modelling Existing Bay – NE Monsoon</i>	129
<b>5.8</b>	<i>Hambatota Harbour Optimization Modelling Option 1 – SW Monsoon</i>	130
<b>5.9</b>	<i>Hambatota Harbour Optimization Modelling Option 1 – NE Monsoon</i>	131

---

<b>5.10</b>	<i>Hambatota Harbour Optimization Modelling Option 1a SW Monsoon</i>	132
-------------	----------------------------------------------------------------------	-----

## Bibliography

<b>Figure</b>	<b>Description</b>	<b>Page No.</b>
1.1	<i>Log-log plot of S44 3rd and 4th Editions.</i>	148
1.2	<i>Log-log plot of SMA implementation of S-44</i>	151
1.3	<i>Log-log plot of USACE standards, and S44 4th Edition Special Order</i>	153
1.4	<i>Log-log plot of Proposed LINZ worst-case sector / IMCA depth uncertainty, and S44 4th Edition Special Order</i>	157
1.5	<i>Compilation of all depth uncertainty standards from s 1 to 4.</i>	160

## LIST OF TABLES

<b>Table</b>	<b>Description</b>	<b>Page No.</b>
<b>3.1</b>	<i>General characteristics of currently available models</i>	11
<b>4.1</b>	<i>Tide level Vs Predicted Water Level</i>	74
<b>4.2</b>	<i>Percentage distribution of CCD-GTZ overall wave data by direction sector</i>	76
<b>4.3</b>	<i>Percentage distribution of CCD-GTZ overall wave data by wave period.</i>	77
<b>4.4</b>	<i>Percentage distribution of CCD-GTZ overall wave data by direction for SW monsoon</i>	79
<b>4.5</b>	<i>Percentage distribution of CCD-GTZ overall wave data by direction for NE monsoon</i>	80
<b>4.6</b>	<i>Percentage distribution of CCD-GTZ overall wave data by direction for IM1 monsoon</i>	81
<b>4.7</b>	<i>Percentage distribution of CCD-GTZ overall wave data by direction for IM2 monsoon</i>	82
<b>4.8</b>	<i>Percentage distribution of CCD-GTZ overall wave data by direction</i>	84
<b>4.9</b>	<i>Summary of MWAVE_REG model runs undertaken</i>	87
<b>4.10</b>	<i>Probability analysis of transformed wave data</i>	90
<b>4.11</b>	<i>Probability Analysis of wave height from direction 180 - 210</i>	93
<b>4.12</b>	<i>Probability Analysis of wave height from direction 210 - 240</i>	93
<b>4.13</b>	<i>Probability Analysis of wave height from direction 240 - 270</i>	93
<b>4.14</b>	<i>Probability Analysis of wave period from direction 180 - 210</i>	93

<b>4.15</b>	<i>Probability Analysis of wave period from direction 210 - 240</i>	94
<b>4.16</b>	<i>Probability Analysis of wave period from direction 240 - 270</i>	94
<b>4.17</b>	<i>Inshore critical wave regions</i>	94
<b>5.1</b>	<i>Tide level Vs Predicted Water Level</i>	101
<b>5.2</b>	<i>Percentage distribution of CCD-GTZ overall wave data by direction sector</i>	103
<b>5.3</b>	<i>Percentage distribution of CCD-GTZ overall wave data by wave period.</i>	104
	<i>Percentage distribution of CCD-GTZ overall wave data by direction for SW monsoon</i>	
<b>5.4</b>	<i>monsoon</i>	106
	<i>Percentage distribution of CCD-GTZ overall wave data by direction for NE monsoon</i>	
<b>5.5</b>	<i>monsoon</i>	107
	<i>Percentage distribution of CCD-GTZ overall wave data by direction for IM1 monsoon</i>	
<b>5.6</b>	<i>monsoon</i>	108
	<i>Percentage distribution of CCD-GTZ overall wave data by direction for IM2 monsoon</i>	
<b>5.7</b>	<i>monsoon</i>	109
	<i>Percentage distribution of Kudawella overall wave data by direction sector for the SW monsoon</i>	
<b>5.8</b>	<i>for the SW monsoon</i>	111
	<i>Percentage distribution of Kudawella overall wave data by direction sector for the SW monsoon</i>	
<b>5.9</b>	<i>for the SW monsoon</i>	111
	<i>Percentage distribution of overall wave data by direction sector for the SW monsoon at Kirinda</i>	
<b>5.10</b>	<i>monsoon at Kirinda</i>	112
	<i>Percentage distribution of overall wave data by direction sector for the NE monsoon at Kirinda</i>	
<b>5.11</b>	<i>monsoon at Kirinda</i>	112
<b>5.12</b>	<i>Summary of MWAVE REG model runs undertaken</i>	115
<b>5.13</b>	<i>Percentage distribution of nearshore wave data at H1 by direction sector</i>	116
<b>5.14</b>	<i>Extreme Wave Heights predicted, for nearshore point H1</i>	117

## Bibliography

<b>Table</b>	<b>Description</b>	<b>Page No.</b>
	<i>Summary of Minimum Standards for Depth Uncertainties</i>	
<b>1.1</b>	<i>from S44 4th Edition (IHO, 1998)</i>	147
<b>1.2</b>	<i>The Swedish implementation of S-44</i>	150
<b>1.3</b>	<i>USACE depth uncertainty standards (2001 draft version)</i>	153
<b>1.4</b>	<i>Proposed LINZ Depth uncertainty specifications</i>	156
<b>1.5</b>	<i>Proposed IMCA Depth Measurement Uncertainty Standards</i>	157



University of Moratuwa, Sri Lanka.  
Electronic Theses & Dissertations  
[www.lib.mrt.ac.lk](http://www.lib.mrt.ac.lk)





## **CHAPTER – 1**

University of Moratuwa, Sri Lanka.  
Electronic Theses & Dissertations  
[www.lib.mrt.ac.lk](http://www.lib.mrt.ac.lk)

## **INTRODUCTION**

## Introduction

Research areas covered herewith are more or less some proven areas where theories of mathematical modelling and concepts of information technology are extensively used in the deriving quantities of quantifiable impacts of coastal processes.

The main objective was laid to study and verify the application of some commercially built coastal mathematical models in real-world scenarios and to design and analyze a numerical model focusing the area of Sediment Transport modelling.

Chapter 3 addresses design details of an Information System (model) which uses several equations of empirical nature which are combined with integrating more elements for a versatile numerical model. Advance paradigms of computer programming are used to design and analyze the model and is enhanced for implementations of Sediment Transport Modelling eliminating many drawbacks in existing designs of Sediment Transport Models.

With Chapter 4 the details would include a case study on applying coastal modelling to a proposed offshore structure (Breakwater) designed for a proposed harbour in Negombo Lagoon. The infrastructure studies had been done for a final year research project details of which are taken into consideration for the current case study. Coastal models used for the investigative approach was Halcrow in-house numerical models.

Chapter 5 is a study carried out under Coastal Resources Management Project, which was undergone with funds of Asian Development Bank, in which the efforts were involved in modelling of Hambanthota fishery harbour. The models used were Halcrow in-house wave models and a complete study including sediment transport modelling was carried out with great details.



**CHAPTER – 2**  
University of Sri Lanka.  
Electronic Theses & Dissertations  
[www.lib.mrt.ac.lk](http://www.lib.mrt.ac.lk)

## **LITERATURE REVIEW**

## 2.0 Literature Review

### 2.1 Hydrodynamics and Sediment Transport Modeling

#### 2.1.1 Hydrodynamics

With the aid of modern computers, multi-dimensional numerical modelling capability has recently been advanced to provide increasingly effective facilities for studies of coastal regions. In fact, seventy years have passed since numerical models were used for the first time in planning major engineering works in a coastal sea. The basis for the tide and storm surge computations for predicting the effect of the closure of the Zuider Zee in the Netherlands was established by the Nobel prize winner, physicist, Lorentz (1926). Even though this approach was a success, computational methods found only limited application outside their country of origin, where a small group of scientists and engineers continued to make effective use of this approach (Mazure, 1937; Schonfeld, 1951; Dronkers and Schonfeld, 1955).

One of the reasons for the limited application of numerical simulation was the development of physical modelling of estuaries. The use of these physical models was found to be much more attractive than complicated, tedious computations. In the last thirty years significant changes have occurred. Industrial development, expansion of navigation and increased habitation of low-lying areas near the coast have necessitated increased construction in coastal seas and estuaries. Physical modelling of these vast regions, often open to the sea on many sides, is difficult and expensive. Moreover, assessments of the fate of discharged pollutants and of the effect of construction on the environment are difficult to make with these models. Consequently, interest in numerical simulation has increased, particularly with the availability of digital computers able to perform effectively the numerous computational operations required. Also, considerable advances in the theory of numerical methods for the solution of partial differential equations, the basis of these numerical simulations, make it possible to design computation procedures with minimum errors.

In 1970, Leendertse (1970) developed an implicit two dimensional, finite difference model, which was an extension of his (Leendertse, 1967) long wave model. A detailed description of the model is presented in a series of reports by Leendertse (1967), Leendertse and Gritton (1971a), Gritton (1972) and Leendertse and Liu (1974a). Fisher (1970) extended the basic hydrodynamic code to include a transport model. Abbott and Ionescu (1967) and Abbott et al (1974) also developed an implicit finite difference model for a vertically integrated two- dimensional system.

Hansen (1956) was the first to apply an explicit finite difference scheme for two-dimensional storm surge computation. The same method was extended by Sundermann (1974) and Laevastu (1975) to analyze three-dimensional multi-level and multi-layer flow systems. The first explicit, two-dimensional finite-difference, water-quality model was developed by Masch et al (1969). The hydrodynamic portion of the computation is an improvement of earlier work of Ried and Bodine (1968), who adopted the basic equations set forth by Hansen (1956,1962) and Dronkers (1964). In recent years, a number of numerical models for estuarine waters were published by researches including Falconer (1974,1976), Falconer & Owens (1987), Kuipers & Vreugdenhil (1973), Nece et al (1976), Weare (1976) and Holmes and Samarawickrama (1996).

Over the last 20 years there has been a significant increase in the number of scientific papers describing the numerical modelling of tides. The quantity of scientific research is such that to produce a comprehensive review of tidal modelling is an impossible task. A good overview of the entire field can be gained from the volume of papers presented at a recent tidal meeting, Parker (1991). Also a brief overview, with a comprehensive set of references to recently published papers, a range of techniques used in tidal hydrodynamic modelling and recent progress in the field can be found in Davies et al (1997) parts I and II. Numerical models of tidal flows are now used for so many purposes in combination with so many other techniques. One of many decompositions of the field application, even in the restricted area of two-dimensional (2D) modelling, is shown in figure 2.1 (Abbott, 1997).

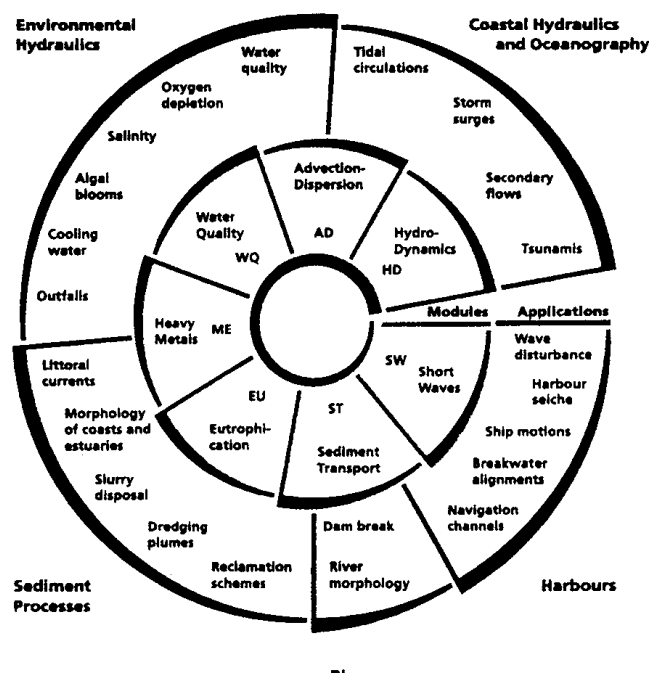


**Figure 2.1 :** Schematization of range of application of Tidal Modelling, showing relations to other areas of modelling activity



University of Moratuwa, Sri Lanka.  
Electronic Theses & Dissertations  
www.lib.mrt.ac.lk

## 2.1.2 Sediment Transportation

Many formulae to predict the bed-load sediment transport rate are described in the literature. The earliest is that of Du boys in 1879, who assumed that the sediment particles move along the bottom in layers of progressively decreasing velocities in the vertical downward direction. The first empirical formula was presented by Meyer-Peter and Muller (1948). They performed flume experiments with particles of uniform size and with particle mixtures. Based on data fitting, a relatively simple formula was obtained, which is still frequently used.


Kalinske (1947) and Einstein (1950) introduced statistical methods to represent the turbulent behaviour of the flow. Kalinske assumed a normal distribution for the instantaneous fluid velocity at the grain level. Einstein gave a detailed but complicated statistical description of the particle motion in which the exchange probability of a particle is related to the hydrodynamic lift force and particle weight. Einstein proposed

the  $d_{35}$  (35% by weight is finer) as the effective diameter for particle mixtures and the  $d_{65}$  (65% by weight is finer) as the effective grain roughness diameter. Frijlink (1952) had very practical approach and simplified the formula of Meyer Peter- Muller and that of Einstein. Bagnold (1966) introduced an energy concept and related the sediment transport rate to the work done by the fluid. Using about one hundred flume data sets, Engelund-Hansen introduced a formula in 1967, based on the concept of Einstein (1950), and Bijker proposed an empirical formula in 1971. In 1973, Ackers-White proposed an empirical formula based on an analysis of about one thousand sets of laboratory and field data. Van Rijn (1984a) solved the equations of motion of an individual bed load particle and computed the saltation characteristics and the particle velocity as functions of the flow conditions and particle diameter.

A large data set of bed load sediment transport rates measured in flume and field conditions was selected by Van Rijn (1984a) from the literature to verify his formula and those formulae of Meyer-Peter and Muller (1948), and Frijlink (1952). Van Rijn (1984) also used four hundred and eighty six sets of river data and one hundred and twenty sets of estuary data, to compare the validity of formulae proposed by Engelund-Hansen (1967), Ackers-White (1973) and Van Rijn (1984). Based on this literature review the latter model was selected for use in the present study, see Section 2.3.2. Recently, Holmes and Samarawickrama (1998) published the application of their numerical model to one of the lagoon regions in Sri Lanka.

Literature review for the coastal sediment transport is given separately in the Chapter 3 of the Thesis.

## CHAPTER – 3

 **COASTAL SEDIMENT TRANSPORT  
MODELLING AND THE DESIGN OF ALONG  
SHORE TRANSPORT MODEL (*SANDPRO*)  
USING ADVANCED PROGRAMMING  
TECHNIQUES  
(GIS BASED)**



## **3.0 Coastal Sediment Transport Modelling and Design of Along Shore Transport Model (*SandPro*) using GIS**

### **3.1 Introduction**

When waves break at an angle to the shoreline they generate an alongshore current, confined primarily to the surf zone. This alongshore current, interacting with the wave surf, in turn produces a sand transport along the beach, parallel to the shoreline often leading to changes in the shoreline and near-shore bathymetry. The need for reliable predictions of shoreline response to man-made or natural modifications is increasing due to environmental concerns and the rising cost of remedial measures.

Studies to determine changes in beach planshape or seabed bathymetry usually involve physical and/or numerical model studies. In situations where the shoreline or bottom topography is very stable and when the structural configurations controlling these features are expected to remain unchanged, future behavior can be forecasted with reasonable confidence, without the use of models. However, in situations where the conditions controlling the changes are either complex or vary during the forecast period, it becomes necessary to use simulation models.

An investigation of shoreline response can proceed by several approaches, with each approach selected for the particular strengths, which it offers. Field programs are costly, usually because of the considerable equipment and extensive time required, but they are essential to quantify the values of constants or parameters, the forms of which may not be available from laboratory measurements or theoretical considerations. Laboratory studies occupy a special niche by allowing the wave conditions and independent variables to be controlled readily, experiments to be repeated and selected measurements to be conducted. Although scale effects are present in laboratory measurements of sediment transport, the physics governing the process should be the same. Laboratory studies can also provide an excellent basis for evaluating certain aspects of a numerical model. Numerical modelling offers the capability of incorporating all the wave hydrodynamic, surf zone and sediment transport knowledge that is available from laboratory and field studies and the

potential to provide accurate predictions of shoreline response to various structural and nourishment alternatives.

Physical models, which have traditionally been used for simulating topographical changes, suffer from serious deficiencies of high costs and scaling problems. For these reasons, and based on improved understanding of the physical process involved, the use of numerical models have grown in recent years. Numerical models possess certain advantages over physical models in allowing the testing of a wide range of parameters, adaptability to a variety of sites, economical operation, and the absence of scale effects. They do, however, require the selection of key parameters, which influence the solution and can, therefore, be considered to have “parameter effects”.

Numerical modelling of sediment transport in coastal regions has received great attention in recent years, not only in connection with the evaluation of the rate of transport itself, but also from the point of view of morphological modelling. Different approaches based on different physical principles have been followed in establishing the models. The complexity of the phenomena described and the lack of adequate description of these phenomena have often resulted in crude simplifying assumptions. Furthermore, the models have frequently been applied to situations well beyond those foreseen when they were developed.

Following the classification of numerical models by spatial and temporal scales presented in Kraus (1983), such models can be grouped into four categories (figure 3.1): one-line models, n-line models, three dimensional models and macro-process models. In one-line models only one contour, the shoreline, is used to represent the beach change. If the beach evolution is represented by changes in more than one contour line, the model is termed an n-line model. In such a model, the cross-shore distribution of alongshore-sand transport as well as on-offshore transport can be taken into account. In 3D-models changes in seabed level caused by local waves and currents are calculated on a two-dimensional (horizontal) grid and such models are the most sophisticated. Macro-process models involve the use of qualitative relationships to simulate trends of shoreline change under simplified conditions. This category includes analytic and numerical solutions of the shoreline change equations under constant wave conditions.

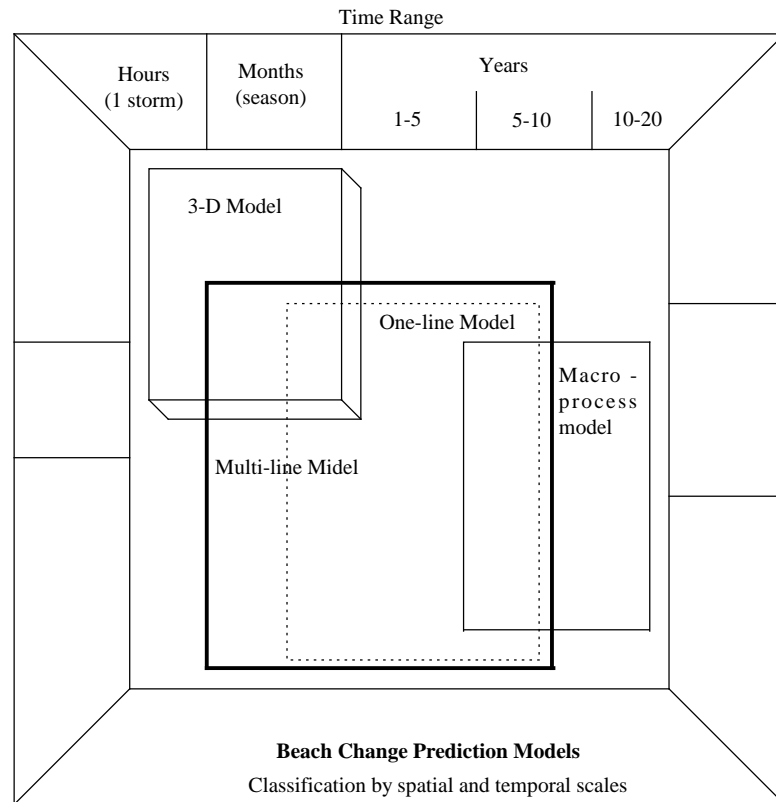


**Figure 3.1:** Classification of beach change prediction models - after Kraus (1983)

The general characteristics of models used today are given in Table 3.1. The computational effort involved increases rapidly with the complexity of the model and at the present time the detailed sediment transport models are essentially in the research stage (3D-models, macro-process models). This leaves a choice between a 1-Line and N-Line models involving a bulk sediment transport relationship (e.g. Shore Protection Manual, 1984; Kamphuis, et al., 1986,1991a) with perhaps an on-offshore distribution (e.g. Fulford as quoted by Perlin and Dean, 1983) for practical computations.

Morphology Model	Wave Transformation	Transport Rate	Area Modelled
1-Line	Snell	Bulk	Large
N-Line	Refrac-Diffrac	Bulk with distribution	Medium
Detailed	Refrac-Diffrac	Locally detailed	Small

**Table 3.1:** General characteristics of currently available models

Since the n-line model can simulate on-offshore sediment motion, steepening of the beach profiles etc., this is often the model of choice. The “n-line” numerical model used in the present study allows simulation of shoreline change due to wave action under a wide variety of user-specified beach and coastal structure configurations, over a period of time. The model evaluates the total alongshore sediment transport rate using the formula developed by Kamphuis (1991a) and distributes it across the surf zone, according to the Perlin and Dean (1983) method. The model uses deep-water wave characteristics for alongshore sediment transport calculations and takes into account the effects of refraction, diffraction at coastal structures and the combined refraction-diffraction behind such structures.

This “n-line” numerical model can be used to investigate the bathymetric response arising from alongshore sediment transport driven by time varying wave conditions. At its present stage of development onshore-offshore transport of sediment is not considered.



## 3.2 Literature Review

University of Moratuwa, Sri Lanka.  
Electronic Theses & Dissertations  
[www.lib.mrt.ac.lk](http://www.lib.mrt.ac.lk)

Systematic study of nearshore processes began in the 1940's and 50's when equations based on classical wave theory, introduced a century earlier by Airy (1845) and Stokes (1847), were used to predict wave-induced currents and sediment transport. These equations represent many characteristics of waveforms, but equations that relate sediment transport to water waves were more difficult to devise.

### 3.2.1 Alongshore transport formulae

With the complexity of sand transport in mind, it is not surprising to note that formulae presented in the literature are extremely simplified. Three basic approaches may be distinguished: the wave power approach, the energetic model approach and the shear stress modification approach. A brief discussion of these three theories is given below.

### 3.2.1.1 Wave power approach

Numerous investigations made in the last decades have indicated a correlation between the sand transport rate,  $Q$ , along a coast and the alongshore component of the incoming wave energy (e.g. Caldwell 1956; Savage 1959; Manohar 1962). The first dimensionally correct expression was presented by Inman and Bagnold (1963):

$$Q = \frac{K^1 P_1}{(\rho_s - \rho)g(1 - p)} \quad (3.1)$$

Where  $K^1$  is a non-dimensional proportionality constant,  $\rho_s$  and  $\rho$  are the densities of the sediment and water ( $\text{kg/m}^3$ ),  $g$  is the acceleration of gravity ( $\text{m/s}^2$ ), and  $p$  is the porosity of the sediment bed.  $P_1$  is usually termed the alongshore component of wave power (or energy flux) and calculated as:

$$P_1 = EC_g (\sin \alpha_{bs} \cos \alpha_{bs})_b \quad (3.2)$$

Where  $E$  is the energy density of the incoming waves ( $\text{J/m}^2$ ),  $C_g$  is the group velocity ( $\text{m/s}$ ),  $\alpha_{bs}$  is the angle of wave crests to the shoreline, and the subscript  $b$  denotes the breaking condition. As shown by Longuet-Higgins (1971), the terminology for  $P_1$  is incorrect and has no physical meaning since scalar quantities, such as power or energy, cannot have components. Equations (3.1 and 3.2) form together what is commonly known as the CERC formula (Shore protection Manual, 1984) for which  $K^1$  is set to 0.77.

If the transport rate is expressed as an immersed-weight transport rate,  $I_1$  ( $\text{N/s}$ ), equation (3.1) can be written in the more practical form:

$$I_1 = (\rho_s - \rho)g(1 - p)Q = K^1 P_1 \quad (3.3)$$

In the literature there have been, and still are, many discussions about the true value of the CERC formula coefficient. Over the years, the recommended value of  $K^1$  has varied by more than a factor of four (Inman, 1978).

The CERC formula has several limitations; it does not explicitly take into account the effects of grain size, beach slope, or bed roughness. Implicitly, however, the two latter parameters appear in the formula, but as a ratio with a constant value for natural beaches. More importantly, only driving forces resulting from waves, uniform alongshore are considered. In spite of this and although basically empirically derived,

without any considerations of the mechanics of sand transport, the CERC formula has been successfully applied in innumerable engineering projects.

More recent studies have suggested that instead of being a constant,  $K^1$  is a function of parameters such as breaker angle, grain size, breaker index  $\left(\frac{H_b}{D_b}\right)$  and bottom slope. Swart (1976), Bailard (1981), Sayao et al (1985), Kamphuis et al.,(1978,1985,1991a) give some of the widely accepted equations, which consider  $K^1$  as a function of these parameters.

### 3.2.1.2 Energetic model approach

Another theory was presented by Bagnold (1963) in which the transport rate is assumed to depend on the combined effect of waves and currents. The wave-induced oscillatory motion is considered as initiating sand movement but with no net transport. Once the sand is in motion, it becomes available for transport by any alongshore uni-directional current,  $V_1$  (m/s). Then, the total immersed-weight transport rate can be calculated as:

$$I_1 = K^{11} \left( E C_g \cos \alpha_{bs} \right)_b \left( \frac{V_1}{U_m} \right) \quad (3.4)$$

where  $K^{11}$  is a non-dimensional proportionality constant and  $U_m$  (m/s) is the maximum near-bottom orbital velocity at wave breaking. The value most commonly used for  $K^{11}$  is 0.28 (Kormar and Inman, 1970). In contrast to equation (3.3), equation (3.4) can be used when the alongshore current,  $V_1$ , results from causes other than wave breaking at an angle to the shore. As shown by Gourlay (1982), it is possible to derive an expression for the alongshore current arising from the effects of both breaker angle and an alongshore gradient of breaking wave height,  $\frac{\partial H}{\partial x}$ . This leads to the relation:

$$I_1 = \left( \frac{K^{11}}{2} \right) \left( E C_g \cos \alpha_{bs} \right)_b \left[ \sin \alpha_{bs} - \left( \frac{K^{111}}{\tan \beta} \right) \left( \frac{\partial H}{\partial x} \right) \right]_b \quad (3.5)$$

where  $K^{111}$  is a non-dimensional proportionality constant and  $\tan \beta$  is the sea-bed slope. For  $\frac{\partial H}{\partial x} = 0$  and small breaking wave angles ( $\cos \alpha_{bs} \approx 1$ ) equation (3.5) becomes identical to the CERC formula. Relations similar to (3.5) have been

proposed by several authors (e.g. Motyka and Willis 1975; Ozasa and Brampton 1980; Kraus 1981).

### 3.2.1.3 *Shear- stress modification approach*

Assuming that the mechanism of sand entrainment is governed by flow-induced bottom shear stresses alone, sand transport relationships used in river sediment computations can be adapted for application in the coastal domain. The bottom shear stress then has to be modified to account for the combined affect of waves and currents. Of this type of analysis the most famous is the work of Bijker (1971), combining the Kalinske-Frijlink bedload equation (Frijlink 1952) with the suspended load relationship developed by Einstein (1950) to determine the total transport rate.

This type of approach tries to model the physical process in more detail than the previous two approaches. Consequently, the method requires detailed knowledge about important physical parameters such as bed form, shear stress under combined waves and currents, and the reduction of wave height due to breaking which, at the present level of knowledge, introduces many assumptions in relation to these values. Moreover the diffusion-type concentration relationship used by Einstein may be questioned when applied to waves because it neglects any mixing due to wave-induced vertical velocities.

### 3.2.2 **Wave Breaking**

The wave breaking criterion is one of the most important aspects of alongshore transport prediction as well as the distribution of alongshore transport across the surf zone. The breaking of waves has been discussed in many papers and expressions are often at variance with each other. Some of the variations are the result of differences in basic definitions. However, much of the confusion must be attributed to combining the wave transformation and wave breaking processes into one single formula relating breaking wave parameters directly to deep water wave parameters.

Stokes (1891) and McCowan (1894) were among the first to develop a criterion for wave breaking, based on the concept that the breaking occurs at the point where the horizontal component of the particle orbital velocity at the surface begins to exceed the velocity of propagation of the wave profile. Miche (1944) proposed a criterion of

wave breaking, taking into account the wavelength in addition to the depth of breaking. Munk's (1949) solution, based on the finding of McCowen (1894) using solitary wave theory, is one of the simplest formulae but is widely used and has been found to work well in alongshore transport prediction models.

In the 1970's Goda (1970), Komar and Cauhan (1972), Weishar and Byrne (1979) and Ostenderf and Madson (1979) proposed expressions for wave breaking. Goda, (1970) being the first to include beach slope into wave breaking calculations. Ostenderf and Madson's solution is similar to that of Goda.

Singamsetti and Wind (1980) and Hanson (1990) also proposed solutions taking beach slope into consideration, but these expressions lead to zero wave height as the beach slope tends to zero, whereas  $H_b$  should approach some finite value at zero beach slope according to Riedel and Byrne (1986). Kamphuis (1991b) modified these equations to overcome this problem.

Shore Protection Manual (1984), Thornton et al (1984) and Kimura (1988) are some of the other widely accepted criteria.

### **3.2.3 One-line models**

The observation that the profile of a particular beach oscillates about an apparent constant shape over the long term led Pelnard-Considere (1956) to develop a mathematical model, now called the one-line model. Grijm (1961) used the one-line theory to derive analytic solutions for delta formations from rivers discharging sand. Bakker and Edelman (1965) further investigated the possibilities of closed form solutions of river delta evolution, assuming a somewhat different sand transport equation to allow for an analytical approach. In Bakker (1969), the one-line theory was extended to include two lines to describe the shoreline change: one line representing the shoreline and another representing an offshore contour. Le Mhaute and Soldate (1977) presented several analytic solutions and discussed the underlying principles of the one-line and two-line theories. Walton and Chiu (1979) gave a brief review of analytic solutions, mainly concerning the dispersion of different beach fill configurations. Larson, Hanson, and Kraus (1987) presented a large number of analytical solutions, concerning shoreline evolution on natural beaches as well as on



beaches protected by various kinds of coastal structures. Hanson and Larson (1987a) compared analytic and numerical solutions of shoreline evolution through the analysis of simple examples.

The one-line theory was first implemented numerically by Price, Tomlinson, and Willis (1973), followed by many others. Rea and Komar (1975) presented a technique for studying shoreline evolution for hooked beaches using a two-dimensional grid. Horikawa, Sasaki, and Sakuramoto (1977) discussed the effect of dredged holes on shoreline evolution. Willis (1977) applied the one-line model to prototype conditions, comparing the traditional CERC formula for calculating alongshore-sand transport with a new expression, including wave refraction over an irregular bottom. Sasaki and Sakuramoto (1978) reported the verification of a one-line model using very precise field data. Perlin (1978) simulated hypothetical case studies involving detached breakwaters. Le Mhoute and Soldate (1977) presented an implicit numerical model and tested it against field data. Mimura, Shimiza, and Horikawa (1983) compared their computer simulations against high quality laboratory data.

As reflected in the previous paragraphs, numerous studies have been made with the one-line model to examine shoreline change in laboratory (physical) conditions. However, only Kraus, Hanson, and Harikai (1985), Kraus et al (1986), and Hanson and Kraus (1987a) and few others attempted to use the model as an engineering tool for making shoreline change forecasts for a real beach.

The model presented by Kraus and Harikai (1983), Kraus et al (1985) and Hanson and Kraus (1986, 1987a) was developed specifically to simulate conditions at Orarai Beach, Japan, and was reformulated in a generalised form by Hanson (1987), leading to the modelling system GENESIS, making the model applicable to an arbitrary open-coast beach.

### **3.2.4 The cross-shore distribution of alongshore transport**

Virtually all of the models proposed to describe the alongshore transport distribution share a central concept: the simultaneous presence of a mechanism which mobilises beach sediments and alongshore current which transports the sediments downdrift. The models vary widely in the description of this mobilising mechanism as well as in

the degree of independence assumed between the sediment mobilising and transporting forces.

Bagnold (1963) proposed that wave orbital motion mobilises beach sands and wave power is expended maintaining the sand in motion so that any mean local alongshore-current  $V_1$  transports the sand. In accordance with this “energetics” approach Bagnold suggested a suspended and bed load model.

In 1969, Savasek proposed a simple distribution model where the local alongshore transport rate is assumed to be proportional to the local loss of wave energy flux.

$$I_1(Z) \propto \left(\frac{d}{dh}\right)(EC_g \sin\alpha \cos\alpha) \quad (3.6)$$

Where  $I_1(Z)$  is the local immersed weight of alongshore sediment transport rate per unit depth.

Thornton (1972) proposed a distributed alongshore transport model based upon the energetics approach of Bagnold. None of the models predicts transport landward of the still-water shoreline and each model exhibits a maximum and a sharp discontinuity at the breakpoint. The latter arises because transport is not predicted seaward of the breakpoint if one assumes no energy losses outside the surf zone.

Komar (1971, 1975, and 1977) extended Bagnold’s (1963) model, envisioning that breaking wave-induced stress at the bed mobilises sediment, making it available for advection by an alongshore current. Therefore, in his popularly called “stress” model, Komar reasoned that the local alongshore transport is related to the product of breaking wave related stress and alongshore current.

Sand transport is predicted seaward of the breakpoint since lateral mixing is considered, but neither model predicts transport above the shoreline in the swash.

Madsen (1978) suggested a distributed alongshore transport model, based upon an experimentally verified expression for sediment transport under oscillatory flow. Like the Komar models, evaluation of the transport landward of the shoreline is not straightforward.

Walton and Chiu (1979) suggested a distributed alongshore transport model. The model typically predicts maximum alongshore transport in the seaward half of the surf zone for a plane beach. A discontinuity is present at the breaker line and transport decreases to zero at the shoreline.

Fulford (1982, 1987) tested a series of simple expressions for the alongshore transport distribution against laboratory data from Savage (1959) and Bijker (1971). Each expression included direct dependence upon the local alongshore-current velocity, for which Fulford used the Longuet-Higgins (1970) formulation for a plane beach.

Tsuchiya (1982) considered the local alongshore transport using a Longuet-Higgins (1970) alongshore current profile with lateral mixing; this suspension-dominant model generally predicts the maximum transport at about three-quarters of the distance from the shoreline to the breaker line. Significant amounts of transport are predicted seaward of the breakpoint for decreasing values of the critical shear stress.

Bailard and Inman (1981) and Bailard (1984) proposed an energetics-based expression, which independently describes the bed load and suspended load, components of the local alongshore transport as functions of the local alongshore, current and water depth. Accordingly, the model is similar in structure to that of Walton & Chiu (1979) and therefore involves the same difficulty of selecting separate bedload and suspended load transport coefficients. The transport maximum is predicted to occur at about nine-tenths of the distance from the shoreline to the breaker line. Transport is described seaward of the breaker line with a slight gradient discontinuity, but is not described above the shoreline.

Abdelrahman (1983) elaborated upon Thornton's (1972) model. He described the gradient in energy flux across the surf zone as a function of breaking wave energy dissipation based on a periodic bore model and bottom friction eventually neglected. The local alongshore current  $V_1(x)$  was expressed as a function of breaking wave energy dissipation after Liu and Dalrymple (1978). Abdelrahman's final expression, which appears to be dimensionally incorrect predicts the peak alongshore, transport at the outer-mid surf zone and predicts transport, which decreases to zero at the shoreline. The model was developed and evaluated for random waves.

Relatively few expressions have been suggested to date for the distribution of alongshore sediment transport across the surf zone. In general, most of the models assume that sediment is locally mobilised either as a function of energy dissipation from the breaking waves, or by the bed shear stress induced by the peak horizontal wave orbital velocities and alongshore current. The mobilised sediment is then assumed to be advected downdrift by the local alongshore current. Accordingly, knowledge of the distribution of alongshore current across the surf zone is important to the prediction of local transport for most models. Many investigators have relied upon the expression for alongshore current across a planar beach suggested by Longuet-Higgins (1970).

Almost all of the existing models suggest that the alongshore sediment transport is the greatest between the mid-surf zone and the breaker line for a planar beach, and that the alongshore transport tends to zero at the shoreline and outside the breaker line. Models which do not include bottom stress due to alongshore current or non-breaking wave orbital motion exhibit discontinuities in transport at the breaker line with no transport seaward of it. Few models explicitly describe or are well conditioned to treat alongshore transport in the swash zone.

Data from field and laboratory studies of alongshore transport indicate that (1) significant levels of transport may occur above the shore-line, i.e., in the swash zone, (2) the contribution of the swash zone transport increases as waves break near or upon the foreshore, (3) about 10% to 30% of the total transport occurs seaward of the breaker line, (4) maximum local transport is at least as likely within the shore-ward half of the surf zone as within the seaward half, (5) greater transport is often associated with shallower depths, i.e., breakpoint bars and the shoreline, and (6) field measurements demonstrate great variability in the shape of the transport distribution profile.

Kamphuis (1991b) from alongshore sediment transport rate distribution experiments concluded that,

- 1) The sediment transport rate distributions are generally bimodal with one peak close to the breaking zone and another in the swash zone.

- 2) The two suspended load peaks come closer and blend together for smaller wave heights and for smaller grain size.

Kamphuis (1991c) proposed expressions for the offshore bed load peak, the inshore bed load peak and for the suspended load peak. These equations give reasonable results for smaller wave heights but with an increase in wave height the predictions become unrealistic.

Other researchers have also found great variability in the shape of the transport distribution profile. These findings undermine widely accepted distribution profiles (Komar, 1977; Tsushiya, 1982; Fulford, 1982; Perlin and Dean; 1983). Even though there is some experimental data showing a bimodal distribution, thus far a reasonable predictor has not been proposed. Therefore the use of any profile for the cross-shore distribution of alongshore sediment transport in engineering applications must be treated with considerable caution.

### **3.2.5 Multi-Line (N-Line) models**

The equilibrium beach profile concept led to the development of the so called “n-line” or “multi-line” type of model, in which cross-shore sand transport, and associated changes in the bottom profile, can be characterised to some extent, as well as the cross shore distribution of the alongshore transport rate. This was first accomplished by treating two contour lines (Bakker, 1969; Bakker, Klein-Breteler, and Ross 1971) in analytic solutions and by Horikawa, Harikai, and Kraus (1979) using a numerical model. A numerical model representing the bathymetry by an arbitrary number of lines was presented by Perlin and Dean (1983).

### 3.3 Sediment Transport Model Development

The wave condition in the solution domain requires a calculation of wave celerity, shoaling, refraction and diffraction, which are summarized here for completeness.

#### 3.3.1 Calculation of Wave Heights for the solution domain

##### 3.3.1.1 Wave Celerity

(i) Deep water  $\left[ \frac{d_{ij}}{(gT^2)} > 0.08 \right]$

$$L_0 = \frac{gT^2}{2\pi}; \quad C_{ij} = C_0 = \frac{L_0}{T} \quad (3.7;3.8)$$

(ii) Transitional zone  $\left[ 0.0025 \leq \frac{d_{ij}}{gT^2} \leq 0.08 \right]$

$$L_{ij} = L_0 \tanh\left(\frac{2\pi d_{ij}}{L}\right); \quad C_{ij} = \frac{L_{ij}}{T} \quad (3.9;3.10)$$

(iii) Shallow water  $\frac{d_{ij}}{gT^2} < 0.0025$

$$C_{ij} = \sqrt{g d_{ij}} \quad (3.11)$$

Where

$C_{ij}$  = wave celerity

$C_0$  = deep water wave celerity

$L_{ij}$  = wave length

$L_0$  = deep water wave length

$T$  = wave period

$d_{ij}$  = water depth

and subscripts ij refer to a point within the calculation domain.

### 3.3.1.2 Coefficient of Shoaling ( $K_s$ )

In deep water the wave profile is sinusoidal. When the water depth shoals to about one half of the deep-water wavelength defined as the horizontal distance between two adjacent wave crests the bottom starts to affect the shape of the wave. The wave height increases, the wavelength, celerity (speed) and group velocity decrease, whereas the wave period is assumed to remain constant. This phenomenon is referred to as wave shoaling. The change of wave height is represented by a shoaling coefficient,  $K_s$ , defined as:

$$(K_s)_{ij} = \left[ \frac{1}{\sqrt{\tanh(K_{ij}d_{ij})(1+G_{ij})}} \right] \quad (3.12)$$

Where:  $K_{ij} = \frac{2\pi}{L_{ij}}$  and  $G_{ij} = 1 + \frac{2K_{ij}d_{ij}}{\sinh(2K_{ij}d_{ij})}$

### 3.3.1.3 Coefficient of Refraction ( $K_r$ )

If the wave propagates into shallow water with the crests making an angle to the depth contours, the waves will be subjected to wave refraction by virtue relative changes in the wave celerity. As a result, the waves tend to become parallel the depth contours. Depending on whether the wave rays defined as paths of wave propagation orthogonal to the wave crests converge or diverge, the wave height will increase or decrease. This change in wave height is represented by a refraction coefficient,  $K_r$ .

Using Snell's Law:  $\sin\alpha_{ij} = \frac{C_{ij}}{C_0} \sin\alpha_0$  (3.13)

Assuming that wave energy is conserved between adjacent orthogonals it can be shown that

$$K_r = \frac{H_{ij}}{H_0} = \sqrt{\frac{\cos\alpha_0}{\cos\alpha_{ij}}} \quad (3.14)$$

where  $\alpha_{ij}$  = wave angle at point ij,

$\alpha_0$  = deep water wave angle,

$C_{ij}$  = wave celerity and

$C_0$  = deep water wave celerity

Because the wave celerity according to linear wave theory is independent of wave height, the wave refraction coefficient,  $K_r$ , is also independent of the wave height.

#### 3.3.1.4 Coefficient of Diffraction ( $K_d$ )

When a wave train passes an impermeable structure, wave energy will be transferred into the shadow zone due to a change in the local wave direction, caused by the strong gradient in wave height. If the depth of water in the lee of the structure is constant the waves will propagate into the shadow zone radially, with decreasing wave height. This phenomenon is referred to as wave diffraction and the change in wave height is represented by a diffraction coefficient,  $K_d$ .

Classical calculations of the diffraction coefficient, such as Penny and Price (1951), are, lengthy and only apply to regular waves. For example; the Penny and Price method gives a  $K_d$  of 0.5 at the edge of the shadow zone, but Goda, Takayama and Suzuki (1978) state that this overestimates the wave height reduction due to diffraction for irregular waves. Based on this earlier work, Goda (1985) describes an “angular spreading method” in which it is simply assumed that the obstruction blocks out a portion of the incoming directional wave spectrum. This method results in a more reasonable diffraction coefficient of 0.7 at the edge of the shadow zone.

Using Goda’s method and simple additional assumptions, the following expressions for diffraction behind a groyne were developed by Kamphuis (1992).



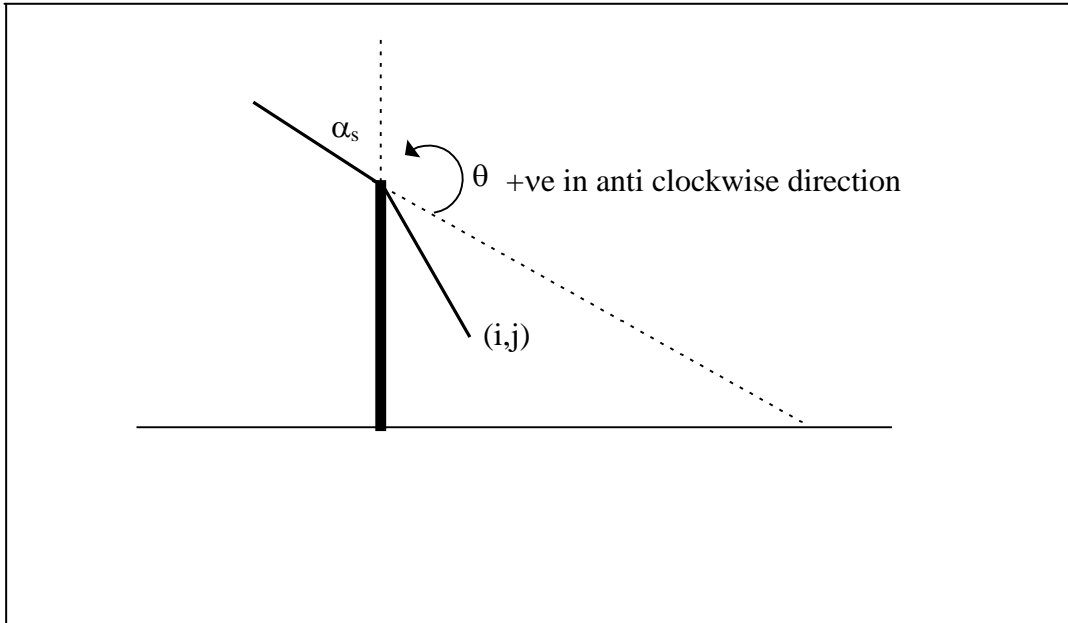


**Figure 3.2:** Diffraction approximation near groyne - after Kamphuis (1992)

$$\begin{aligned}
 (K_d)_{ij} &= 0.69 + 0.008\theta && \text{for } -90^\circ \leq \theta \leq 0^\circ \\
 (K_d)_{ij} &= 0.71 + 0.37 \sin \theta && \text{for } 0^\circ < \theta \leq 40^\circ \\
 (K_d)_{ij} &= 0.83 + 0.17 \sin \theta && \text{for } 40^\circ < \theta \leq 90^\circ
 \end{aligned} \tag{3.15}$$

Where  $\theta$  is expressed in degrees.

The calculated values of  $K_d$  will reduce the wave heights behind the structure as a result of which, and the corresponding smaller depths of wave breaking, the breaking angle behind the structure will be reduced. This phenomenon is discussed further in section 3.3.4.

Combining the effects of Shoaling, Refraction and Diffraction (if there is a structure), the wave height in shallow water can be expressed as

$$H_{ij} = \left[ (K_r)_{ij} (K_s)_{ij} (K_d)_{ij} \right] H_0 \tag{3.16}$$

$H_{ij}$  - wave height;  $H_0$  - deep water wave height

Deep water Wave Height,  $H_0=1.5\text{m}$ , Wave Direction,  $\alpha_0=30^\circ$  and a uniform bed slope of 1:200 was used in this example.

### 3.3.2 Calculation of Wave angles for the solution domain

Wave angles at all grid points can simply be calculated using Snell's Law

$$\alpha_{ij} = \sin^{-1} \left[ \left( \frac{C_{ij}}{C_0} \right) \sin \alpha_0 \right] \quad (3.17)$$

### 3.3.3 Calculation of Wave Height ( $H_{sb}$ ) and Wave Angle ( $\alpha_b$ ) at breaking

The most widely used is (Munk, 1949), was used in the present model.

$$H_b = 0.78 D_b \quad (3.18)$$

### 3.3.4 Correction for Combined refraction and diffraction behind a structure

The success of a rigorous calculation of the combined refraction/ diffraction of waves behind structures is largely limited by the lack of precise knowledge of the wave breaking phenomena and the two-dimensionality of the problem. Also, from a computer run time point of view, the procedure for calculating the wave angle behind a structure should be as simple as possible. However, from an engineering standpoint, the calculated results must show reasonable agreement with actual data.

The breaking wave angle behind the groyne is modified by two processes: diffraction around the structure and continuous refraction (even broken waves will refract since their celerity is a function of depth of water). Kamphuis, (1992) developed a relationship to account for these two processes, given as:

$$(\alpha_{bd})_i = (\alpha_b)_i (K_d)_i^{0.375} \quad (3.19)$$

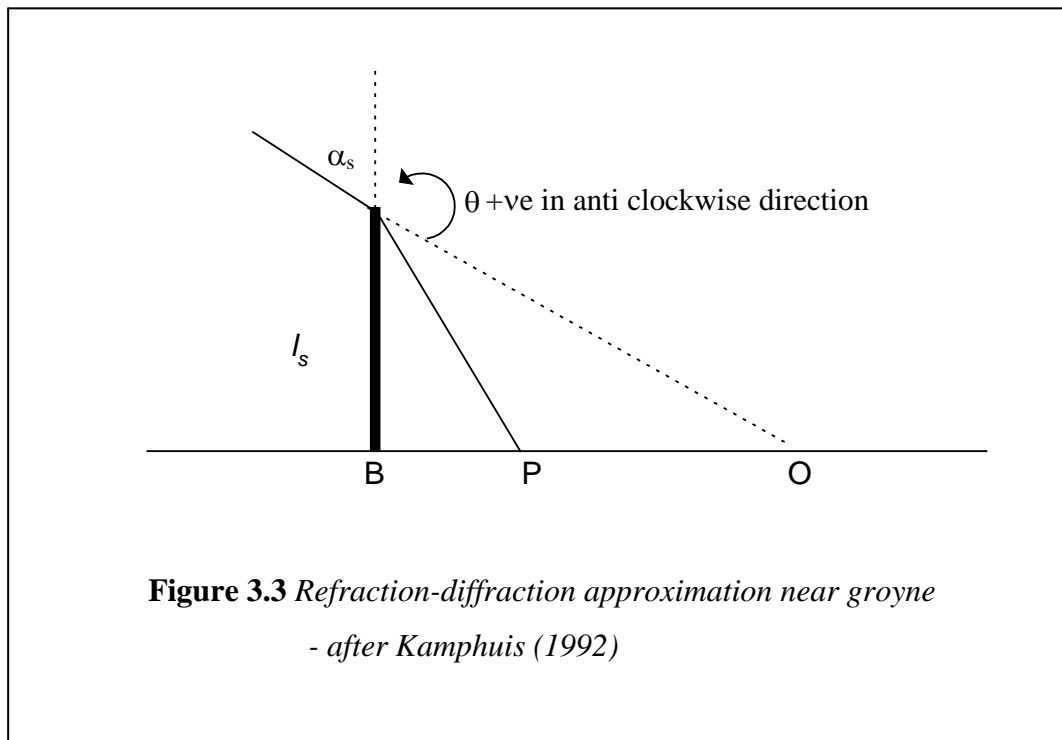
Except when

$$\theta < 0 \quad \text{and} \quad \frac{PB}{l_s} < 0.5 \left\{ \tan(\alpha_s) + \tan \left[ (0.88(\alpha_b)_i) \right] \right\}$$

In which case

$$(\alpha_{bd})_i = (\alpha_b)_i (K_d)_i^{0.375} \left\{ \frac{2PB}{[l_s (\tan \alpha_s + \tan(0.88(\alpha_b)_i))]} \right\} \quad (3.20)$$

PB is defined in figure 3.3



Obviously, greater sophistication could be used in the refraction and diffraction computations. However, the limited quality of the input data and the number of assumptions made to arrive at the n-line model normally would make greater sophistication unnecessary and time-consuming in numerical solution.

### 3.3.5 Groyne By-passing and Permeability

Although a groyne is a simple structure, the interaction between groyne and the beach is complex, and the number of variables needed to specify the problem is large. These variables include: wave direction, height, and period, and their temporal and spatial variability; tidal range; sand size, availability of sand, and beach topography (particularly beach slope); groyne length, construction material, elevation, porosity, and orientation with respect to the shoreline.

From an operational viewpoint, many of the aforementioned factors can be accounted for by two quantities categorizing alongshore-sand transport at groynes in a shoreline response model. These two quantities are bypassing and permeability.

### 3.3.5.1 Bypassing

Bypassing refers to alongshore movement of sand around the seaward end of a groyne. The factors believed to have leading control on the amount of by-passing are,

1. The length of the groyne relative to the width of the active zone of alongshore transport
2. The slope of the cross-shore distribution of the alongshore transport

Normally in 1-line models, sand bypassing is simulated by multiplying the calculated alongshore sand transport rate at the updrift grid section immediately adjacent to the groyne by the by-passing factor  $B$  defined as:

$$B = 1 - \frac{D_G}{D_{LT}} (D_G \leq D_{LT}) \quad (3.21)$$

in which  $D_G$  is the water depth at the seaward end of the groyne (which is a function of the calculated shoreline position and equilibrium beach slope), and  $D_{LT}$  is the depth limit for active alongshore transport (will be discussed in 3.3.7.1). Equation 3.27 implies a rectangular distribution of the alongshore-sand transport rate from the mean shoreline position at the groyne to the location of  $D_{LT}$ , with the amount by-passed proportional to the effective length of the groyne. If  $D_G \geq D_{LT}$  (very long groyne), then  $B = 0$ . The value of  $B$  therefore ranges between 0 and 1, with  $B = 0$  signifying no bypassing and  $B = 1$  signifying that all sand can potentially pass the position of the groyne.

In the case of n-line models, since the amount of sand transport at each cell across the shore is calculated, there is no need to incorporate a separate criterion for bypassing. However, the calculation of the amount of sand by-passed with reference to the groyne length is an important factor in deciding a suitable groyne length in a design context. The amount of sand needed for not depriving downdrift beaches of sand and groyne permeability has to be known in addition to the amount of sand by-passing to decide on a suitable groyne length.

In addition to sand by-passing due to alongshore transport, a small percentage of sand may be transported by waves around groynes due to a combination of alongshore and on-offshore transport. Since the model does not have the facility to calculate the on-

offshore transport at its present stage of development, it is not possible to calculate this component of sand bypassing.

#### 3.3.5.2 *Permeability*

The term groyne permeability encompasses the factors

- 1) Groyne porosity
- 2) Elevation of the groyne with respect to the wave and water level at a given time (controlling sand over-topping), and
- 3) By-passing of sand around the landward end of the groyne

In contrast to the bypassing factor, which depends on the wave conditions, the permeability factor  $P$  is, in the absence of hard data, taken to be a constant for a particular groyne. By definition, a “transparent” groyne is assigned a permeability of 1, and a very high, structurally tight groyne which extends landward so as to prevent landward sand by-passing is assigned a permeability factor of 0. The value of  $P$  for a particular groyne therefore lies in the range of  $0 \leq P \leq 1$  and is specified through the judgment of the modeler based on, for example, the structural characteristics of the groyne, its elevation, and the tidal range at the site.

#### 3.3.6 **Alongshore Sediment Transport Rate**

An extensive literature review was carried out by Samarawickrama (1999) in selecting the most appropriate alongshore transport predictor for this n-line model. It was found that Kamphuis et al equations are the most consistent and have given the best predictions for almost all cases. Kamphuis proposed his first alongshore transport equation in 1978 and has subsequently published improvements; the latest version was in 1991. Earlier equations tend to give inaccurate predictions in storm conditions and in situations with larger wave angles. The most recent equation has overcome these problems and it was therefore decided to use Kamphuis, 1991 formula for this study.

#### 3.3.7 **Alongshore Sediment Transport Rate - Kamphuis, 1991a**

The reasoning behind Kamphuis’ development of his equations is as follows. Alongshore sediment transport rate is a function of a combination of wave, fluid, sediment and beach-profile parameters. A general expression is:

$$Q = f(H, T, \alpha, d, \rho, \mu, g, x, y, z, t, \rho_s, D, m) \quad (3.22)$$

Where

$Q$  = alongshore sediment transport rate, expressed in kilograms of immersed mass per second,

$H, T, \alpha$  = wave height, period and angle of approach respectively,

$d$  = depth of water,

$\rho, \mu$  = fluid density and viscosity respectively,

$g$  = gravitational acceleration,

$x, y, z$  = space coordinates,

$t$  = time,

$\rho_s$  = sediment density,

$D$  = nominal grain size,

$m$  = beach slope, which is a simplified representation of the beach profile.

Because of the large number of parameters in the above equation, whose effects are interrelated, it is necessary to simplify the analysis by making use of the dimensional properties of the various parameters.

This result in

$$\pi_Q = \phi \left\{ \frac{H}{gT^2}, \alpha, \frac{H}{d}, \frac{H \left( \frac{H}{T} \right)}{\left( \frac{\mu}{\rho} \right)}, \frac{x}{gT^2}, \frac{y}{gT^2}, \frac{z}{d}, \frac{t}{T}, \frac{\rho_s}{\rho}, \frac{H}{D}, m \right\} \quad (3.23)$$

Where  $\pi_Q$  is a dimensionless sediment transport parameter: and  $\phi$  denotes “function of”.

Since the present analysis is concerned with sediment transport in the breaking zone,

$\frac{H}{d}$  is determined by the breaking process itself and is therefore not a true “variable”.

Because the breaking zone is highly turbulent the viscosity term is not important.

Overall sediment transport rate is discussed here, rather than sediment transport details through the breaking zone, hence geometric parameters containing  $x, y$  and  $z$  are not

needed; also since sediment transport rate is averaged over many wave periods, the  $\frac{t}{T}$

term becomes irrelevant. Only sand/water combinations had been used in the experiments, hence the  $\frac{\rho_s}{\rho}$  term was not investigated. Because the objective of the study was to derive a bulk sediment transport expression, which is normally assumed to be closely related to alongshore wave thrust (or alongshore component of wave power), the wave-angle term should be expressed as a function of  $(\sin 2\alpha_b)$ . The characteristic grain size used is  $D_{50}$ , and the beach profile parameter used is the beach slope in the breaking zone,  $m_b = \frac{d_b}{\lambda_b}$ , where  $\lambda_b$  is the distance from the shoreline to the breaker line. Finally, the  $\left(\frac{H}{gT^2}\right)$  term can be replaced by wave steepness. Thus the resulting relationship is:

$$\frac{Q}{\left(\frac{\rho H^3}{T}\right)} = \left(\frac{H}{L_0}\right)^p m_b^q \left(\frac{H}{D_{50}}\right)^r \sin^s(2\alpha_b) \quad (3.24)$$

Where  $p$ ,  $q$ ,  $r$  and  $s$  are unknown exponents. Sediment transport is thus a function of wave steepness, beach slope, relative grain size, and wave angle.

Kamphuis found the values for  $p$ ,  $q$ ,  $r$  and  $s$ , which fit well with full-scale data.

$$\frac{Q}{\left(\frac{\rho H_{sb}^3}{T_p}\right)} = 1.3 \times 10^{-3} \left(\frac{H_{sb}}{L_{op}}\right)^{-1.25} m_b^{0.25} \sin^{0.6}(2\alpha_b) \quad (3.25)$$

$H_{sb}$  is the breaking significant wave height,  $T_p$  is the peak period of the offshore wave spectrum, and  $L_{op}$  is the deep-water wavelength corresponding to the peak wave period. The exponents cannot be simply determined by multiple regression analysis, since the parameters involved are not truly independent; they were determined by successive approximations. Firstly, the exponent of the parameters that exerts the most influence was determined. Then the next most important exponent was found and the interaction between the first two exponents was determined. Once the interaction was understood, a relationship of best fit was determined. Then a third exponent was introduced and so on. Eventually the interaction between all four parameters was found and the process was repeated several times to improve the fit.

Equation 3.37 may be reduced to the form

$$Q=1.3 \times 10^{-3} \rho \left( \frac{g}{2\pi} \right)^{1.25} H_{sb}^2 T_p^{1.5} m_b^{0.75} D_{50}^{-0.25} \sin^{0.6}(2\alpha_b) \quad (3.26)$$

Thus

$$Q=2.27 H_{sb}^2 T_p^{1.5} m_b^{0.75} D_{50}^{-0.25} \sin^{0.6}(2\alpha_b) \left( \frac{kg}{s} \right) \quad (3.27)$$

$$Q=0.00203 (H_{sb})_i^2 T_p^{1.5} m_b^{0.75} D_{50}^{-0.25} \sin^{0.6}[2(\alpha_{bd})_i] \left[ \left( \frac{m^3}{s} \right) \right] \quad (3.28)$$

The final form equation takes into consideration wave steepness, beach slope, relative grain size in addition to breaking wave height, breaking wave angle and peak wave period and was adopted in the present model for the calculation of alongshore sediment transport rate.

It is seen that the sediment transport rate is proportional to  $H^2$ , the exponent of  $H$  being smaller than earlier Kamphuis equations. This reduced sensitivity to wave height corrects the criticism of earlier expressions that they over predicted the sediment transport rate in major storms. The present expression is more sensitive to wave period than earlier expressions.

### 3.3.8 Distribution of the Alongshore Sediment Transport Rate Across the Surf Zone

Based on the review by Samarawickrama (1999) of the limited number of models of the distribution the Perlin & Dean method was selected for use in this study and a detailed description of the method is given below.

### 3.3.9 The Cross- Shore Distribution of Alongshore Sediment Transport Rate Perlin & Dean, 1983

To represent the Fulford distribution analytically, a function of the following form was chosen:

$$q(y)=(B)(y)^{n-1} e^{-(y)^n} \quad (3.29)$$



This type of equation is convenient because it is easily integrable, and by properly choosing the constant,  $B$ , the integral of the equation from zero to infinity can be required to equal a particular value. This too is highly desirable because the integral is set equal to one and then multiplying by the value of the total alongshore transport, the value of the transport at any location across the surf zone can be determined. Further investigations suggested a value of  $n = 3$  to produce a curve similar to Fulford's curve. A more general form of the equation which allows more flexibility and curve fitting is,

$$q(y) = B(y + a)^2 e^{-\left[\frac{(y+a)}{cy_b}\right]^3} \quad (3.30)$$

Where,

$y_b$  = distance to the point of breaking,

$a$  = constant to allow sediment transport above the mean water line

(MWL) (swash transport or transport in the region of wave setup) to be included,

$c$  = a constant establishing the spread of the curve on the  $y$ -axis

(to be determined).

on the condition  $\int_0^{\infty} q_x(y) dy = 1.0$  then  $B = \frac{3}{c^3 y_b^3}$

Based on Fulford's (1982) results and considering " $a$ " to be proportional to the breaking wave height divided by the beach slope, the constant of proportionality was determined to be unity

i.e.  $a = \frac{h_b}{\left(\frac{\partial h}{\partial y}\right)}$

By carrying out non-linear least square regression analysis on measured and predicted values, the value of  $c$  was determined to be 1.25. The final form of the equation for the relative sediment transport at a location,  $y$ , in the surf zone results:

$$q(y) = \left\{ \frac{3}{[1.25^3 y_b^3]} \right\} \left\{ (y + a)^2 e^{-\left[\frac{(y+a)}{cy_b}\right]^3} \right\} \quad (3.31)$$

To obtain the fraction of transport between two  $y$  coordinates, the integral of the above equation from  $y_1$  to  $y_2$ , must be used.

$$Q_{x[ND]} = Q \int_{y_2}^{y_1} q(y) dy = e^{-\left[\frac{(y_1+a)}{cy_b}\right]^3} - e^{-\left[\frac{(y_2+a)}{cy_b}\right]^3} \quad (3.32)$$

$Q_{x[ND]}$  is dimensionless: therefore, to compute a value in, say, cubic meters per second, it must be multiplied by the total transport along a perpendicular to the shoreline, obtained from the total alongshore transport equation used in the model.

$$Q(I, J) = Q_{x[ND]} * Q = \left\{ e^{-\left[\frac{(y_1+a)}{cy_b}\right]^3} - e^{-\left[\frac{(y_2+a)}{cy_b}\right]^3} \right\} Q \quad (3.33)$$

In the present numerical model,  $Q(I, J)$  is determined by using the above equation except for the shoreline contour,  $J=1$ , and the farthest offshore contour simulated,  $J=JMAX$ . In order to include swash-zone transport, the shoreline contour alongshore transport,  $Q(I, 1)$ , is determined from the same equation; however, the first term is set equal to 1.0.

$$Q(I, 1) = \left\{ 1 - e^{-\left[\frac{(y_2+a)}{cy_b}\right]^3} \right\} Q \quad (3.34)$$

The transport at the most seaward contour,  $Q(I, JMAX)$ , neglects the second term of the initial equation in order to include any alongshore transport not yet accounted for, that is, it accounts for transport from  $y(I, JMAX)$  to infinity.

$$Q(I, JMAX) = \left\{ e^{-\left[\frac{(y_1+a)}{cy_b}\right]^3} \right\} Q \quad (3.35)$$

### 3.4 Design of Along Shore Transport Model (*SandPro*) using Advance Programming Techniques (GIS Based) – Design and Details

- Identification of nature of theories and equations.
- Solutions and explicit equations for corrections for combined refraction diffraction behind a structure.
- Algorithm design and Verification
- Technical Implementation with ArcView GIS Platform with a programmed and customized interface using avenue and C++.

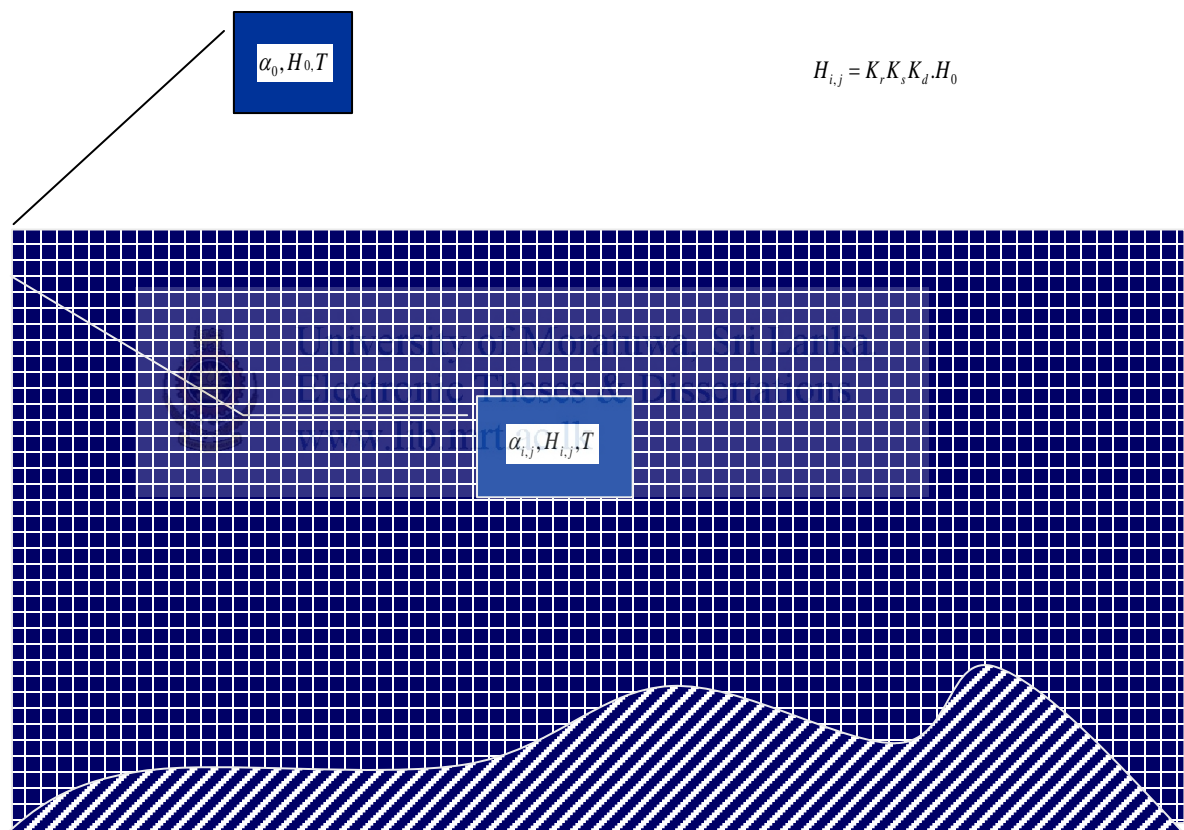


**Figure 3.4:** *Grid space for bathymetry*

- Identifying Universal Direction (X)
- Identifying Universal Direction (Y)
- Grid Area
  - Grid resolution of static nature – 500 \* 500
  - Transfer the nature from static to Dynamic
- In-Shore Boundary

- Below M.S.L. depth values are positive
- Above M.S.L. depth values are negative
- Coastal structures should be attached to shore line boundary with negative depth values
- Off-shore boundary
  - The off-shore boundary should be along the universal X direction.

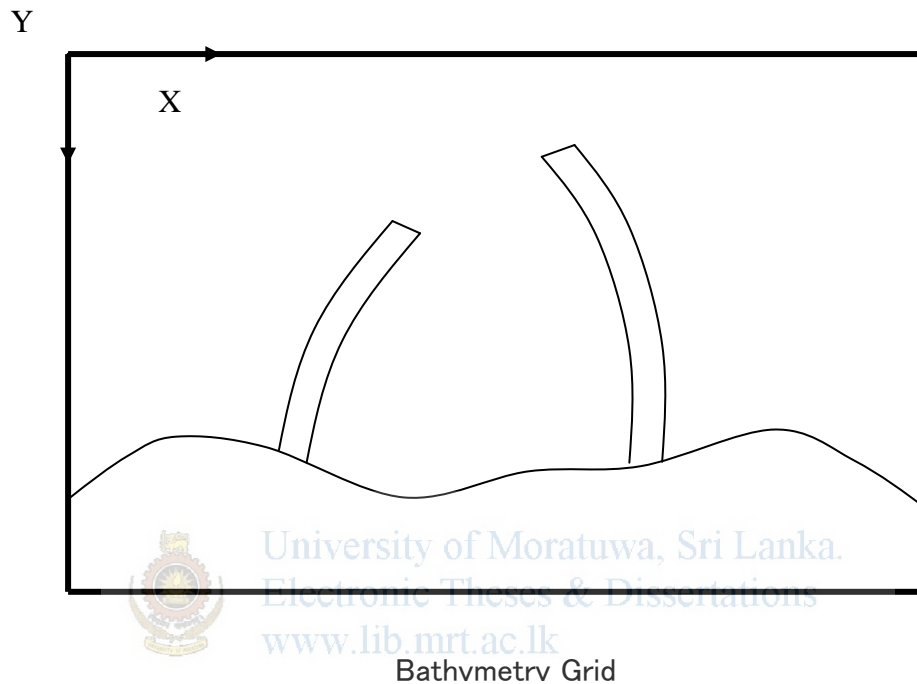


**Figure 3.5:** *structures defined alongshore*

Universal Direction - X

- Where Y-coordinate value doesn't change
- Where only X-coordinate value changes

**Important:** The offshore wave climate is considered and taken as  $\alpha_{i,j}, H_{i,j}, T$  at the offshore boundary along the universal x-direction.

- Wave climate transformation is done along the Y-direction.

**Note:** T is a constant for the processing for a particular instance of the model run. With a Global variable called “**Bathymetry\_Update\_Interval**”, the model would run throughout the initial bathymetry producing bathymetry updates after each such interval, making the model dynamic with short time periods.

These sets of offshore wave climates have to be defined with ASCII formatted text file as parameters for the model along with a value for “**Bathymetry\_Update\_Interval**”.

Universal Direction – Y

- Where X-coordinate value doesn't change
- Where only Y-coordinate value changes

Grid Area

- The Grid area initially is taken as 500\*500 where all the sub-functions of grid climate transformations are done using a statically defined two-dimensional array of 500\*500 elements.
- With the working prototype, the nature of application will be transferred where all the array definitions will be decided run-time.

**Note:** Before the task is taken to the main processing, the dimensions have to be input as parameters.

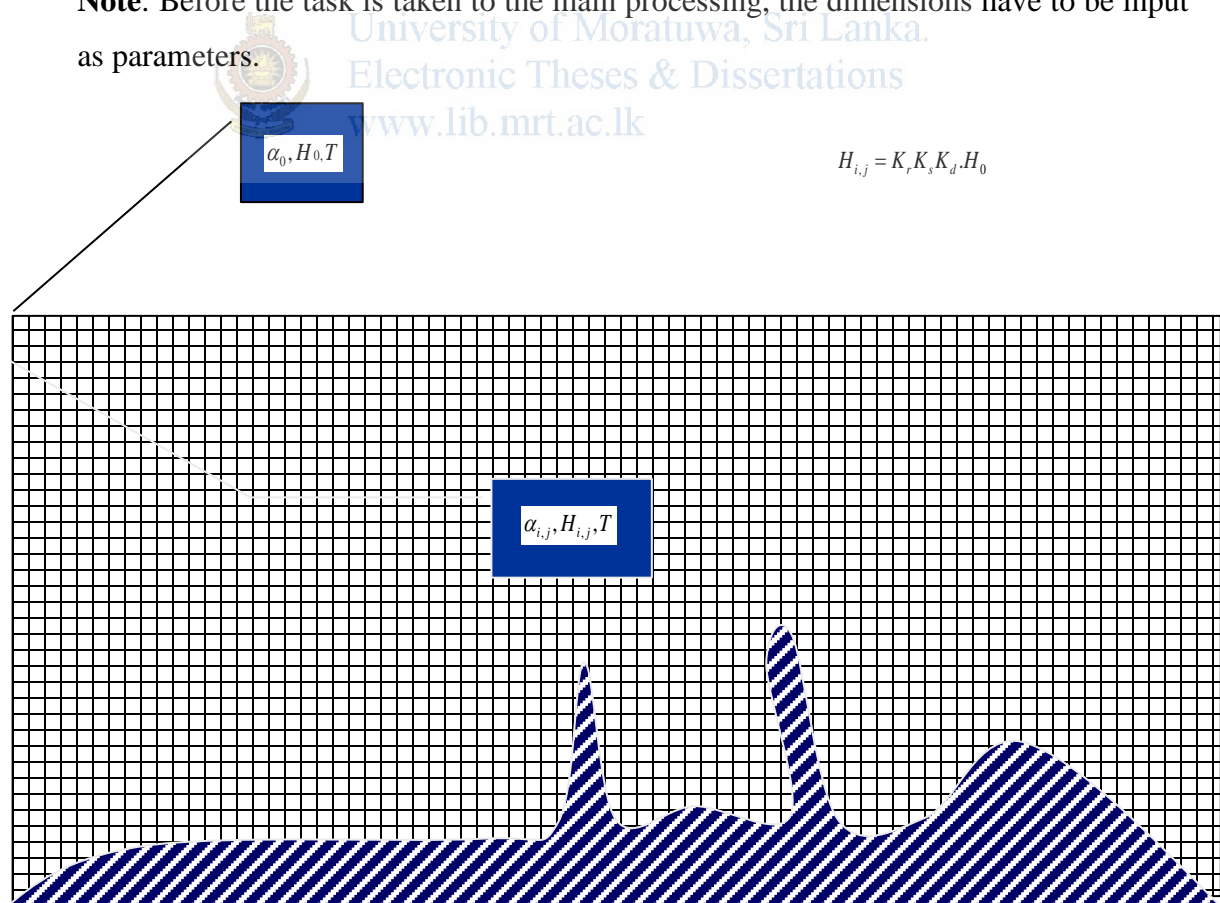


**Figure 3.6:** Bathymetry Space with the Grid with structures defined with the shoreline

### In-shore Boundary

- Surface Generated Bed Surface should be a continuous and uniform bathymetry.
- Land including structures should be defined separately with the depth values.

### Depth values

- Under sea level, all the depth values must be defined as positive. Above the mean-sea-level (0m or user defined) depth values must be defined as negative.

**Note:** The in-shore boundary can be irregular and in-shore structures should be combined with the shore boundary, and should be defined with negative depth values which will be modelled as a part of bathymetry.

### Offshore boundary

- The offshore boundary should be along the universal X direction as shown in figure 3.5 and 3.6.

### 3.4.1 Wave Climate Transformation

#### System Memory Space Required

- Storage of Z values (Depth)
- Storage of  $\alpha$  values
- Storage of C values
- Storage of  $K_r$  values
- Storage of  $K_s$  values
- Storage of  $K_d$  values

#### Storage of Z Values :zArray

Note: The grid-formatted value used with program is taken from the ASCII output of ArcView GIS grid.

[format]

- The values have to be read from each column and row
- The delimiter for each value is ' ' (space) character.

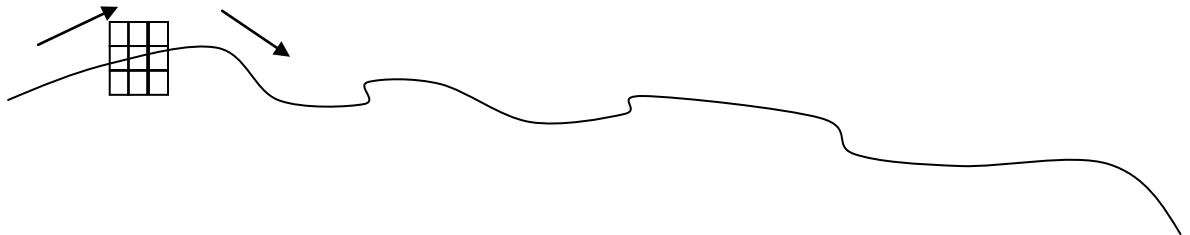
The function to isolate each depth value  $\rightarrow$  *StrChopCol()*; refer Bibliography

- Each value is taken and stored in the array.

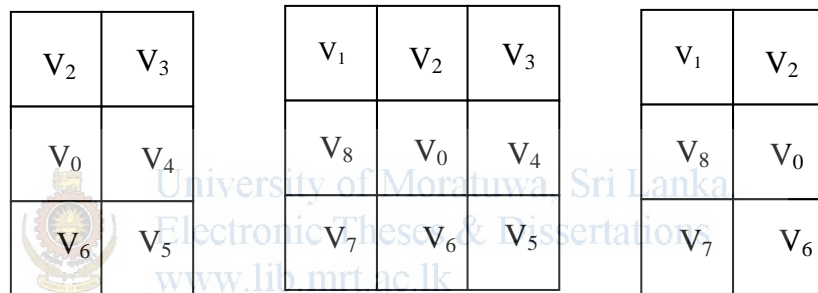
### 3.4.1.1 Identifying shore-line-boundary

Shore Line Boundary is stored in an array: *shoreLine* – using function *ScanShore()*

**Note:** The function stores the co-ordinates of the grid, which is the boundary of shore and structures proposed/existing.



col index  $> 0 \leq \text{max columns} - 2$



col index = 0

col index = max columns - 1

**Figure 3.7:** Grid Templates for beach slope calculation and to identify shoreline

#### Algorithm 3.1: ScanShore

//System Variables:

//M.S.L.: Mean Sea Level value to identify land values and sea.

Accept the model control parameter for Mean Sea Level

Initialize *shoreLine* array

Along the first column start searching Cell\_Value, which is greater than specified value for Mean Sea Level

Obtain the co-ordinates for the cell, which breaks the condition

Store co-ordinates as the first cell along the coastal shoreline

Define the grid template for col\_index = 0 (figure 3.7)

Obtain the Cell\_Coordinates where Cell\_Value is closest to the M.S.L. ( $|M.S.L. - Cell\_Value|$  is the minimum.)

Store in *shoreLine* array

*Column\_index* = *column\_index* of *Cell\_Coordinates*

Store the co-ordinates of the current cell as the *previous\_coordinates*

While *column\_index* < *max\_columns* - 1

Begin

Define the Grid Template (figure 3.7)

Obtain the *Cell\_Coordinates* where *Cell\_Value* is closest to the M.S.L. (  
| M.S.L. - *Cell\_Value* | is the minimum.)

If obtained *Cell\_Coordinate* is not *previous\_coordinate*

Then

Store in *shoreLine* array

*Column\_index* = next *column\_index* of *Cell\_Coordinates*

End if

End

Repeat the above Task for *Column\_index* = *max\_columns* - 1 and *Column\_index* =  
*max\_columns*

End



University of Moratuwa, Sri Lanka.  
Electronic Theses & Dissertations  
[www.lib.mrt.ac.lk](http://www.lib.mrt.ac.lk)

### Algorithm 3.2: Compute Beach Slope

Initialize **beachSlope** Array

Use the same structure as above for scanning

For *col\_index* = 0

Obtain *Cell\_Value* ( $V_0$ ) of Grid at M.S.L. from **shoreLine**

Obtain values of surrounding cells out of ( $V_{2-6}$ )

Obtain values those are greater than  $V_0$

Compute the Average

Calculate beach slope from  $V_0$ , Computed Average and  $\Delta y$ ;  $(\text{Average} - V_0) / \Delta y$

Store the values as the slope along the coastal line in **beachSlope** array

For each point in *shoreLine* array next to first cell and up to the cell before last cell

Begin

Obtain *Cell\_Value* ( $V_0$ ) of Grid at M.S.L. from **shoreLine**

Obtain values of surrounding cells out of ( $V_{0-8}$ )

Obtain values those are greater than  $V_0$



*Compute the Average*

*Calculate beach slope from  $V_0$ , Computed Average and  $\Delta y$ :  $(\text{Average} - V_0) / \Delta y$*

*Store the values as the slope along the coastal line in **beachSlope** array*

*End*

*col\_index = max\_columns - 1*

*Obtain Cell\_Value ( $V_0$ ) of Grid at M.S.L. from **shoreLine***

*Obtain values of surrounding cells out of ( $V_{1-2, 6-8}$ )*

*Obtain values those are greater than  $V_0$*

*Compute the Average*

*Calculate beach slope from  $V_0$ , Computed Average and  $\Delta y$ :  $(\text{Average} - V_0) / \Delta y$*

*Store the values as the slope along the coastal line in **beachSlope** array*

**Storage of C values : cArray**

- For Storage of C values, an array of the same size (500\*500) should be defined.

- Applied Criteria

1. Deep water  $\left[ \frac{d_{ij}}{(gT^2)} > 0.08 \right]$

$$L_0 = \frac{gT^2}{2\pi}; C_{ij} = C_0 = \frac{L_0}{T}$$

2. Transitional zone  $\left[ 0.0025 \leq \frac{d_{ij}}{gT^2} \leq 0.08 \right]$

$$L_{ij} = L_0 \tanh\left(\frac{2\pi d_{ij}}{L}\right); C_{ij} = \frac{L_{ij}}{T}$$

3. Shallow water  $\frac{d_{ij}}{gT^2} < 0.0025$

$$C_{ij} = \sqrt{gd_{ij}}$$

where

$C_{ij}$  = wave celerity

$C_0$  = deep water wave celerity

$L_{ij}$  = wave length

$L_0$  = deep water wave length

$T$  = wave period

$d_{ij}$  = water depth

and subscripts ij refer to a point within the calculation domain.

**Algorithm 3.3: Celerity\_Generation**

/\*\*\*\*\*\*

**Refer Bibliography Listing 2.1**

\*\*\*\*\*/

Initialize cArray with 1.0s

For Column\_Index = 0 to col\_maximum

Begin

For Row\_Index = 0 to row\_maximum

Begin

If Cell\_Value > M. S. L. then

Begin

Do

Case (i) ; Calculate  $C_{ij}$  and store

Case (ii) ; Calculate  $C_{ij}$  and store

Case (iii) ; Calculate  $C_{ij}$  and store

End Case

End if

End if

End for

**Storage of  $\alpha$  values : *alPhaArray***

- Define an array of Same size (500 \* 500) and dimensions as the grid space
- Use the array of C values

**Criteria**

$$\sin\alpha_{ij} = \frac{C_{ij}}{C_0} \sin\alpha_0$$

**Algorithm 3.4: *alpha\_generation***

Initialize *alPhaArray* with 0s



University of Moratuwa, Sri Lanka.  
Electronic Theses & Dissertations  
www.ho.mrt.ac.lk

```

For Column_Index = 0 to col_maximum
Begin
    For row_index = 0 to row_maximum
    Begin
        If Cell_Value > M.S.L. then
        Begin
            Obtain C value      Cij → Calculate αij
        End if
    End For
End For
End For

```

/\*\*\*\*\*\*

**Refer Bibliography Listing 2.2**

\*\*\*\*\*/

Storage of K<sub>s</sub> Values : **KsArray**

- An array of similar capacity is needed



University of Moratuwa, Sri Lanka.  
Electronic Theses & Dissertations  
www.lib.mrt.ac.lk

**Criteria**

$$(K_s)_{ij} = \left[ \frac{1}{\sqrt{\tanh(K_{ij} d_{ij})(1 + G_{ij})}} \right] \tag{3.12}$$

where:  $K_{ij} = \frac{2\pi}{L_{ij}}$  and  $G_{ij} = 1 + \frac{2K_{ij}d_{ij}}{\sinh(2K_{ij}d_{ij})}$

L<sub>ij</sub> →

- Deep Water

- $L_0 = \frac{gT^2}{2\pi}$ ;

- Transition Zone  $\left[ 0.0025 \leq \frac{d_{ij}}{gT^2} \leq 0.08 \right]$

- $L_{ij} = L_0 \tanh\left(\frac{2\pi d_{ij}}{L}\right)$ ;  $C_{ij} = \frac{L_{ij}}{T}$

- Shallow Water

$$○ C_{ij} = \sqrt{gd_{ij}} \quad ; L_{i,j} = C_{i,j} \alpha_{ij} T$$

stored in algorithm : **Celerity\_Generation**

/\*\*\*\*\*\*

**Refer to Bibliography Listing 2.1**

\*\*\*\*\*/

**Storage of  $K_r$  Values : *KrArray***

- A similar sized array-space is required.

**Criteria**

$$K_r = \frac{H_{ij}}{H_0} = \sqrt{\frac{\cos\alpha_0}{\cos\alpha_{ij}}} \quad \text{Calculation 1}$$

$$(K_r)_{i,j} = \sqrt{\frac{\cos\alpha_{i,j-1}}{\cos\alpha_{ij}}} \quad \text{Calculation 2}$$



University of Moratuwa, Sri Lanka.  
Electronic Theses & Dissertations  
www.ho.mrc.ac.lk

**Algorithm 3.5: refraction generation**

Initialize *KrArray* with 1.0 s

For Column\_Index = 0 to col\_maximum - 1

Begin

Find max\_row\_number at which it meets first cell at landward boundary

For row\_index = 0 to max\_row\_number

Begin

While Cell\_Value > M.S.L.

If row\_index = 0 then

Begin

**Calculation 1**

Else

**Calculation 2**

End if

End While

End For

End For

Storage of  $K_d$  Values :  $KdArray$

**Criteria**

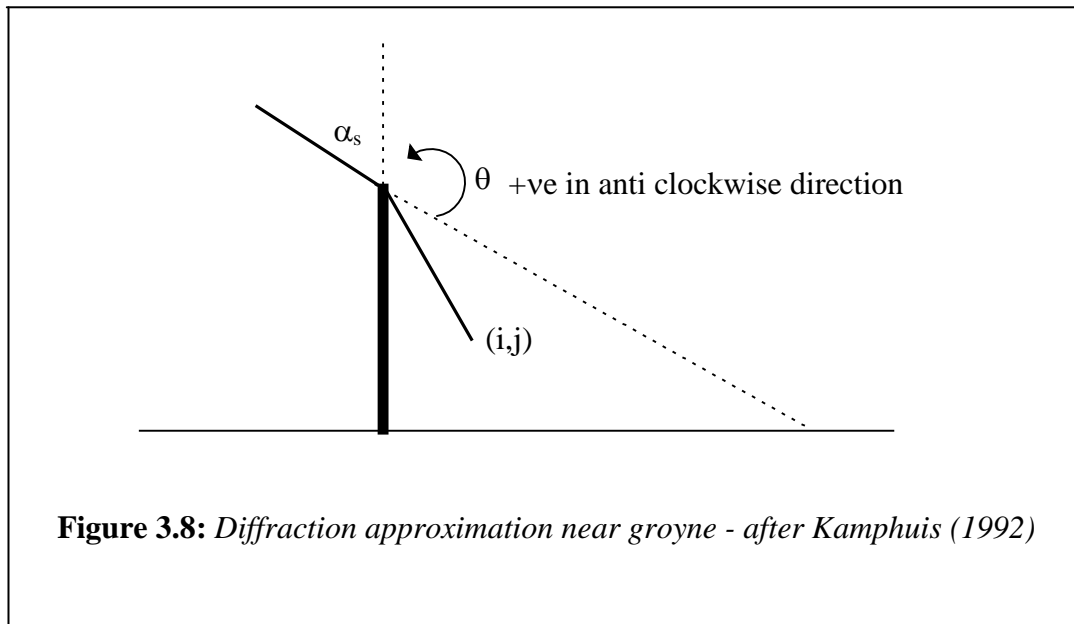


**Figure 3.8:** Diffraction approximation near groyne - after Kamphuis (1992)

$$\begin{aligned}
 (K_d)_{ij} &= 0.69 + 0.008\theta && \text{for } -90^\circ \leq \theta \leq 0^\circ \\
 (K_d)_{ij} &= 0.71 + 0.37 \sin \theta && \text{for } 0^\circ < \theta \leq 40^\circ \\
 (K_d)_{ij} &= 0.83 + 0.17 \sin \theta && \text{for } 40^\circ < \theta \leq 90^\circ
 \end{aligned}
 \tag{3.15}$$

Where  $\theta$  is expressed in degrees.

At the shore boundary

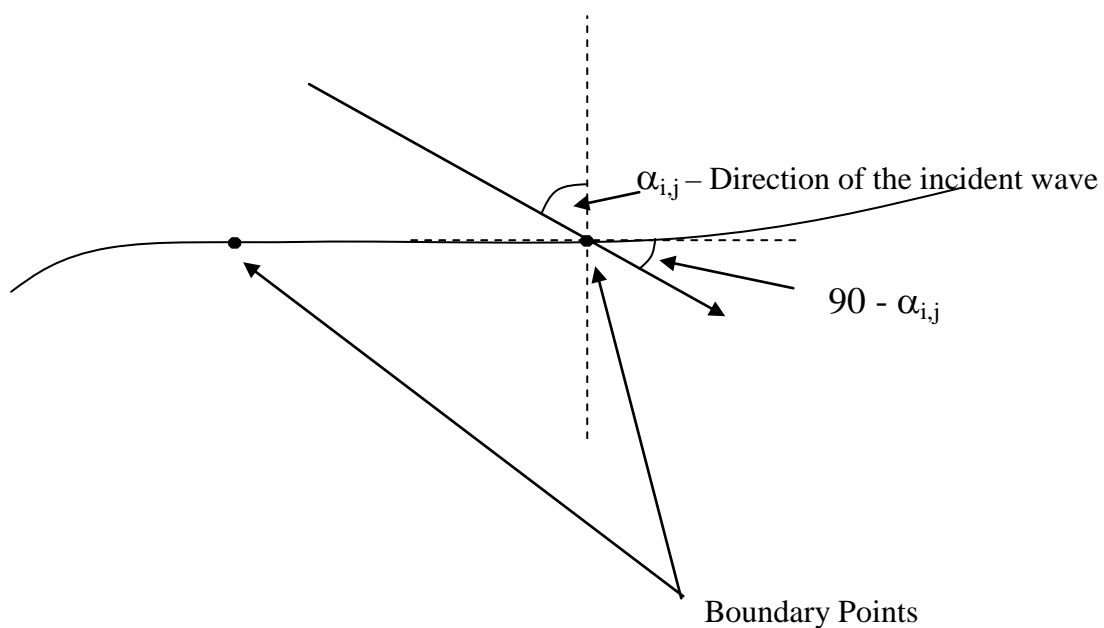


**Figure 3.9:** Identifying points of diffraction

### 3.4.2 Calculation of wave-directional gradient

Gradient  $_{i,j} = \text{Cot } \alpha_{i,j} = G_{i,j}$

Range of Tolerance =  $\pm (1^\circ - 2^\circ)$  (To be decided with Sample data sets).

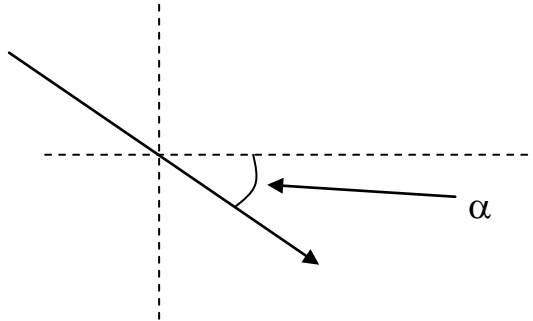


**Figure 3.10:** Considered Angle for Calculations

$$\begin{aligned} \tan(\alpha + \delta\theta) &= \frac{(\tan \alpha + \tan \delta\theta)}{(1 - \tan \alpha \tan \delta\theta)} \\ &= \frac{(\tan \alpha + \delta\theta)}{(1 - \delta\theta \tan \alpha)} \end{aligned}$$

$$\tan(\alpha + \delta\theta) - \tan \alpha = \frac{(\tan \alpha + \delta\theta)}{(1 - \delta\theta \tan \alpha)} - \tan \alpha = \Delta G$$

$$\Delta G = \frac{(1 + \tan^2 \alpha) \delta\theta}{(1 - \delta\theta \tan \alpha)}$$

$$\Delta G = \frac{\delta\theta \text{Sec}^2 \alpha}{(1 - \delta\theta \tan \alpha)}$$

Range of Tolerance for G (Directional Gradient)

$$\pm \Delta G = \frac{\pm \delta\theta \text{Sec}^2 \alpha}{(1 - \delta\theta \tan \alpha)} \quad - \alpha, \delta\theta \text{ is in radians}$$

$$\alpha \longrightarrow (90 - \alpha_{i,j})$$

$$\pm \Delta G = \frac{\pm \delta\theta \text{cosec}^2 \alpha_{i,j}}{(1 - \delta\theta \cot \alpha_{i,j})}$$

### Calculation of Directional Gradient along shoreline boundary

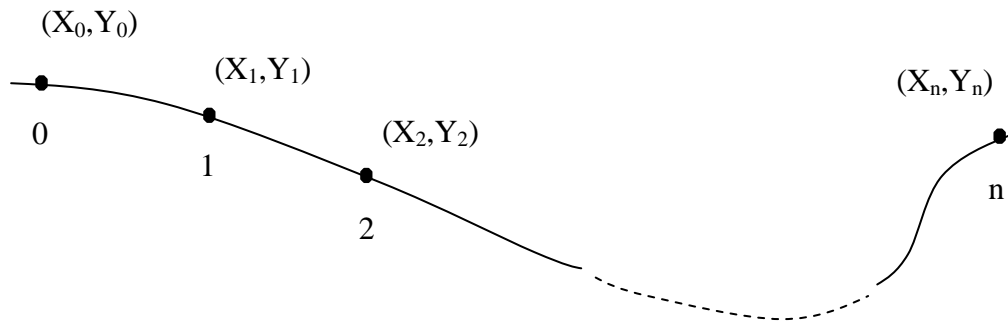


**Figure 3.11:** Calculating shoreline gradient

With 0<sup>th</sup> node; (Along *shoreLine* array)

Use Co-ordinates such as  $(X_0, Y_0)$ ,  $(X_1, Y_1)$  and calculate  $g$  with respect to universal X direction.

$$g_0 = \frac{(Y_1 - Y_0)}{(X_1 - X_0)}$$

For the n<sup>th</sup> node (Along *shoreLine* array)

Use nodes such as  $(X_n, Y_n)$ ,  $(X_{n-1}, Y_{n-1})$

$$g_n = \frac{(Y_n - Y_{n-1})}{(X_n - X_{n-1})}$$

For all intermediate points

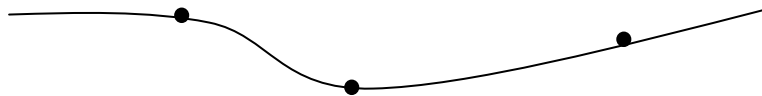


**Figure 3.12:** Calculating gradient at middle points along shoreline

$$g_n = \frac{\left(\frac{Y_N - Y_{N-1}}{X_N - X_{N-1}}\right) + \left(\frac{Y_{N+1} - Y_N}{X_{N+1} - X_N}\right)}{2}$$

Calculate  $|G - g|$  and if the value is held within  $\Delta G$  the wave vector proceeds beyond the shore point and diffraction is applied accordingly.

*Area under influence of diffraction*

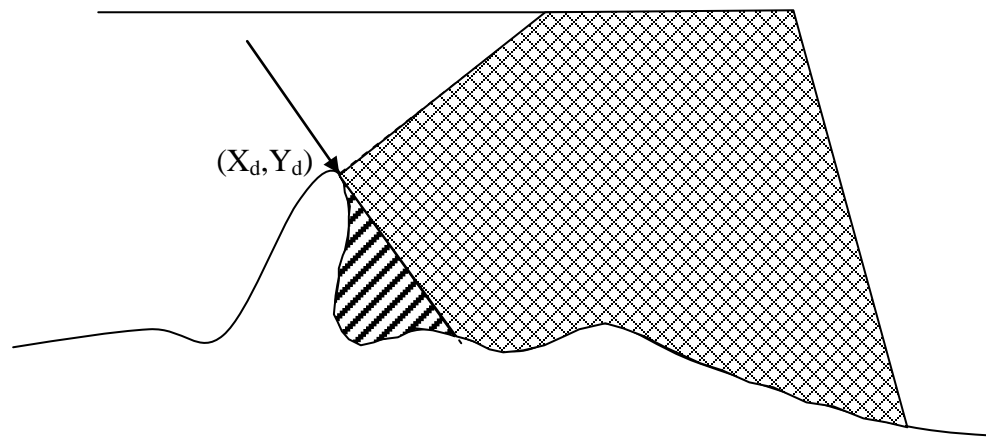


**Figure 3.13:** Influence zone under diffraction

If a point satisfied with the above condition, the point co-ordinate is used to calculate  $K_d$  for points located within the influence zone.

- $(P_{i,j}) \equiv (X_p, Y_p)$

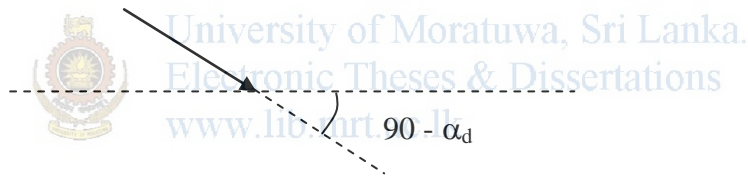


**Figure 3.14:** Considered Angle from Incident Angle for Diffraction Calculations

$\alpha_d$  = incident angle

Angle produced by the point  $P$  on point of diffraction with respect to universal  $X$ -direction.

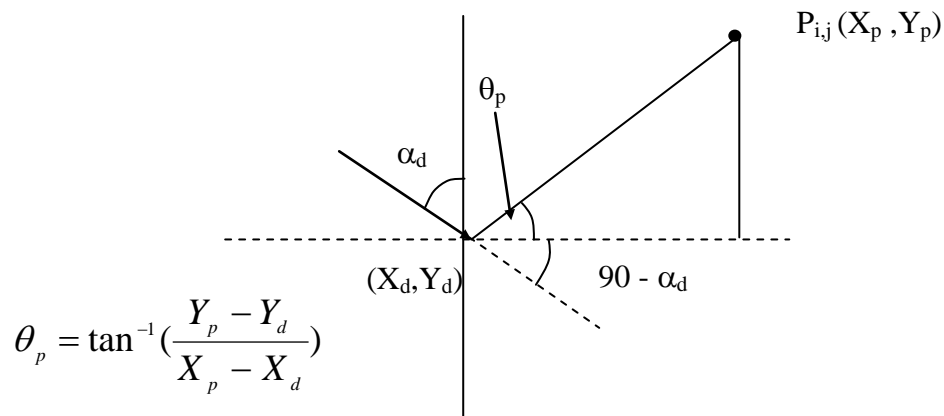


**Figure 3.15:** Angles derived for Diffraction Calculations



Angle with respect to the incident direction;

$$\theta = (\theta_p + 90 - \alpha_d)$$

$$\text{if } -90^0 \leq \theta \leq 0^0 \quad (K_d)_{ij} = 0.69 + 0.008\theta$$

$$\text{elseif } 0^0 < \theta \leq 40^0 \quad (K_d)_{ij} = 0.71 + 0.37 \sin \theta$$

$$\text{elseif } 40^0 < \theta \leq 90^0 \quad (K_d)_{ij} = 0.83 + 0.17 \sin \theta$$

$$\text{else } (K_d)_{i,j} = 1$$

**Algorithm 3.6: diffraction\_generation**

Computation of Co-efficient of diffraction

Initialize an array **KdArray** with dimensions equivalent to bathymetry grid-dimensions

Define an Array of structures to store diffraction points along the shore-line – **diffPoints** structure { **point\_cell** (x,y), **incident\_angle**}

Initialize all its values to 1.0

Traverse through **shoreLine** array (**shoreLine**) and array of incident angles (**alphaArray**)

With each **Cell\_Value**

Calculate shoreline gradient (g) from shoreline co-ordinates.

Calculate wave directional gradient from the incident angle at each relevant co-ordinate

Compare the different with  $\Delta G$

If the point under consideration is a point of diffraction

Then

Add the diffraction point to **diffPoints**

Define the influence zone of diffraction and through a traverse of the whole bathymetry, update array of diffraction points (**KdArray**) with Coefficient of diffraction (Only if  $K_d > 0$ )

**Note:** Always the co-efficient of diffraction (**cell\_value**) is multiplied by the value that is computed

End if

*End with*

*Initialize an array of  $H_0$  values (**hArray**) with same capacity as other storages.*

*Initialize with  $H_0$  values only for those cells, which are sea.*

*For each Cell that is water*

$$hArray[i][j] = hArray[i][j] * KrArray[i][j] * KsArray[i][j] * KdArray[i][j]$$

*End For*

**Algorithm 3.7: store\_breaking\_zone**

**Resources: zArray, alPhaArray, hArra**

*Identification of breaking zone*

*Define a new storage space for wave breaking zone points:→ **BreakArray** (Statically defined/ an array of structure)*

*For  $i = 0$  to  $max\_columns - 1$*

*Begin*

*For  $j = 0$  to  $max\_rows - 1$*

*Begin*

*If  $H_{i,j} \geq 0.78 * D_{i,j}$*

*Then*

*Store co-ordinates  $[i,j]$  in 'BreakArray'*

*Store  $\alpha$  values in 'BreakArray'*

*Store  $H$  values in 'BreakArray'*

*Break*

*End if*

*End for*



University of Moratuwa, Sri Lanka.  
Electronic Theses & Dissertations  
www.lib.mrt.ac.lk

### 3.4.3 Correction for combined refraction and diffraction behind a structure

Two Cases:

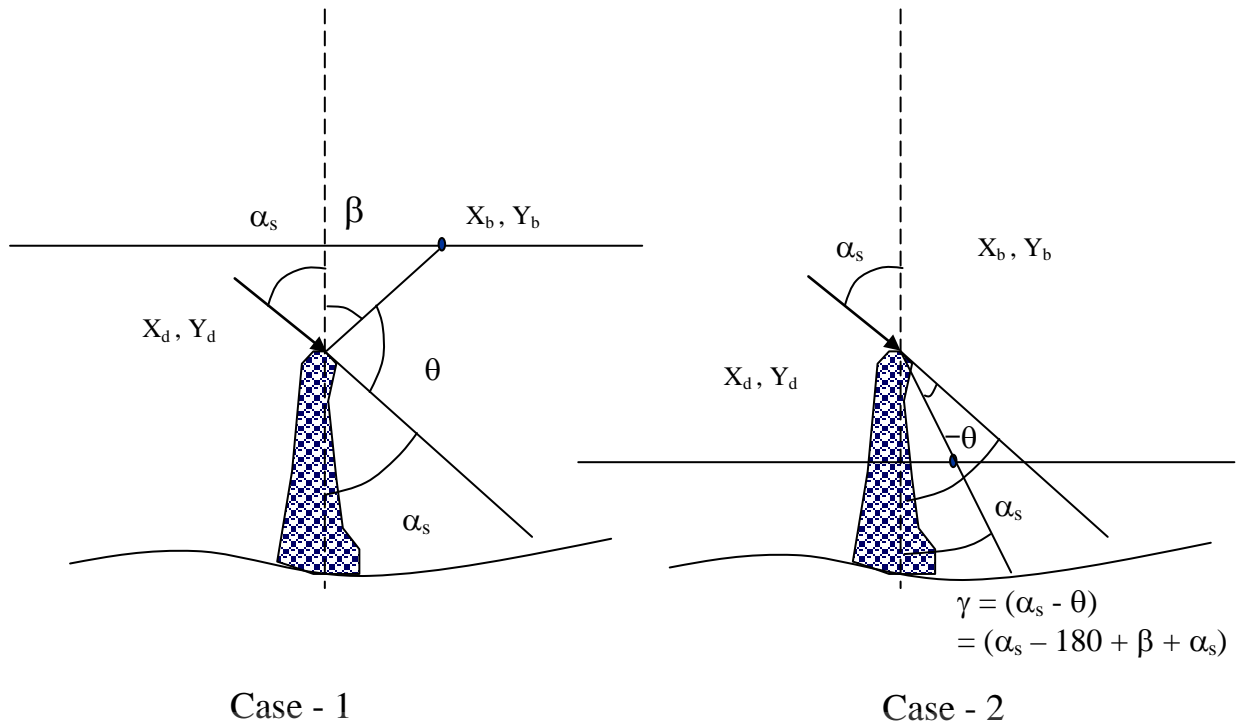


**Figure 3.16:** Two cases for the correction of combined refraction and diffraction

Case - 1

$$\alpha_{bd} = \alpha_b * (K_d \text{ at break point of the column})^{0.375}$$

Case - 2

$$\tan \beta = \left( \frac{Y_b - Y_d}{X_b - X_d} \right) \quad \beta = \tan^{-1} \left( \frac{Y_b - Y_d}{X_b - X_d} \right)$$

$$\theta = (180 - \beta - \alpha_s) \quad \gamma = (2\alpha_s + \beta - 180)$$

$$\text{Condition:} \quad \theta < 0 \quad \text{and} \quad \frac{PB}{l_s} < 0.5 \left\{ \tan(\alpha_s) + \tan \left[ (0.88(\alpha_b)_i) \right] \right\}$$

$$\gamma = PB/l_s ;$$

$$\text{Condition:} \quad \theta < 0 \quad \text{and} \quad \tan \gamma < 0.5 \left\{ \tan(\alpha_s) + \tan \left[ (0.88(\alpha_b)_i) \right] \right\}$$

in which case

$$(\alpha_{bd})_i = (\alpha_b)_i (K_d)_i^{0.375} \left\{ \frac{2PB}{[l_s (\tan \alpha_s + \tan(0.88(\alpha_b)_i))]} \right\}$$

Becomes

$$\alpha_{bd} = \alpha_b * (K_d)^{0.375} \left\{ \frac{2 \tan \gamma}{(\tan \alpha_s + \tan(0.88\alpha_b))} \right\}$$

**Algorithm 3.8: apply\_Combined\_refraction\_and\_diffraction**

For each point in diffPoints

    Begin

        Obtain co-ordinates  $\rightarrow (X_d, Y_d)$

        For col\_index =  $X_{d+1}$  to max

            Obtain the co-ordinate from BreakArray (col\_index,  $Y_b$ )

            Calculate  $\theta$

            If  $\theta > 0$

                Then

$$\alpha_{bd} = \alpha_b * (K_d \text{ at break point of the column})^{0.375}$$

        elseif( $\theta \leq 0$ ) AND  $\tan \gamma < 0.5 \{ \tan \alpha_s + \tan[0.88\alpha_{bi}] \}$ ,  $\gamma = (2\alpha_s + \beta - 180)$

            Then

$$\alpha_{bd} = \alpha_b * (K_d)^{0.375} \left\{ \frac{2 \tan \gamma}{(\tan \alpha_s + \tan(0.88\alpha_b))} \right\}$$

            End if

        End for

End For

$\alpha_b$  – incident wave angle at the breaking zone as stored in the BreakArray

$\alpha_{bd}$  – Corrected incident wave angle



### 3.4.4 Implementing the Sediment Balance

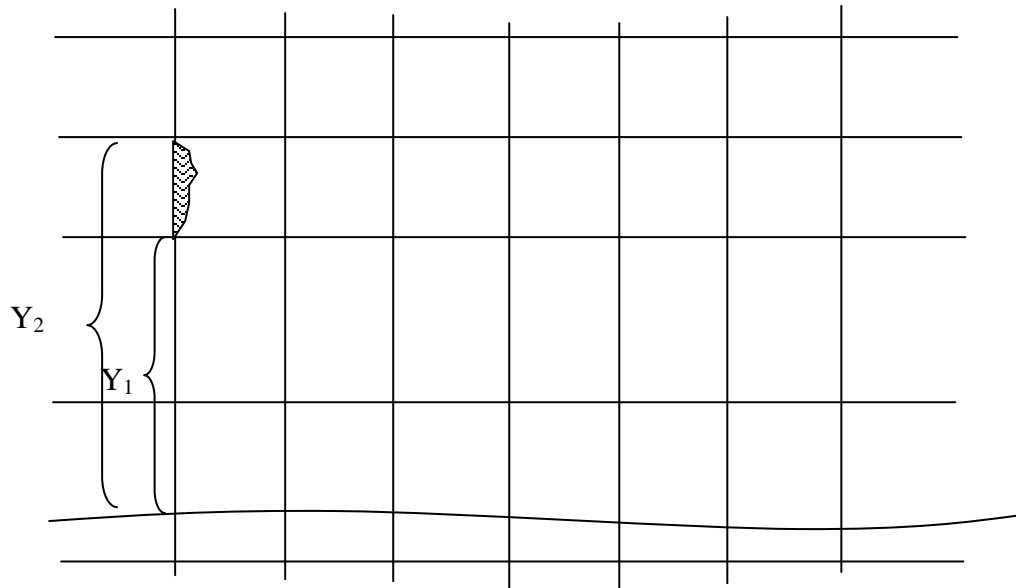


**Figure 3.17:** Calculating sediment flow for intermediate cells of the grid

For the first Node:

$$Q_{cell} = \left\{ 1 - e^{-\left[ \frac{y_2+a}{Cy_b} \right]^3} \right\} Q$$

For intermediate Nodes:

$$Q_{cell} = \left\{ e^{-\left[ \frac{y_1+a}{Cy_b} \right]^3} - e^{-\left[ \frac{y_2+a}{Cy_b} \right]^3} \right\} Q$$

For the Last Node:

$$Q_{cell} = \left\{ e^{-\left[ \frac{y_1+a}{Cy_b} \right]^3} \right\} Q$$

(Should be most 5% or less of the  $Q_{max}$ )

Resources – BreakArray, shoreline

**Algorithm 3.9: flow\_calculation**

Initialize **qArray** for similar capacity of grid-space.

For *col\_index* = 0 to *max\_columns*

Begin

Obtain relevant  $H_b$  for the column from **BreakArray**,  $H_{sb} = H_b$

Obtain respective  $y$  from **BreakArray** at relevant  $x$

Obtain average gradient along the column with 10 coordinates towards offshore or until  $y$  reaches offshore boundary:  $m_b$

Obtain  $\alpha_{bd}$  from **BreakArray**

$$a = \frac{H_{sb} \text{ taken from BreakArray at corresponding } x}{m_b}$$

$$C = 1.25$$

Calculate the Total  $Q$  across a section (for each column)

$$Q_i = 0.00203 * (H_{sb})^2 * T_p^{1.5} * m_b^{0.75} * D_{50}^{-0.25} * \text{Sin}^{0.6}(2(\alpha_{bd})_i)$$

( $D_{50}$  – Input parameter for the model)



University of Moratuwa, Sri Lanka.  
Electronic Theses & Dissertations

Search first found *row\_number* at landward boundary => *row\_number*

$$y_2 = \Delta y$$

$$qArray[i, row\_number] = \left\{ 1 - e^{-\left[ \frac{y_2 + a}{C y_b} \right]^3} \right\} Q_i$$

$$y_b = (-\Delta y) * (Y_b \text{ from BreakArray} - Y_{shoreline} \text{ from shoreline})$$

For *row\_index* = *row\_number* - 1 to 1

Begin

If *Cell\_Value* >= *M.S.L*

$Y_1 = (\text{row\_index} - \text{row\_number}) * (-\Delta y)$  // First found point at landward boundary

$$Y_2 = ((\text{row\_index} - 1) - \text{row\_number}) * (-\Delta y)$$

$$qArray[i, j] = \left\{ e^{-\left[\frac{(y_1+a)}{Cy_b}\right]^3} - e^{-\left[\frac{(y_2+a)}{Cy_b}\right]^3} \right\} Q_i$$

// i = col\_index, j = row\_index

End if

End For

$$Y_1 = Y_{shoreline} * (\Delta y)$$

$$qArray[i, j] = \left\{ e^{-\left[\frac{y_1+a}{Cy_b}\right]^3} \right\} Q$$

If (  $Q_{i,j} \geq 0.05 * Q_i$  )

Then

Report Error: (Message: Bathymetry insufficient Re-submit your bathymetry)

Abort

End if

End For



University of Moratuwa, Sri Lanka.  
Electronic Theses & Dissertations  
[www.lib.mrt.ac.lk](http://www.lib.mrt.ac.lk)

### 3.4.5 Implementing the flow distribution

- First Row, Last Column of the Grid space are avoided from sediment transfer quantity computations.
- The following cases are identified in the area other than the avoided region as specified above.

▪ General Case

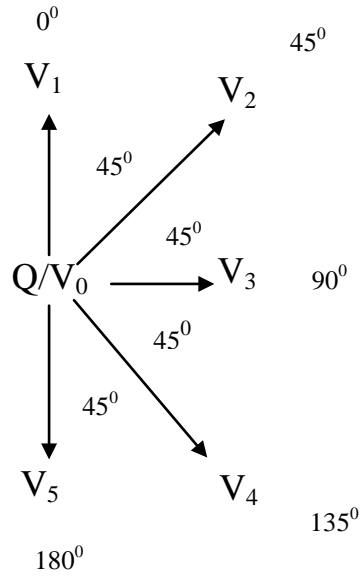
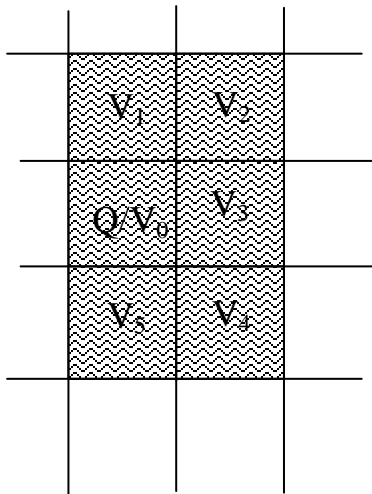


**Figure 3.18:** General Case

▪ Corner starting Column, middle cell

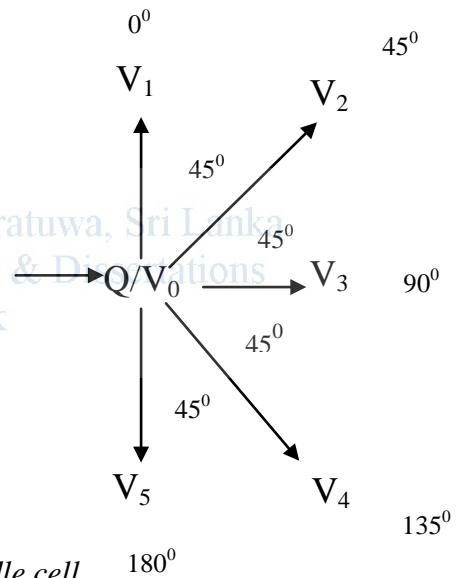
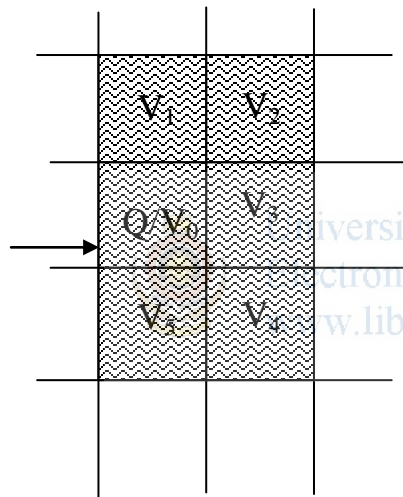


**Figure 3.19:** Corner starting Column, middle cell

▪ Corner Starting Column, Lower Cell

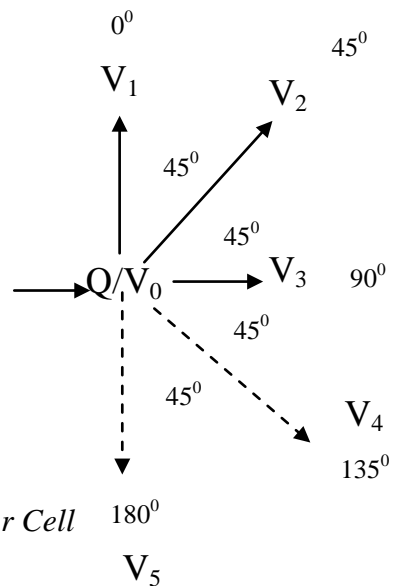
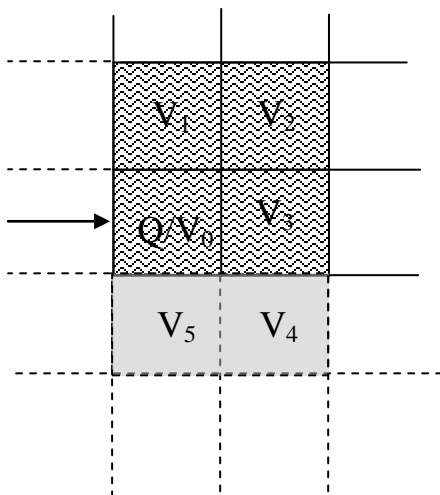


**Figure 3.20:** Corner Starting Column, Lower Cell



▪ Corner Middle Column, Lower Cell

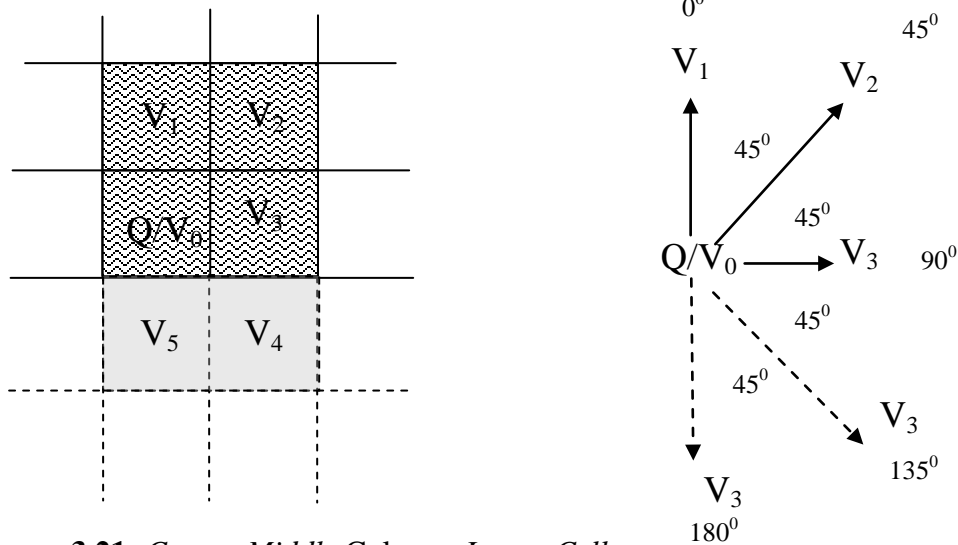


**Figure 3.21:** Corner Middle Column, Lower Cell

3.4.6.1 Methodology of solution

From the considered Cell, the flow of sediment is distributed to surrounding cells on the condition where bathymetry depth value ( $V$ ) is same or higher than the value of the cell. Depending on the cell value and the angle, a co-efficient of distribution is created to each direction. In this researched Sand transport Model, with use of special Technique, Sand Transport is modelled mainly along the Bathymetry streamlines. Calculated values are equally transferred to adjacent cells, updating the bathymetry value. The following array is used for each cell to compute the co-efficient of distribution.

Array structure to be defined:

Offset	
Angle	
Bathymetry Value ( $V$ )	
$(V - V_0)$	
If positive $1/(V - V_0)^n (x)$	
Proportioned $x$ by Total : $y$	
Distributed $Q (y * Q * T_u)$	

**Figure 3.22:** Structure for Flow\_Distributig\_Array

$T_u$  - Bathymetry Update Interval

#### 3.4.6.1.1 Offset

It is the offset of the system Array (**Flow\_Distributing\_Array**). It ranges from 0 to 180 to support the worst case with cells being with lower elevation than the considered cell.

#### 3.4.6.1.2 Angle

Angle is considered from 0 – 180 towards the direction of wave propagation. Only those directions where there's a possibility of sediment transfer are fed into the array.

#### 3.4.6.1.3 Bathymetry Value

Bathymetry depth for each corresponding cell is stored against the angle. First, major directions are stored (0, 45, 90, 135, 180), with which intermediate values are calculated through linear regression.

#### 3.4.6.1.4 $(V - V_0)$

$V_0$  value is deducted from each bathymetry value ( $V_1, V_2, V_3, V_4, V_5$ ) and the resultant is stored. Linear Regression is used to calculate values in between.

#### 3.4.6.1.5 $1/(V - V_0)^n(x)$

For values except for negative values, inverse is calculated with the power n for the denominator. The value for n, shore **parallel dominance parameter** is sensitive for the nature of bathymetry that is considered. For a bathymetry that is not irregular in nature would suit a higher value for n so that shore parallel dominance is calculated so that cells along the true stream line is promoted and is given prominence in the process of Sand Transport. For a bathymetry that is very irregular in its basin shape, shore parallel dominance should hold a value much lesser (1.0).

#### 3.4.6.1.6 Proportioned $x$ by Total : $y$

Results from above procedure are proportioned by the total of inverse values.

#### 3.4.6.1.7 Distributed $Q (y * Q * T_u)$

Q is calculated for each direction by multiplying proportioned value with Q in the cell that is considered.

- *If angle segment 0 - 30 is present, the accumulated  $Q$  for 0 – 30 segment would be transferred and would update V1.*
- *If angle segment 30 - 60 is present, the accumulated  $Q$  for 30 – 60 segment would be transferred and would update V2.*
- *If angle segment 60 - 90 is present, the accumulated  $Q$  for 60 – 90 segment would be transferred and would update V3.*
- *If angle segment 90 - 120 is present, the accumulated  $Q$  for 90 – 120 segment would be transferred and would update V4.*
- *If angle segment 120 - 150 is present, the accumulated  $Q$  for 120 – 150 segment would be transferred and would update V5.*
- *If angle segment 150 - 180 is present, the accumulated  $Q$  for 150 – 180 segment would be transferred and would update V6.*

With the above methodology, most of sediment will be transferred to the cell where bathymetry elevation is along the **same streamline**. With this methodology flow distribution would coincide with contours of the bathymetry. With linear distribution of flow to each direction, sediments would be modelled in more realistic manner than any other method.

*Algorithm 3.10: flow\_distribution*

Resources: *qArray ,zArray*

System Variables used: *To be specified by the user*

*Bathymetry\_Update\_Interval*: Time interval during which a particular model run is carried out.

*residual\_control\_value*: Parameter which would control the lowest value for the residual that is calculated when sediment quantity difference is quantified amongst cells. This parameter more or less would have influence on promoting wave direction towards the streamlines.

*beachslope\_ControlValue*: In order to differentiate between shoreline structures (Breakwaters, Piers, Groynes) from typical beaches, this parameter is introduced. For a particular bathymetry created with shoreline structures, user should specify a value

for this system variable. All the points along the shoreline where beach slope is lesser than this amount, can be subjected to erosion.

*n, shore parallel dominance parameter:* The value for *n*, shore parallel dominance parameter is sensitive for the nature of bathymetry that is considered. For a bathymetry that is not irregular in nature would suit a higher value for *n* so that shore parallel dominance is calculated greater than for the other directions. For a bathymetry that is very irregular in its basin shape, shore parallel dominance should hold a value much lesser (1.0).

*Initialize Flow\_Distributing\_Array with 6 rows of 181 elements in each.*

*Obtain Bathymetry\_Update\_Interval as a system parameter*

*Model\_Interval = Bathymetry\_Update\_Interval*

*For column\_index = 0 to max\_columns - 2*

*Begin*

*Obtain row\_number of the firstly found landward boundary along the column*

*For row\_index = 1 to row\_number*

*Begin*

*Do Case*

*Case: Cell is at starting column at the middle and at lower boundary*

*Begin*

*Store Flow\_Distributing\_Array with bathymetry values of surrounding Cells ( $V_1 - V_5$ )*

*Calculate ( $V - V_0$ ) for each direction ( $0^\circ, 45^\circ, 90^\circ, 135^\circ, 180^\circ$ )*

*Interpolate between values and make a distribution for each angle within the valid range. (Linear Regression)*

*For each positive value*

*Begin*

*If ( $V - V_0$ ) < residual\_control\_value then*

*Replace ( $V - V_0$ ) with residual\_control\_value*

*End if*

*Obtain  $1/(V - V_0)^n$ :  $x$*

*End for*

*Calculate sum of  $x$ , (Sum of  $1/(V - V_0)^n$ )*

*For each Positive value*

*Obtain proportioned value of x*

$$y = x * qArray[column\_index, row\_index] * Model\_Interval$$

*End for*

*Sum up Sediment flow for each segment:  $0^0 - 30^0, 30^0 - 60^0, 60^0 - 90^0, 90^0 - 135^0, 135^0 - 180^0$*

*For each direction*

*If  $V \leq V_0$  then*

*Transfer Sediment // **Note:** Deduct value from target cell, and Source Cell value remains unchanged*

*End if*

*End for*

*End*

*Case: Cell is at Middle Column or at Lower boundary/Cell is at end column middle or at lower boundary*



*Store **Flow\_Distributing\_Array** with bathymetry values of surrounding Cells ( $V_1 - V_5$ )*

*Calculate  $(V - V_0)$  for each direction ( $0^0, 45^0, 90^0, 135^0, 180^0$ )*

*Interpolate between values and make a distribution for each angle within the valid range. (Linear Regression)*

*For each positive value*

*Begin*

*If  $V < residual\_control\_value$  then*

*Replace the value with residual\_control\_value*

*End if*

*Obtain  $1/(V - V_0)^n : x$*

*End for*

*Calculate sum of  $1/(V - V_0)^n$*

*For each Positive value*

*Obtain proportioned value of x*

$$y = x * qArray[column\_index, row\_index] * Model\_Interval$$

*End for*

*Sum up Sediment flow for each segment:  $0^0 - 30^0, 30^0 - 60^0, 60^0 - 90^0, 90^0 - 135^0, 135^0 - 180^0$*

```

    For each direction
    If  $V \leq V_0$  then
        Transfer Sediment // Note: Deduct value from target
        cell, and add transferred value to the source Cell value
    End if
    End for
    End
    End Case
    End For
End For
Update Corner end column  $col\_index = (max\_columns - 1)$  values with  $col\_index =$ 
 $(max\_columns - 2)$  values
Update  $row\_index = 0$  values with  $row\_index = 1$  values
// In order to account for shore-erosion the following procedure is carried out for all
the points defining the shoreline boundary
For each element in shoreLine array
    Obtain relevant beach slope from beachSlope array
    If beachSlope  $\leq$  beachslope_ControlValue Then
        Obtain  $z$  value of point at shoreline
         $\Delta Diff = beachSlope * \Delta y$ 
        //Consider a grid as shown in figure 3.7
         $Old\_Average = \Delta Diff + V_0$ 
        //As method shown in algorithm 3.2 calculate New_Average of
        surrounding cells, Note: Consider Starting Cell Grid as shown in
        figure 3.7
        If New_Average  $>$  Old_Average then
            Distribute (Transfer) from Land (From Cells in the first Row at
            Landward boundary) the difference:  $New\_Average -$ 
             $Old\_Average$  in proportion of selected cell values // cells of
            which values are considered to calculate the average depth
            value
        End if
    End if
End for

```

**IMPORTANT:** When Bathymetry Values (**zArray[i,j]** values) are updated, the new transferred value should be deducted from the available value, since the model uses values below sea level as positive.

### 3.4.6 Main Algorithm

*Begin*

*Through ArcView obtain point theme of bathymetry data*

*Incorporate shoreline structures*

*Generate surface with realistic surface generation parameters*

*Export with ASCII grid format*

*Initialize zArray with grid capacity*

*Read Exported file with and update zArray //Listing 2.6 , 2.5 , 2.4*

*Input values for system variables:*

*Bathymetry\_Update\_Interval*

*M.S.L.*

*Obtain delta x, delta y from ASCII grid file*

*residual\_control\_value*

*beachslope\_ControlValue*

*n, shore parallel dominance parameter*

*Read external series of offshore wave climate*

*For each offshore wave climate*

*Begin*

*Do Case:*

*Case: offshore direction is positive  $0^{\circ} < \alpha < 180^{\circ}$*

*ScanShore*

*Compute\_Beach\_Slope*

*Celerity\_Generation*

*alpha\_generation*

*refraction\_generation*

*diffraction\_generation*

*store\_breaking\_zone*

*apply\_Combined\_refraction\_and\_diffraction*

*flow\_calculation*

*flow\_distribution*

*End*

*Case: offshore direction is negative  $0^\circ > \alpha > -180^\circ$*

*Obtain mirror image of zArray and consider offshore direction as positive*

*ScanShore*

*Compute\_Beach\_Slope*

*Celerity\_Generation*

*alpha\_generation*

*refraction\_generation*

*diffraction\_generation*

*store\_breaking\_zone*

*apply\_Combined\_refraction\_and\_diffraction*

*flow\_calculation*

*flow\_distribution*

*Obtain mirror image of zArray*

*End*

*End for*

*Write zArray into ASCII Grid format*

*Update bathymetry graph via ArcView*

- Use Updated Bathymetry, and next offshore wave climate parameters to start the process from the very beginning.
- After pre-defined period for the sediment transformation the model-run should be aborted and new bathymetry values (**zArray**) should be written to ASCII grid format.
- With ArcView GIS platform the new surface with the new shoreline would be visible through Grid-Surface.

**NOTE:** To run the model, the bathymetry has to be setup with Sea at the upper boundary of the grid and land being at the lower boundary of the grid.



### 3.4.7 Technical guidelines for the development of *SanPro*

#### 3.4.8.1 Flow chart of *SandPro*

- Identification of theories and numerical solutions for the whole process
- Validity of theories behind the period for which the entire process is implemented
- Reliability of theories and the degree of suitability for the real-world implementation of *SandPro*
- Overall design for data flow between elements
- Decomposition of the whole process
- Detailed design of each process
- Design and Analysis of each modularized process
- Walkthrough the design
- Nature of development (Isolated program or As a part of another application platform)
- Coding and Testing (Development)
- Development *As identified*
- Develop *SandPro* as a part of ArcView GIS engine
  - Develop Dynamic Link Libraries for each modularized process
  - Develop avenue modules for internal data processing
    - Input data
    - Surface interpolation and create bathymetry
    - Defining Structures and other coastal elements alongshore
  - Create customized GUI through ArcView GIS and Invoke Win 32 Library APIs for external operations
  - Test the development with number of testing data
  - Determine how realistic the results are
  - Fine-tune the design
  - Sensitivity Analysis and determine global system variables
  - Revise the development
  - Modify the GUI to make the program consider about System dependant variables

- Once the development proves to be reliable and suitable in its results, incorporate all functionality and carry out an isolated design

#### 3.4.8.2. Discussion

Equations identified by Kamphuis (1992) for modelling of sediment transport model here are based on empirical co-relations and dimensional analysis of properties. The form that is interpreted is directly used in the numerical calculations of quantities of coastal processes. Since the form of equation can be directly used in the form of numerical equations, algorithm designed for the process has used equations as they are mentioned in the thesis.

The equations used in *SandPro* have been developed eliminating many drawbacks in other sediment transport models that had been carried out so far. Details and a comparison with other available equations are described at Literature Review at section 3.2.

The original raw data of bathymetry surveys are of high importance. Hydrographic survey or digitizing the bathymetry charts has to be done very accurately such that irregularities of the sea bed are reflected within the data that is used for surface generation of the bathymetry. For the ease of development during first stages, bathymetry could be prepared using *Surfer Ver 7.0*. Many surface generating algorithms could be attempted to select the best option to suit the data existing. Preferred option that can be used is *kriging*. Structures that are to be built or had been built should be defined along with the bathymetry it self as a part of the shoreline boundary. With the aid of tools of *Surfer* or with use of scripting, these could be defined. It is important to make sure that the slope of the shoreline, where shoreline structures are defined, are significantly different from general beach slope to slopes existing, where structures (breakwaters, groynes, piers, jetties etc) are located.

As one possible option, the exported *ASCII* Grid output could be taken for the testing of the program. (**Note:** File reading algorithm has to be modified according to the specific *ASCII* grid output that is produced by *Surfer Ver 7.0*.) With invoking all the procedures, the final bathymetry could be updated back in *ASCII* Grid format and could be viewed with *Surfer*.

The other alternative is to customize ArcView GIS engine and use avenue scripting to input bathymetry data and invoke surface interpolation though the general method. The GUI could be customized such that user interaction could be

incorporated and shoreline structures could be defined methodically will full control over bathymetry. Sediment Transportation modeling could be executed within avenue scripting through *dll* calling, and final bathymetry could be updated back from results of modelling taken in memory.

The bathymetry layout provided as an input parameter should conform to several assumptions.

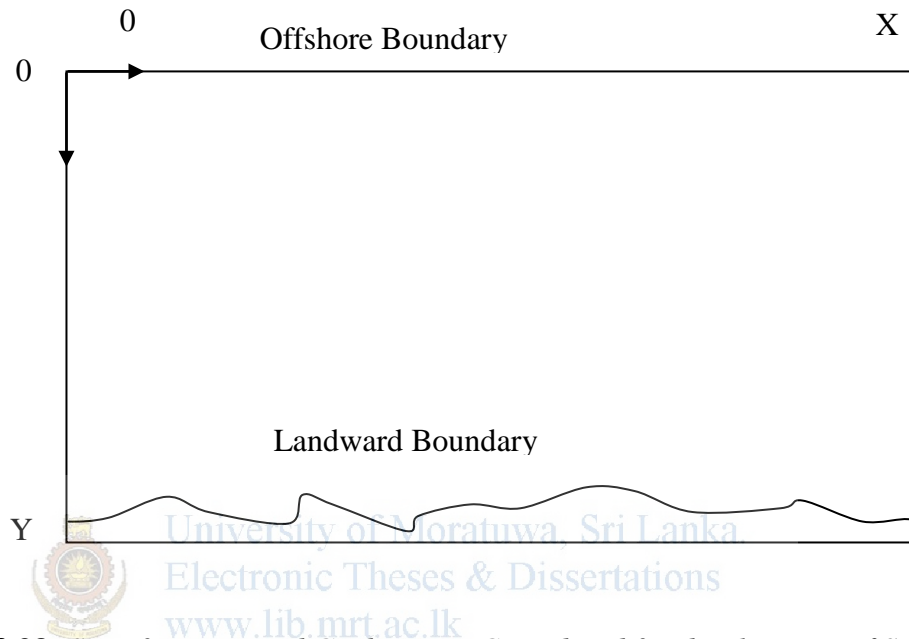


**Figure 3.23:** *Specifications and Grid Layout Considered for development of SandPro*

As shown in the figure, axis of the grid should be as specified, Offshore Boundary should be at  $y = 0$  boundary, while Landward boundary should be at other side of the grid space. At  $y = 0$  column shore boundary should appear and up to the other corner column along the grid space.

Across the grid space land values are of negative amounts while below M.S.L. values are positive. Isolated land values shouldn't appear in offshore region, as the model at current stage is not dealing with situations with islands.

During testing of the model, test cases have to be defined such that the range of tolerance can be determined in order to identify points of diffraction. With current design, the grid space defined is of static nature and angle of tolerance determined and the number of points considered in order to obtain shoreline gradient (3) have to be dependant with the resolution selected for the grid space in the next stage of development when it changes from static nature to dynamic nature.

Sufficient test cases have to be defined and implemented to determine ranges of values and influence on the results. Each model dependant variable is detailed at each relevant module.



University of Moratuwa, Sri Lanka.  
Electronic Theses & Dissertations  
[www.lib.mrt.ac.lk](http://www.lib.mrt.ac.lk)

## CHAPTER – 4



University of Moratuwa, Sri Lanka.  
Electronic Theses & Dissertations  
[www.lib.mrt.ac.lk](http://www.lib.mrt.ac.lk)

# NUMERICAL MODELLING – CASE STUDY – PROPOSED HARBOUR AT THE NEGOMBO LAGOON

## **4.0 Numerical Modelling –Case Study – Proposed Harbour Layout at Negombo Lagoon**

### **4.1 Introduction**

Negombo is a major town in the coastal zone developing rapidly. Its main economic activities fishery and tourism need to be developed in a systematic way to avoid certain adverse effects to various other sub systems in the environment. In such projects, many alternatives are assessed to determine answers to 'What', 'why' and 'how' in a formal study process known as Environmental Impact Assessment (EIA).

The closest major town to the country's only international Airport, Negombo serves as the hub for the tourist industry. Nevertheless, the majority of the population is still dependants on the fishery industry. Thus, the need to cater the contrasting requirements of two industries in two extreme directions is a challenging task to be induced especially when the rate of development is very high and almost beyond controllable limits.



University of Moratuwa, Sri Lanka.  
Electronic Theses & Dissertations  
[www.lib.mrt.ac.lk](http://www.lib.mrt.ac.lk)

#### **4.1.1. Need for Development**

Any development project will incur a large amount of costs in terms of money, time and labour. Thus, before commencing any project, it is necessary to evaluate the need of the project, which enables the correct focus of the project to satisfy the needs and thereby to come up with the most appropriate and cost effective design.

Hence, the following aspects need to be given careful consideration

- Due to difficulties in mooring closer to the markets, some fishermen are compelled to tie them in the Hamilton Canal, which aggravates the problems.
- Fishery industry is developing rapidly
- There are over 3000 boats and yet no organized places to moor the boats.
- Mooring of boats at the mouth of the lagoon is causing lot of problems to the lagoon in terms of its marine environment and ecological environment.

- The two main bridges block the entering of large vessels (multi-day boats) into the lagoon, hence the fiber boats are being anchored even in the middle of the lagoon disabling the lagoons' beauty and usage for any other purpose.
- Most fishermen use only temporary piers and these cause additional problems of safety, hindering beauty and wastage.
- There is a great potential to develop the industry to increase the nation's productivity and at the same time use the available resources to provide employment opportunities.
- Avoid the conflict of interests between the two industries (Tourism and Fishery) trying to utilize the same resources.
- Give sufficient space to the tourism industry and recreational facilities like water sports, boat rides, bathing, etc.
- At present all types of boats (multi- day, single day, fiber, motored, oared and sailed boats) are being moored together even though their requirements for space and depths vary from one to the other.
- Specially, the moorage right at the mouth of the lagoon affects the special species and plants in that zone and the sea-lagoon interactions.
- High concentration of human settlement at the lagoon entrance is causing problems
- Excessive human settlement causes encroachment of the lagoon thereby further narrowing the entrances.
- Negombo has no rain forests. Thus mangrove islands are a precious asset.
- Unhygienic practices of the fisher folk causing lot of environmental problems. Specially the use of the beach as the toilet.
- Need to develop the whole sale market and may be to process fish for export, etc.

These factors suggest the importance of regulating the activities of the fishery industry, which will benefit both the fishery industry and others as well.

#### 4.1.2. Introduction to Alternatives

With the data available about the present activities, it has been strongly recommended that there should be some regulation of activities in the area to avoid wastage and other prevailing problems and those, which may be faced in the future.

Nevertheless, the development proposal should have an advantage positive balance in a Cost – Benefit analysis. Therefore it is necessary to analyze and critically assess the feasibility of any proposals not only in financial terms but also in other long term and non-quantifiable impacts.

Thus, having considered many alternatives, which were believed to be feasible, the following one is considered for the technical feasibility.

#### 4.1.3 Alternative: Construction of Breakwaters and Associated Facilities at Morawala



**Figure 4.1:** *Proposed Fisheries Harbour at Morawala*

*Source: Sri Lanka Fisheries sector Project – HR Wallingford, UK*



## 4.2 Data Review and Analysis

### 4.2.1 Data collection

Numerous reports have been collated and reviewed during the initial stages of the project. The following section describes the data found and reviewed.

#### 4.2.1.1 Bathymetry and Topography

Regional bathymetry data were obtained from Admiralty Charts no. 813, 3700 3265 1587 and 1583. Detailed bathymetry close to the proposed fishing harbour area was obtained from existing Ceylon Fishery Harbour Corporation (CFHC) surveys carried out prior to 2000 and new surveys undertaken by the National Hydrographic Office -National Aquatic Resources Research and Development Agency (NARA) on behalf of CFHC in 2001. The results of the recent bathymetry and topography survey carried out for Hambantota are contained on drawing numbers MISC 003/01 (1:5000) and MISC 008/02 (1:1000) surveyed between September and November 2001 which was used in the case study. In all cases a digitizer was used to convert the data to ASCII format, after which regular depth grids of varying mesh sizes were created by applying a surface-fitting algorithm to the depth data. Details of the specific grids used for the wave models are given in the following sections.

#### 4.2.1.2 Water Level Data

Predicted water levels relative to Admiralty Chart Datum were obtained from Admiralty Tide Tables Volume 3 (2001). Proposed Negombo fishery harbour is located close to Negombo Bay, which is towards north from the Admiralty Standard Ports of Colombo. The water levels at Negombo were obtained from applying published Admiralty Secondary Port corrections to the water level data at Colombo. These are summarized in Table 4.1 below.

<b>Tide Level</b>	<b>Predicted Water Level (m above CD)</b>
Mean High Water Springs (MHWS)	0.6
Mean High Water Neaps (MHWN)	0.4
Mean Sea Level (MSL)	0.4
Mean Low Water Neaps (MLWN)	0.3
Mean Low Water Springs (MLWS)	0.1

**Table 4.1:** *Predicted water levels*

#### 4.2.1.3 Wave Data

The near-shore wave climate at Negombo is influenced by two distinct wave systems. Swell waves are generated in the deep sea of the Indian Ocean and have propagated out of the generating area to the Negombo region. These waves exhibit typically long wave periods and are more or less unidirectional. Sea waves are generated by the local wind fields and have wave periods less than the swell waves. In contrast to swell waves, sea waves occur from a variety of directions.

The directional distribution of sea and swell wave conditions outside the Negombo area were established from four different sources:

- Directional wave statistics were available from a directional wave climate study covering the south west coast of Sri Lanka carried out by the Coast Conservation Department (CCD) under a German Technical Cooperation (GTZ) programme based on wave measurements conducted using a WAVEC type pitch and roll buoy in 70m water depth offshore of Galle for the periods February 1989 -August 1992 and May 1994 –September 1995.
- Non-directional wave measurements conducted by LHI for SLPA in approximately 20m water depth off Galle harbour, over intermittent periods during 1984 -1986 and on a continuous basis during September 1988 -August 1995.

#### *4.2.1.4 Preliminary Analysis of Off-shore Wave Data*

The CCD-GTZ data set was obtained in electronic format from Lanka Hydraulic Institute in the form of ASCII files of wave height, period, and direction. Analysis of this data was undertaken to show the percentage distribution of offshore waves with direction and period for overall waves, as well as for the sea and swell components separately.

Table 4.2 shows the distribution of the overall wave climate by direction and Table 4.3 shows the distribution of the overall wave climate by period.



University of Moratuwa, Sri Lanka.  
Electronic Theses & Dissertations  
[www.lib.mrt.ac.lk](http://www.lib.mrt.ac.lk)

Wave Height (m)	Wave Direction (degrees)											
	0 – 30	30 – 60	60 – 90	90 – 120	120 – 150	150 – 180	180 – 210	210 – 240	240 – 270	270 – 300	300 – 330	330 – 360
0.00 – 0.25	0.02	0	0	0.01	0	0	0	0	0	0	0	0
0.25 – 0.50	0	0	0	0	0	0	0	0.03	0.01	0	0	0
0.50 – 0.75	0	0	0	0	0.25	1.13	0.92	0.24	0.02	0	0	0
0.75 – 1.00	0	0	0	0.05	1.78	5.16	3.91	1.05	0.22	0.02	0	0
1.00 – 1.25	0.01	0	0.01	0.20	2.68	6.73	4.74	1.34	0.68	0.08	0.02	0
1.25 – 1.50	0.01	0	0.02	0.22	1.61	2.55	5.21	2.07	1.41	0.18	0.02	0.02
1.50 – 1.75	0	0	0	0.05	0.23	0.55	4.93	2.97	1.24	0.12	0.02	0
1.75 – 2.00	0	0	0	0.01	0.03	0.20	4.64	5.23	1.70	0.02	0	0
2.00 – 2.25	0	0	0	0	0	0.26	3.94	5.51	2.40	0.06	0	0
2.25 – 2.50	0	0	0	0	0	0.25	2.73	4.45	3.15	0.17	0	0
2.50 – 2.75	0	0	0	0	0	0.02	1.07	2.69	2.05	0.13	0	0
2.75 – 3.00	0	0	0	0	0	0	0.43	1.31	0.98	0.06	0	0
3.00 – 3.25	0	0	0	0	0	0	0.17	0.43	0.47	0.09	0	0
3.25 – 3.50	0	0	0	0	0	0	0.01	0.12	0.16	0.06	0	0
3.50 – 3.75	0	0	0	0	0	0	0	0.05	0.05	0.02	0	0
3.75 – 4.00	0	0	0	0	0	0	0	0.01	0.02	0	0	0
4.00 – 4.25	0	0	0	0	0	0	0	0	0.04	0.01	0	0
4.25 – 4.50	0	0	0	0	0	0	0	0	0	0.02	0	0
4.50 – 4.75	0	0	0	0	0	0	0	0	0	0	0	0
4.75 – 5.00	0	0	0	0	0	0	0	0.02	0	0	0	0
5.00 – 5.25	0	0	0	0	0	0	0	0.02	0.01	0	0	0
5.25 – 5.50	0	0	0	0	0	0	0	0	0	0	0	0
5.50 – 5.75	0	0	0	0	0	0	0	0	0	0	0	0
5.75 – 6.00	0	0	0	0	0	0	0	0	0	0	0	0
<b>Total</b>	<b>0.03</b>		<b>0.03</b>	<b>0.54</b>	<b>6.58</b>	<b>16.85</b>	<b>32.70</b>	<b>27.53</b>	<b>14.62</b>	<b>1.03</b>	<b>0.07</b>	<b>0.02</b>

Numbers refer to 3hr wave records

**Table 4.2:** Percentage distribution of CCD-GTZ overall wave data by direction sector

Wave Height (m)	Wave Period (seconds)											
	0 - 1	1 - 2	2 - 3	3 - 4	4 - 5	5 - 6	6 - 7	7 - 8	8 - 9	9 - 10	10 - 11	11 - 12
0.00 – 0.25	0.02	0	0	0.01	0	0	0	0	0	0	0	0
0.25 – 0.50	0	0	0	0	0	0	0	0	0.02	0.02	0	0
0.50 – 0.75	0	0	0	0.12	0.63	0.92	0.67	0.16	0.06	0	0	0
0.75 – 1.00	0	0	0	0.15	2.53	4.26	2.88	1.74	0.58	0.02	0	0
1.00 – 1.25	0	0	0	0.02	2.19	6.05	4.15	2.68	1.07	0.33	0	0
1.25 – 1.50	0	0	0	0	1.27	5.44	2.78	2.15	1.20	0.28	0.17	0.02
1.50 – 1.75	0	0	0	0	0.45	4.13	3.56	1.15	0.43	0.31	0.07	0.01
1.75 – 2.00	0	0	0	0	0.07	3.51	6.35	1.43	0.25	0.14	0.04	0.02
2.00 – 2.25	0	0	0	0	0.01	1.63	7.07	2.79	0.56	0.08	0	0.02
2.25 – 2.50	0	0	0	0	0	0.61	5.42	3.81	0.86	0.02	0	0.01
2.50 – 2.75	0	0	0	0	0	0.36	2.64	2.19	0.76	0.03	0	0
2.75 – 3.00	0	0	0	0	0	0.09	1.25	0.85	0.54	0.05	0	0
3.00 – 3.25	0	0	0	0	0	0.01	0.56	0.42	0.17	0.01	0	0
3.25 – 3.50	0	0	0	0	0	0.02	0.20	0.10	0.03	0.0	0	0
3.50 – 3.75	0	0	0	0	0	0	0.09	0.02	0.01	0.01	0	0
3.75 – 4.00	0	0	0	0	0	0	0	0.03	0	0	0	0
4.00 – 4.25	0	0	0	0	0	0	0.02	0.03	0	0	0	0
4.25 – 4.50	0	0	0	0	0	0	0.01	0.01	0	0	0	0
4.50 – 4.75	0	0	0	0	0	0	0	0	0	0	0	0
4.75 – 5.00	0	0	0	0	0	0	0	0.01	0.01	0	0	0
5.00 – 5.25	0	0	0	0	0	0	0	0.01	0.02	0	0	0
5.25 – 5.50	0	0	0	0	0	0	0	0	0	0	0	0
5.50 – 5.75	0	0	0	0	0	0	0	0	0	0	0	0
5.75 – 6.00	0	0	0	0	0	0	0	0	0	0	0	0
<b>Total</b>	<b>0.02</b>	<b>0</b>	<b>0</b>	<b>0.31</b>	<b>7.15</b>	<b>27.04</b>	<b>37.66</b>	<b>19.58</b>	<b>6.56</b>	<b>1.32</b>	<b>0.27</b>	<b>0.09</b>

Number refer to 3hr wave records

**Table 4.3:** Percentage distribution of CCD-GTZ overall wave data by wave period

In addition, analysis was undertaken to investigate how the off-shore wave climate varied with season. The wave climate was broken down into four seasons in accordance with previous studies as follows:

1. The South-West monsoon (SW) – from May to September;
2. The first Inter-monsoon (IM1) – from October to November;
3. The North-East monsoon (NE) – from December to February;
4. The Second Inter-monsoon (IM2) – from March to April.

The conclusion from the analysis of the CCD-GTZ offshore wave data was:

- a) Analysis of the data set into monsoon periods has highlighted very few waves in the NW or NE direction sectors for the NE monsoon period. It has therefore been concluded that this data set does not accurately represent the NE monsoon period and hence it should not be used to derive typical wave climates at the proposed harbour for the NE monsoon period.
- b) The original data files and the precise position of the wave rider buoy were not available from CCD or LHI. Therefore it has not been possible to check the raw ASCII data files received from LHI and hence there is no way of assuring these files are correct or have not been filtered in anyway during their previous analysis.
- c) The wave climate for the SW monsoon is predominantly from the 150-300 degree sectors. There are a very small proportion of the waves, which are generated between 300 – 360 degrees but the wave height is relatively small ( $< 1.5$  m) . Hence these have been ignored for all subsequent wave modeling since they are not capable of having a significant impact on the final derived wave climates at Negombo.

Wave Height (m)	Wave Direction (degrees)											
	0 - 30	30 - 60	60 - 90	90 - 120	120 - 150	150 - 180	180 - 210	210 - 240	240 - 270	270 - 300	300 - 330	330 - 360
0.00 – 0.25	0.03	0	0	0.02	0	0	0.02	0	0	0	0	0
0.25 – 0.50	0	0	0	0	0	0	0	0.06	0.03	0	0	0
0.50 – 0.75	0	0	0	0	0	0	0	0	0	0	0	0
0.75 – 1.00	0	0	0	0	0	0.05	0.09	0	0	0	0	0
1.00 – 1.25	0	0	0	0	0	0.39	0.94	0.39	0.26	0	0	0
1.25 – 1.50	0	0	0	0	0	0.26	2.07	1.46	1.78	0	0	0
1.50 – 1.75	0	0	0	0	0	0.26	4.29	3.62	1.77	0	0	0
1.75 – 2.00	0	0	0	0	0	0.21	6.99	8.88	2.90	0.02	0	0
2.00 – 2.25	0	0	0	0	0	0.45	6.67	10.01	4.29	0.08	0	0
2.25 – 2.50	0	0	0	0	0	0.45	4.65	8.18	5.74	0.26	0	0
2.50 – 2.75	0	0	0	0	0	0.05	1.98	4.89	3.73	0.23	0	0
2.75 – 3.00	0	0	0	0	0	0	0.95	2.94	2.17	0.14	0	0
3.00 – 3.25	0	0	0	0	0	0	0.50	1.42	1.28	0.32	0	0
3.25 – 3.50	0	0	0	0	0	0	0.08	0.35	0.48	0.29	0	0
3.50 – 3.75	0	0	0	0	0	0	0	0.12	0.14	0.05	0	0
3.75 – 4.00	0	0	0	0	0	0	0	0.03	0.06	0.05	0	0
4.00 – 4.25	0	0	0	0	0	0	0	0	0.06	0.03	0	0
4.25 – 4.50	0	0	0	0	0	0	0	0	0.02	0.05	0	0
4.50 – 4.75	0	0	0	0	0	0	0	0	0	0	0	0
4.75 – 5.00	0	0	0	0	0	0	0	0.03	0	0	0	0
5.00 – 5.25	0	0	0	0	0	0	0	0.03	0.02	0	0	0
5.25 – 5.50	0	0	0	0	0	0	0	0	0	0	0	0
5.50 – 5.75	0	0	0	0	0	0	0	0.02	0	0	0	0
5.75 – 6.00	0	0	0	0	0	0	0	0	0	0	0	0
<b>Total</b>	<b>0</b>	<b>0</b>	<b>0</b>	<b>0</b>	<b>0</b>	<b>2.11</b>	<b>29.21</b>	<b>72.44</b>	<b>24.71</b>	<b>1.48</b>	<b>0</b>	<b>0</b>

Number refer to 3hr wave records

**Table 4.4:** Percentage distribution of CCD-GTZ overall wave data by direction for SW monsoon

Wave Height (m)	Wave Direction (degrees)											
	0 – 30	30 - 60	60 - 90	90 - 120	120 - 150	150 - 180	180 - 210	210 - 240	240 - 270	270 - 300	300 - 330	330 - 360
0.00 – 0.25	0	0	0	0	0	0	0	0	0	0	0	0
0.25 – 0.50	0	0	0	0	0	0	0	0	0	0	0	0
0.50 – 0.75	0	0	0	0	0	0.16	0.6	1.20	0.11	0	0	0
0.75 – 1.00	0	0	0	0	0	2.73	4.15	4.59	0.93	0	0	0
1.00 – 1.25	0	0	0	0.16	0.77	8.47	6.23	3.99	2.30	0.16	0	0
1.25 – 1.50	0	0	0	0	0.6	4.15	11.53	5.41	2.30	0.38	0	0
1.50 – 1.75	0	0	0	0	0.05	1.26	11.86	5.68	2.08	0.60	0.11	0
1.75 – 2.00	0	0	0	0	0.05	0.38	4.32	2.95	1.15	0.05	0	0
2.00 – 2.25	0	0	0	0	0	0.05	1.75	1.04	0.98	0.05	0	0
2.25 – 2.50	0	0	0	0	0	0	1.26	0.55	0.66	0.16	0	0
2.50 – 2.75	0	0	0	0	0	0	0.05	0.55	0.66	0.05	0	0
2.75 – 3.00	0	0	0	0	0	0	0	0.11	0.22	0	0	0
3.00 – 3.25	0	0	0	0	0	0	0	0.05	0.05	0	0	0
3.25 – 3.50	0	0	0	0	0	0	0	0	0	0	0	0
3.50 – 3.75	0	0	0	0	0	0	0	0	0.05	0	0	0
3.75 – 4.00	0	0	0	0	0	0	0	0	0.11	0	0	0
4.00 – 4.25	0	0	0	0	0	0	0	0	0.05	0	0	0
4.25 – 4.50	0	0	0	0	0	0	0	0	0	0	0	0
4.50 – 4.75	0	0	0	0	0	0	0	0	0.05	0	0	0
4.75 – 5.00	0	0	0	0	0	0	0	0	0	0	0	0
5.00 – 5.25	0	0	0	0	0	0	0	0	0	0	0	0
5.25 – 5.50	0	0	0	0	0	0	0	0	0	0	0	0
5.50 – 5.75	0	0	0	0	0	0	0	0	0	0	0	0
5.75 – 6.00	0	0	0	0	0	0	0	0	0	0	0	0
<b>Total</b>	<b>0</b>	<b>0</b>	<b>0</b>	<b>0.16</b>	<b>1.48</b>	<b>17.21</b>	<b>41.75</b>	<b>26.12</b>	<b>11.69</b>	<b>1.48</b>	<b>0.11</b>	<b>0</b>

Number refer to 3hr wave records

**Table 4.5:** Percentage distribution of CCD-GTZ overall wave data by direction for NE monsoon



Wave Height (m)	Wave Direction (degrees)											
	0 – 30	30 – 60	60 – 90	90 – 120	120 – 150	150 – 180	180 – 210	210 – 240	240 – 270	270 – 300	300 – 330	330 – 360
0.00 – 0.25	0	0	0	0	0	0	0	0	0	0	0	0
0.25 – 0.50	0	0	0	0	0	0	0	0	0	0	0	0
0.50 – 0.75	0	0	0	0	1.23	5.11	3.69	0.44	0.08	0	0	0
0.75 – 1.00	0	0	0	0.24	8.49	17.05	8.60	1.47	0.36	0.08	0	0
1.00 – 1.25	0.04	0	0.04	0.87	11.62	14.04	4.48	1.31	0.79	0.28	0.12	0
1.25 – 1.50	0.04	0	0.12	1.11	6.82	4.56	1.94	0.63	0.40	0.59	0.08	0.08
1.50 – 1.75	0	0	0	0.24	1.07	0.59	0.48	0.16	0	0.12	0.04	0
1.75 – 2.00	0	0	0	0.04	0.12	0.04	0.20	0.04	0	0	0	0
2.00 – 2.25	0	0	0	0	0	0	0.04	0	0	0.04	0	0
2.25 – 2.50	0	0	0	0	0	0	0	0	0	0	0	0
2.50 – 2.75	0	0	0	0	0	0	0	0	0	0	0	0
2.75 – 3.00	0	0	0	0	0	0	0	0	0	0	0	0
3.00 – 3.25	0	0	0	0	0	0	0	0	0	0	0	0
3.25 – 3.50	0	0	0	0	0	0	0	0	0	0	0	0
3.50 – 3.75	0	0	0	0	0	0	0	0	0	0	0	0
3.75 – 4.00	0	0	0	0	0	0	0	0	0	0	0	0
4.00 – 4.25	0	0	0	0	0	0	0	0	0	0	0	0
4.25 – 4.50	0	0	0	0	0	0	0	0	0	0	0	0
4.50 – 4.75	0	0	0	0	0	0	0	0	0	0	0	0
4.75 – 5.00	0	0	0	0	0	0	0	0	0	0	0	0
5.00 – 5.25	0	0	0	0	0	0	0	0	0	0	0	0
5.25 – 5.50	0	0	0	0	0	0	0	0	0	0	0	0
5.50 – 5.75	0	0	0	0	0	0	0	0	0	0	0	0
5.75 – 6.00	0	0	0	0	0	0	0	0	0	0	0	0
<b>Total</b>	<b>0.08</b>	<b>0</b>	<b>0.16</b>	<b>2.50</b>	<b>29.34</b>	<b>41.4</b>	<b>19.43</b>	<b>4.04</b>	<b>1.63</b>	<b>1.11</b>	<b>0.24</b>	<b>0.08</b>

Numbers refer to 3hr wave records

**Table 4.6:** Percentage distribution of CCD-GTZ overall wave data by direction for IM1 monsoon

Wave Height (m)	Wave Direction (degrees)											
	0 - 30	30 - 60	60 - 90	90 - 120	120 - 150	150 - 180	180 - 210	210 - 240	240 - 270	270 - 300	300 - 330	330 - 360
0.00 – 0.25	0	0	0	0	0	0	0	0	0	0	0	0
0.25 – 0.50	0	0	0	0	0	0	0	0	0	0	0	0
0.50 – 0.75	0	0	0	0	0	0.76	0.76	0	0	0	0	0
0.75 – 1.00	0	0	0	0	0.59	9.31	11.36	0.53	0	0	0	0
1.00 – 1.25	0	0	0	0	1.64	17.63	17.28	1.99	0.35	0	0	0
1.25 – 1.50	0	0	0	0	0.82	5.68	14.47	2.64	0.53	0	0	0
1.50 – 1.75	0	0	0	0	0	0.64	0.48	1.52	0.35	0	0	0
1.75 – 2.00	0	0	0	0	0	0.18	0.20	1.17	0.35	0	0	0
2.00 – 2.25	0	0	0	0	0	0	0.04	0.23	0	0	0	0
2.25 – 2.50	0	0	0	0	0	0	0	0	0	0	0	0
2.50 – 2.75	0	0	0	0	0	0	0	0	0	0	0	0
2.75 – 3.00	0	0	0	0	0	0	0	0	0	0	0	0
3.00 – 3.25	0	0	0	0	0	0	0	0	0	0	0	0
3.25 – 3.50	0	0	0	0	0	0	0	0	0	0	0	0
3.50 – 3.75	0	0	0	0	0	0	0	0	0	0	0	0
3.75 – 4.00	0	0	0	0	0	0	0	0	0	0	0	0
4.00 – 4.25	0	0	0	0	0	0	0	0	0	0	0	0
4.25 – 4.50	0	0	0	0	0	0	0	0	0	0	0	0
4.50 – 4.75	0	0	0	0	0	0	0	0	0	0	0	0
4.75 – 5.00	0	0	0	0	0	0	0	0	0	0	0	0
5.00 – 5.25	0	0	0	0	0	0	0	0	0	0	0	0
5.25 – 5.50	0	0	0	0	0	0	0	0	0	0	0	0
5.50 – 5.75	0	0	0	0	0	0	0	0	0	0	0	0
5.75 – 6.00	0	0	0	0	0	0	0	0	0	0	0	0
<b>Total</b>	<b>0</b>	<b>0</b>	<b>0</b>	<b>0</b>	<b>3.05</b>	<b>34.21</b>	<b>19.43</b>	<b>8.08</b>	<b>1.58</b>	<b>0</b>	<b>0</b>	<b>0</b>

Numbers refer to 3hr wave records

**Table 4.7:** Percentage distribution of CCD-GTZ overall wave data by direction for IM2 monsoon

### 4.3 Model Basis

The regional wave model MWAV\_REG is based on an evolution of the mild slope equation for water waves, which is described in more detail in Li (1994). It has been used in a wide range of different wave modelling applications and incorporates the effects of wave refraction, diffraction, breaking and bottom friction on a monochromatic wave field. Like MWAV\_REG the local wave model MWAV\_LOC is also based on an evolution equation of the mild slope equation for water waves (Li, 1994), but in addition also includes the effects of wave reflection off quay walls and other structures.

### 4.4 Regional Wave Modelling

The regional wave model MWAV \_REG was used for a large area to generate a wave matrix for transforming the offshore wave data to inshore. The model was set up using a 400m mesh size with 460 x 537 node points in the grid, covering an approximate area of 184km x 215km. The grid was set up by applying a surface- fitting algorithm to the Admiralty chart data for the area. The boundary conditions used were the time series of offshore wave data at Galle CCD-GTZ (70m). The layout used for the wave modelling is shown in Figure 4.3.

Offshore wave data analysis at Galle offshore 70m contour point is shown in table 4.8. Wave data are selected from all the periods of the year and the dominant direction of wave data seem to be from SW direction.

The data was analyzed by MWAVE\_FIT module of Halcrow in-house wave model.

		Wave Direction (degrees)											
		30	60	90	120	150	180	210	240	270	300	330	360
Wave height		-	-	-	-	-	-	-	-	-	-	-	-
		0	30	60	90	120	150	180	210	240	270	300	330
5.75	- 6	0.00	0.00	0.00	0.00	0.00	0.00	0.00	0.00	0.00	0.00	0.00	0.00
5.5	- 5.75	0.00	0.00	0.00	0.00	0.00	0.00	0.00	0.00	0.00	0.00	0.00	0.00
5.25	- 5.5	0.00	0.00	0.00	0.00	0.00	0.00	0.00	0.00	0.00	0.00	0.00	0.00
5	- 5.25	0.00	0.00	0.00	0.00	0.00	0.00	0.00	0.02	0.01	0.00	0.00	0.00
4.75	- 5	0.00	0.00	0.00	0.00	0.00	0.00	0.00	0.02	0.00	0.00	0.00	0.00
4.5	- 4.75	0.00	0.00	0.00	0.00	0.00	0.00	0.00	0.00	0.00	0.00	0.00	0.00
4.25	- 4.5	0.00	0.00	0.00	0.00	0.00	0.00	0.00	0.00	0.00	0.02	0.00	0.00
4	- 4.25	0.00	0.00	0.00	0.00	0.00	0.00	0.00	0.00	0.04	0.01	0.00	0.00
3.75	- 4	0.00	0.00	0.00	0.00	0.00	0.00	0.00	0.01	0.02	0.00	0.00	0.00
3.5	- 3.75	0.00	0.00	0.00	0.00	0.00	0.00	0.00	0.05	0.05	0.02	0.00	0.00
3.25	- 3.5	0.00	0.00	0.00	0.00	0.00	0.00	0.01	0.12	0.16	0.06	0.00	0.00
3	- 3.25	0.00	0.00	0.00	0.00	0.00	0.00	0.17	0.43	0.47	0.09	0.00	0.00
2.75	- 3	0.00	0.00	0.00	0.00	0.00	0.00	0.43	1.31	0.98	0.06	0.00	0.00
2.5	- 2.75	0.00	0.00	0.00	0.00	0.00	0.02	1.07	2.69	2.05	0.13	0.00	0.00
2.25	- 2.5	0.00	0.00	0.00	0.00	0.00	0.25	2.73	4.45	3.15	0.17	0.00	0.00
2	- 2.25	0.00	0.00	0.00	0.00	0.00	0.26	3.94	5.51	2.40	0.06	0.00	0.00
1.75	- 2	0.00	0.00	0.00	0.01	0.03	0.20	4.64	5.23	1.70	0.02	0.00	0.00
1.5	- 1.75	0.00	0.00	0.00	0.05	0.23	0.55	4.93	2.97	1.24	0.12	0.02	0.00
1.25	- 1.5	0.01	0.00	0.02	0.22	1.61	2.55	5.21	2.07	1.41	0.18	0.02	0.02
1	- 1.25	0.01	0.00	0.01	0.20	2.68	6.73	4.74	1.34	0.68	0.08	0.02	0.00
0.75	- 1	0.00	0.00	0.00	0.05	1.78	5.16	3.91	1.05	0.22	0.02	0.00	0.00
0.5	- 0.75	0.00	0.00	0.00	0.00	0.25	1.13	0.92	0.24	0.02	0.00	0.00	0.00
0.25	- 0.5	0.00	0.00	0.00	0.00	0.00	0.00	0.00	0.03	0.01	0.00	0.00	0.00
0	- 0.25	0.02	0.00	0.00	0.01	0.00	0.00	0.00	0.00	0.00	0.00	0.00	0.00
	<b>Total</b>	0.03	0.00	0.03	0.54	6.58	16.85	32.70	27.53	14.62	1.03	0.07	0.02

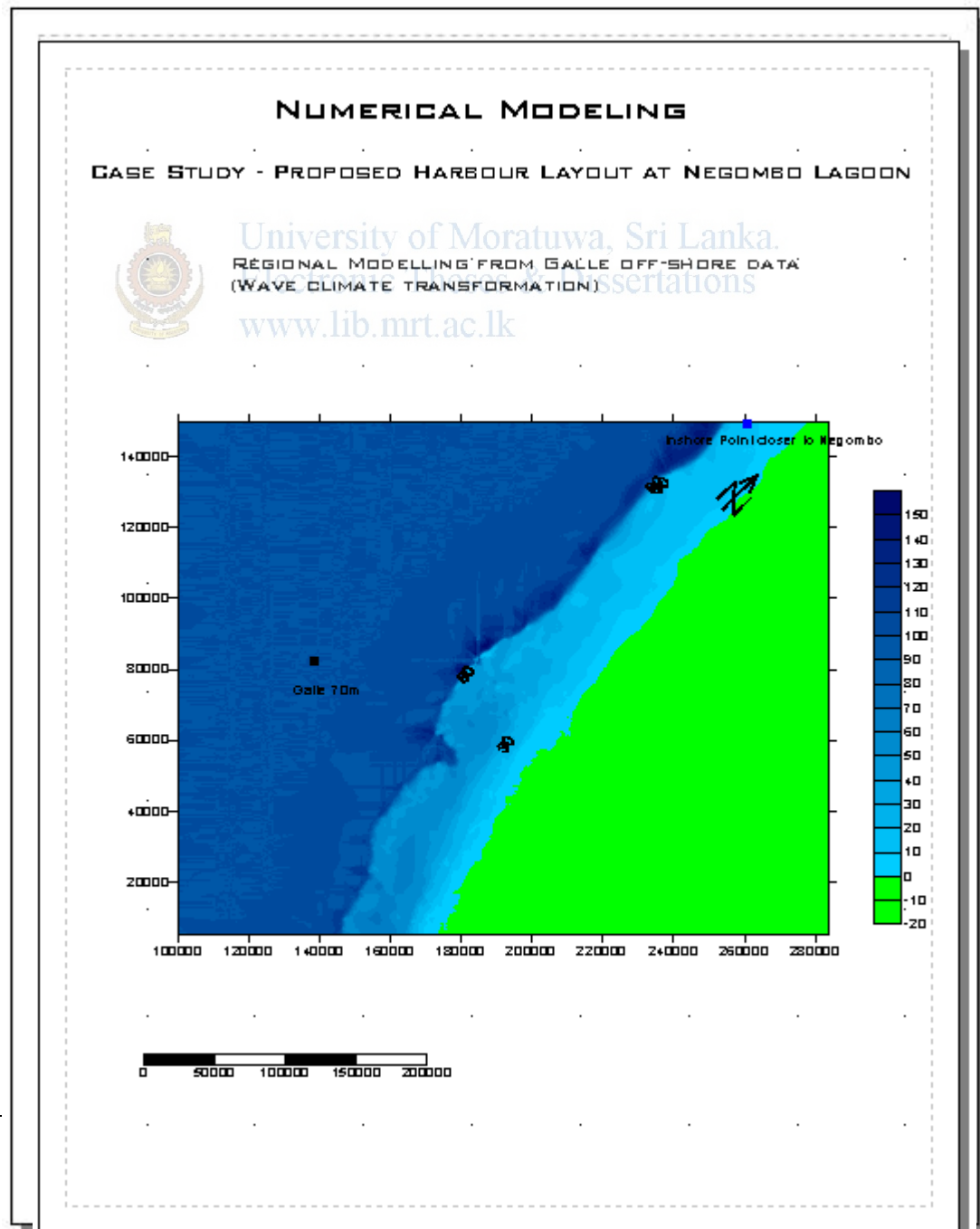
Number refer to 3hr wave records

**Table 4.8:** Percentage distribution of CCD-GTZ overall wave data by direction

The following figure 4.1 gives the wave rose produced by MWAVE\_ROS module and was plotted through “Surfur Ver 7.0 – surface generation software.

**Figure 4.2:** Wave rose produced from Galle 70m offshore wave data

**Figure 4.3:** Bathymetry for Regional wave modeling and wave climate transformation



In order to derive the wave matrix for transforming the offshore wave data to inshore a total of 165 runs were undertaken. These runs consisted of 5 wave periods, 11 directions and 3 water levels as summarized in Table 4.9 below.

Parameter	Values modelled	Number of runs
Wave Height (m)	Unity (1.0)	1 No.
Wave Period (s)	3.0,6.0,9.0,12.0,15.0	5 No.
Wave Directions (degrees)	150, 165, 180, 195, 210, 225, 240, 255, 270, 285, 300	11 No.
Water Level (m)	-1.0,0.0,1.0	3 No.
	Total	165 No.

**Table 4.9:** Summary of MWAVE\_REG model runs undertaken

#### 4.4.1 Wave Penetration Modelling

The wave model used to study wave penetration into the proposed fishing harbour is MWAV\_LOC. The model was developed from an evolution equation solution to the mild slope equation for water waves (Li, 1994). The evolution equation is a time dependant parabolic equation and its solutions will approach the results of the elliptical mild-slope equation as time increases. A perturbation method was used to derive the evolution equation. The equation takes into account the combined effects of refraction, diffraction, wave reflections and wave breaking. The mild slope equation is derived from the exact linearised governing equations of irrotational flow in the three dimensional domain under the assumption that the bottom varies very slowly over one wavelength. It reduces to the Helmholtz diffraction solution for constant water depth on the one hand and to the long wave equation for shallow water on the other hand. The accuracy of the equation is still satisfactory for a bottom slope of the order of unity.

The results obtained from the regional wave model MWAV\_REG were used as the boundary conditions for the wave penetration model MWAV\_LOC. Like the local MWAV\_REG modelling discussed above, a total of 95 MWAV\_LOC model runs were undertaken. The grid spacing for the wave penetration model was 5 metres so that waves propagating into the harbour can be calculated accurately with a fine grid size.

A typical model result is shown in **Figure 1.3** for a 1 in 50 year wave extreme from the NE monsoon direction. This model result clearly demonstrates that the wave heights within the proposed harbour are significantly reduced when compared to the wave heights outside the harbour. The worst wave directions are for the NE monsoon period when waves approach the harbour entrance from 90 -120 degrees. The local wave modelling study reveals that there is no significant wave penetration ( $H_s > 0.3\text{m}$ ) for the proposed harbour and hence no downtime calculations have been determined.

Halcrow's wave data transformation model MWAV\_TRN, was then used to transform each offshore wave record to a point in the shallower (20m depth) water nearer to the study site, and typical of the depth at the boundary of the local wave model. This inshore point is referred to as H1. This process results in a time series that represents a nearshore transformation of the offshore time series data. This model and processes has been successfully used for many similar projects around the world.

#### 4.4.2 Wave Model Setup for Regional Model

With Halcrow model limitations the region has to be transformed by rotation as follows. So that wave directions chosen could be run through the model with all the directional vectors that are selected from off-shore wave climate.

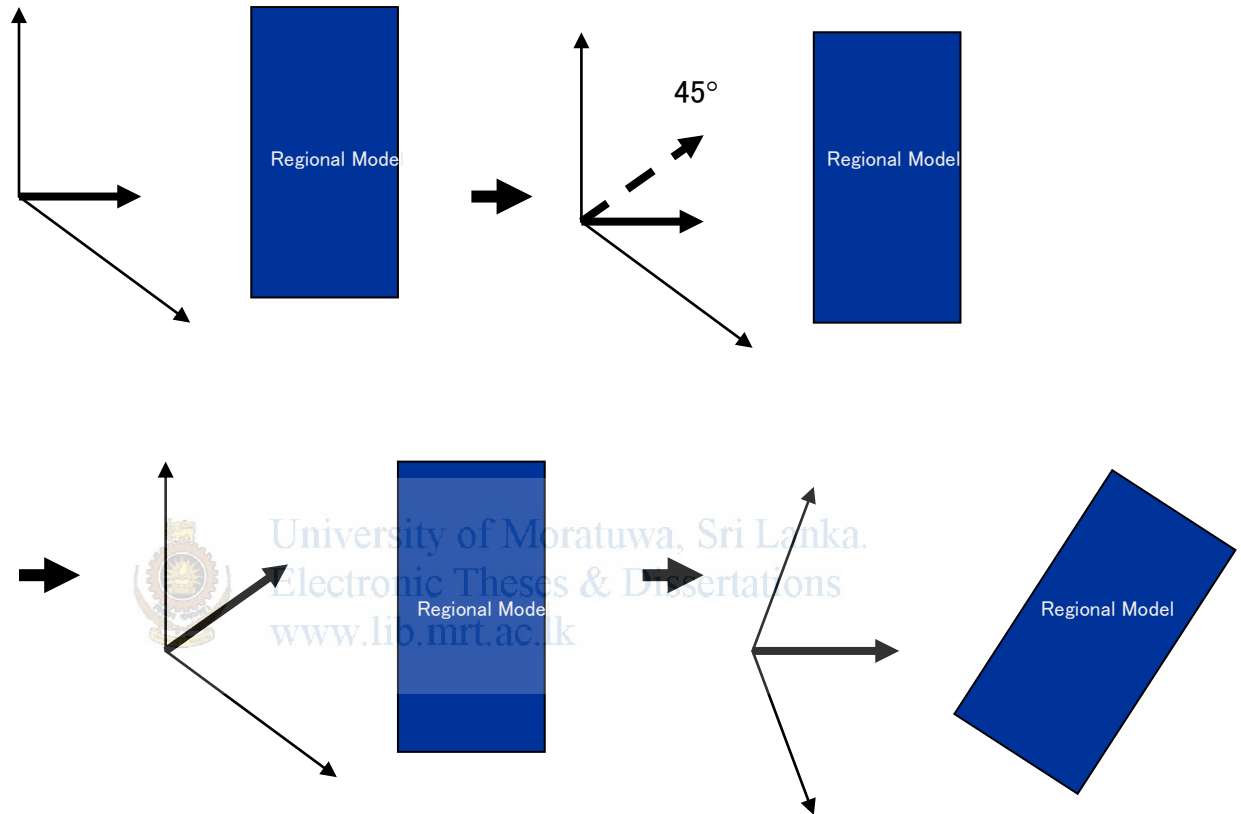


**Figure 4.4:** *Regional Model Setup*



After Wave transformation inshore wave series was analyzed as follows. MWAVE\_FIT module was implemented in deriving the following table

		Wave Direction (degrees)											
		30	60	90	120	150	180	210	240	270	300	330	360
Wave height		0	30	60	90	120	150	180	210	240	270	300	330
5.75	- 6	0.00	0.00	0.00	0.00	0.00	0.00	0.00	0.00	0.00	0.00	0.00	0.00
5.5	- 5.75	0.00	0.00	0.00	0.00	0.00	0.00	0.00	0.00	0.00	0.00	0.00	0.00
5.25	- 5.5	0.00	0.00	0.00	0.00	0.00	0.00	0.00	0.00	0.00	0.00	0.00	0.00
5	- 5.25	0.00	0.00	0.00	0.00	0.00	0.00	0.00	0.00	0.00	0.00	0.00	0.00
4.75	- 5	0.00	0.00	0.00	0.00	0.00	0.00	0.00	0.03	0.00	0.00	0.00	0.00
4.5	- 4.75	0.00	0.00	0.00	0.00	0.00	0.00	0.00	0.02	0.00	0.00	0.00	0.00
4.25	- 4.5	0.00	0.00	0.00	0.00	0.00	0.00	0.00	0.00	0.00	0.00	0.00	0.00
4	- 4.25	0.00	0.00	0.00	0.00	0.00	0.00	0.00	0.00	0.00	0.00	0.00	0.00
3.75	- 4	0.00	0.00	0.00	0.00	0.00	0.00	0.00	0.01	0.00	0.00	0.00	0.00
3.5	- 3.75	0.00	0.00	0.00	0.00	0.00	0.00	0.00	0.03	0.05	0.00	0.00	0.00
3.25	- 3.5	0.00	0.00	0.00	0.00	0.00	0.00	0.00	0.06	0.04	0.00	0.00	0.00
3	- 3.25	0.00	0.00	0.00	0.00	0.00	0.00	0.00	0.14	0.12	0.00	0.00	0.00
2.75	- 3	0.00	0.00	0.00	0.00	0.00	0.00	0.00	0.60	0.46	0.01	0.00	0.00
2.5	- 2.75	0.00	0.00	0.00	0.00	0.00	0.00	0.00	1.65	1.01	0.00	0.00	0.00
2.25	- 2.5	0.00	0.00	0.00	0.00	0.00	0.00	0.00	3.85	2.14	0.00	0.00	0.00
2	- 2.25	0.00	0.00	0.00	0.00	0.00	0.00	0.00	6.91	3.13	0.02	0.00	0.00
1.75	- 2	0.00	0.00	0.00	0.00	0.00	0.00	0.28	9.76	2.36	0.01	0.00	0.00
1.5	- 1.75	0.00	0.00	0.00	0.00	0.00	0.00	1.49	9.62	1.65	0.02	0.00	0.00
1.25	- 1.5	0.00	0.00	0.00	0.00	0.00	0.00	2.84	6.82	1.65	0.08	0.00	0.00
1	- 1.25	0.00	0.00	0.00	0.00	0.00	0.00	2.37	4.86	1.02	0.13	0.00	0.00
0.75	- 1	0.00	0.00	0.00	0.00	0.00	0.00	3.39	4.69	0.30	0.04	0.00	0.00
0.5	- 0.75	0.00	0.00	0.00	0.00	0.00	0.00	7.36	4.43	0.05	0.01	0.00	0.00
0.25	- 0.5	0.00	0.00	0.00	0.00	0.00	0.00	10.02	1.51	0.01	0.00	0.00	0.00
0	- 0.25	0.00	0.00	0.00	0.00	0.00	0.00	2.97	0.01	0.00	0.00	0.00	0.00
<b>Total</b>		0.00	0.00	0.00	0.00	0.00	0.00	30.72	54.98	13.99	0.31	0.00	0.00

Number refer to 3hr wave records

**Table 4.10:** Probability analysis of transformed wave data

Wave distribution could be represented in the following wave rose output. It was produced with the use of MWAVE\_ROS and Surfer Ver 7.0 surface generation software.



University of Moratuwa, Sri Lanka.  
Electronic Theses & Dissertations  
[www.lib.mrt.ac.lk](http://www.lib.mrt.ac.lk)

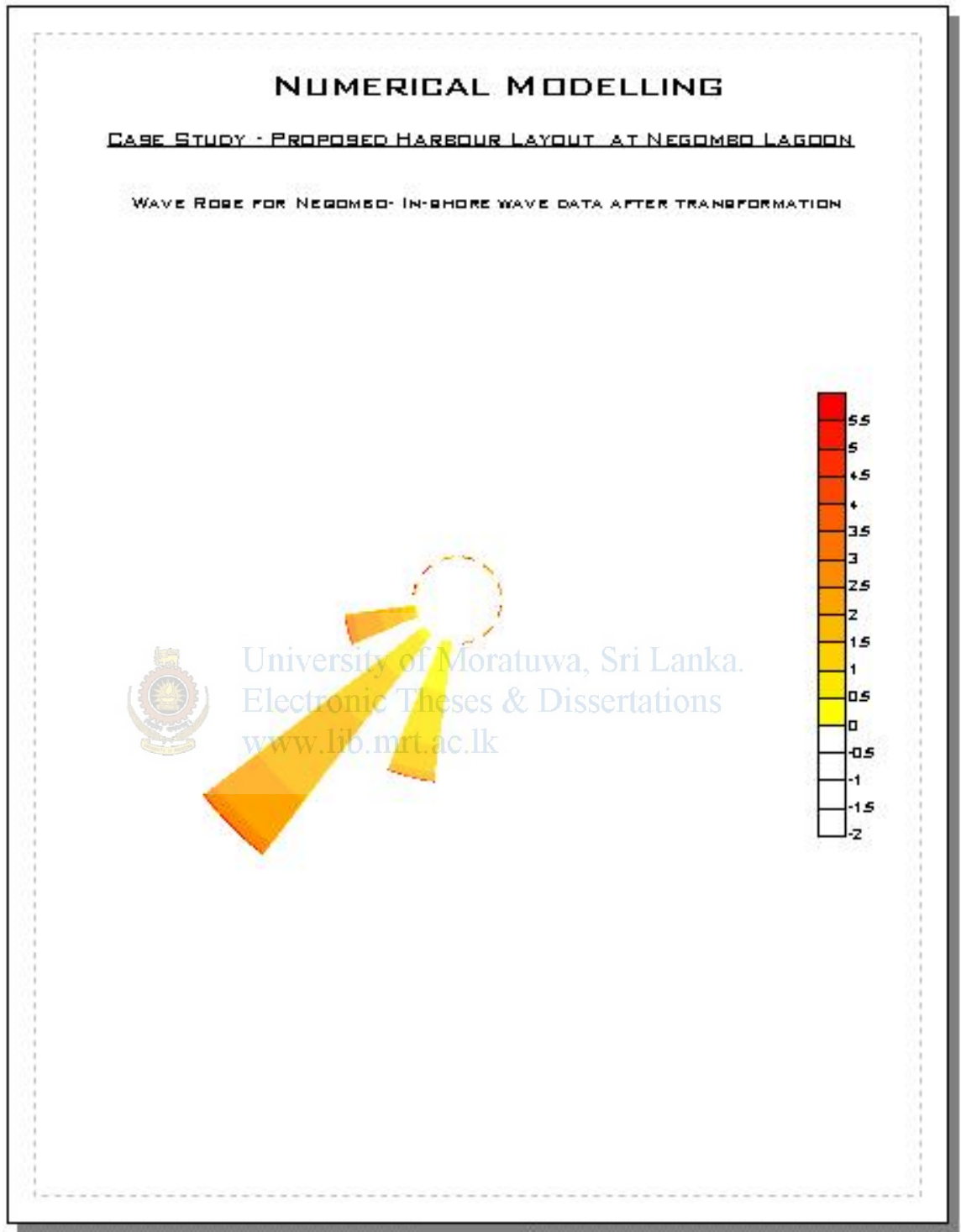


**Figure 4.5:** Wave Rose for Negombo-Inshore wave data after transformation

With the implementation of MWAVE\_JON, the joint probability analysis was derived from the Negombo in-shore wave series.

Angle sec: 180 - 210 : heights		
Return period	weibull	gumbell
1	2.395	2.385
5	2.784	2.85
10	2.944	3.051
20	3.101	3.251
50	3.303	3.516
100	3.453	3.716
150	3.539	3.834
200	3.6	3.917
300	3.685	4.034
1000	3.932	4.385

Table 4.11: Wave Height

Angle sec: 210 - 240: heights		
Return period	weibull	gumbell
1	3.338	3.931
5	3.571	4.553
10	3.663	4.821
20	3.751	5.088
50	3.861	5.442
100	3.94	5.71
150	3.985	5.865
200	4.016	5.981
300	4.059	6.138
1000	4.183	6.617

Table 4.12: Wave Height

Angle sec: 240 - 270: heights		
Return period	weibull	gumbell
1	3.069	3.534
5	3.253	4.126
10	3.323	4.381
20	3.388	4.636
50	3.468	4.973
100	3.525	5.227
150	3.557	5.376
200	3.579	5.482
300	3.61	5.63
1000	3.695	6.077

Table 4.13: Wave Height

Angle sec: 180 - 210 : periods		
Return period	weibull	gumbell
1	7.141	11.07
5	7.29	12.472
10	7.347	13.075
20	7.4	13.678
50	7.465	14.477
100	7.511	15.078
150	7.536	15.431
200	7.554	15.681
300	7.578	16.034
1000	7.647	17.092

Table 4.14: Wave Period

Angle sec: 210 - 240: periods		
Return period	weibull	gumbell
1	9.11	11.519
5	9.305	12.808
10	9.379	13.363
20	9.449	13.917
50	9.535	14.651
100	9.596	15.206
150	9.63	15.527
200	9.654	15.767
300	9.686	16.092
1000	9.778	17.084

Table 4.15: Wave Period

Angle sec: 240 - 270: periods		
Return period	weibull	gumbell
1	7.921	8.081
5	8.184	8.827
10	8.282	9.148
20	8.372	9.47
50	8.483	9.894
100	8.561	10.215
150	8.604	10.404
200	8.634	10.537
300	8.675	10.724
1000	8.79	11.286

Table 4.16: Wave Period

The following in-shore wave climate was derived from joint probability analysis as critical cases.



Electronic Theses & Dissertations  
www.lib.mrt.ac.lk

Wave Direction (Degrees)	1 in 1 year		1 in 20 year		1 in 50 year	
	Hs	Tz(s)	Hs	Tz(s)	Hs	Tz(s)
180 - 210	2.395	11.07	3.251	13.678	3.516	14.477
210 - 240	3.931	11.519	5.088	13.917	5.442	14.651
240 - 270	3.534	8.081	4.636	9.47	4.973	9.894

Table 4.17: Inshore critical wave regions

The results in above table along with other derived wave extremes were used to estimate the design conditions at the boundary of the local wave model.

## 4.5 Local Wave Modelling

Local wave modelling consisted of two phases. The first phase was the harbour layout optimization and the second phase was the wave penetration (or harbour disturbance) modelling. The following section briefly discusses the modelling work undertaken.

### 4.5.1 Wave Model Setup for Local Model

With Halcrow model limitations the region has to be transformed by rotation as follows. So that wave directions chosen could be run through the model with all the directional vectors that are selected from in-shore wave climate.

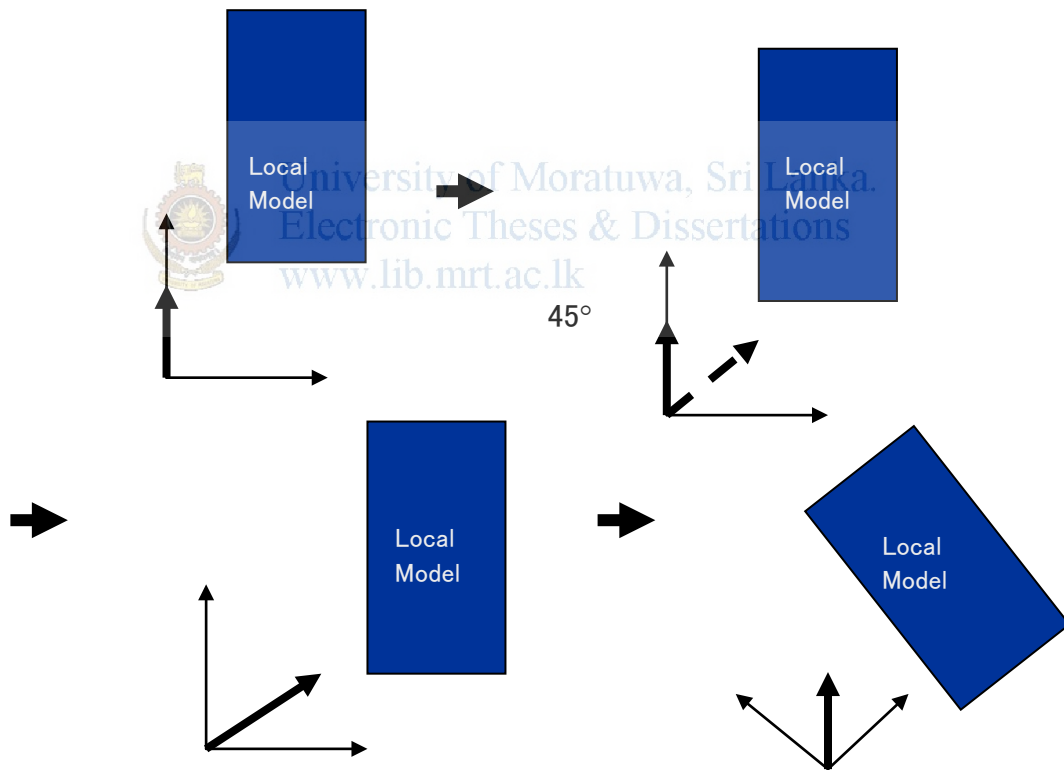


**Figure 4.6:** *Local Model Setup*

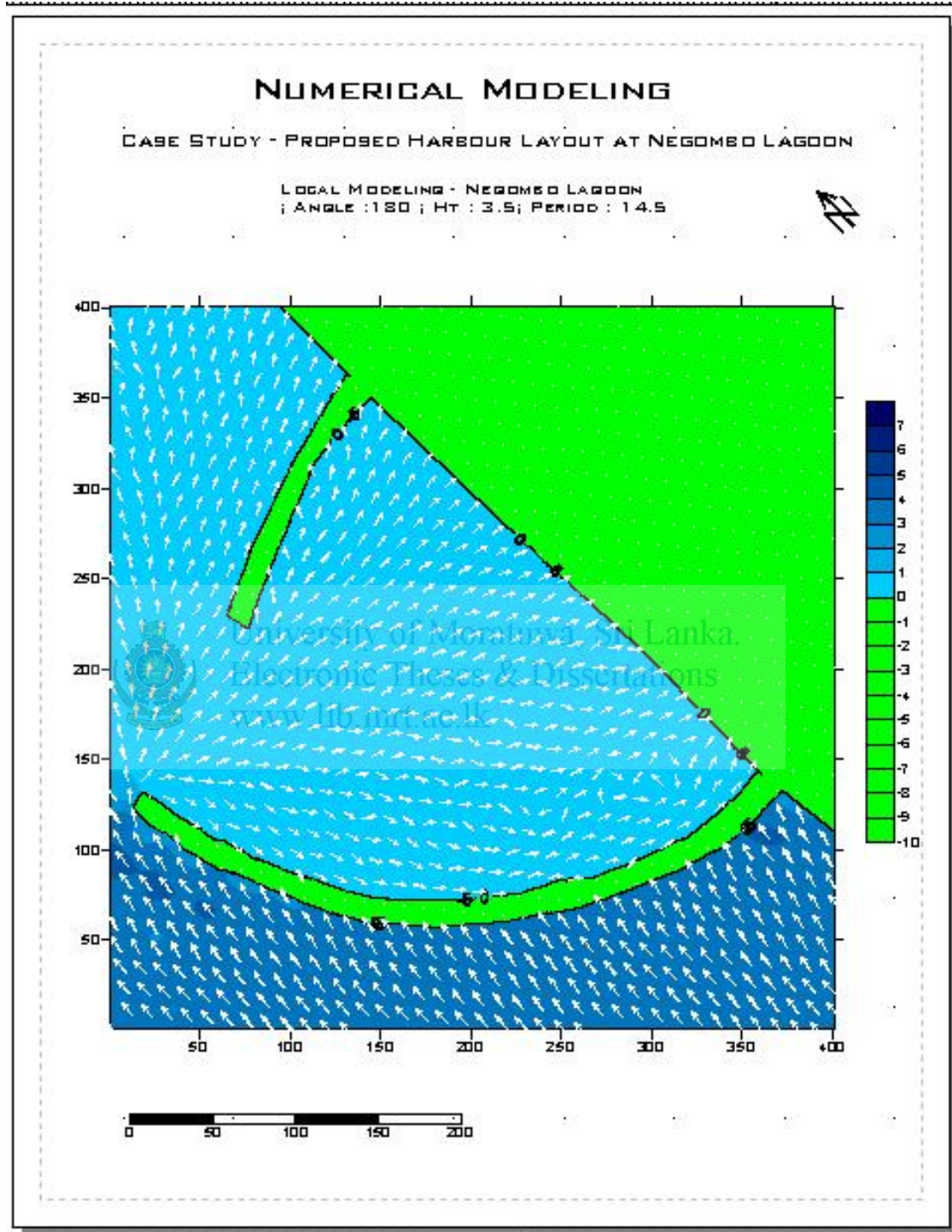


**Figure 4.7:** Local Model Critical Cases Run no 1

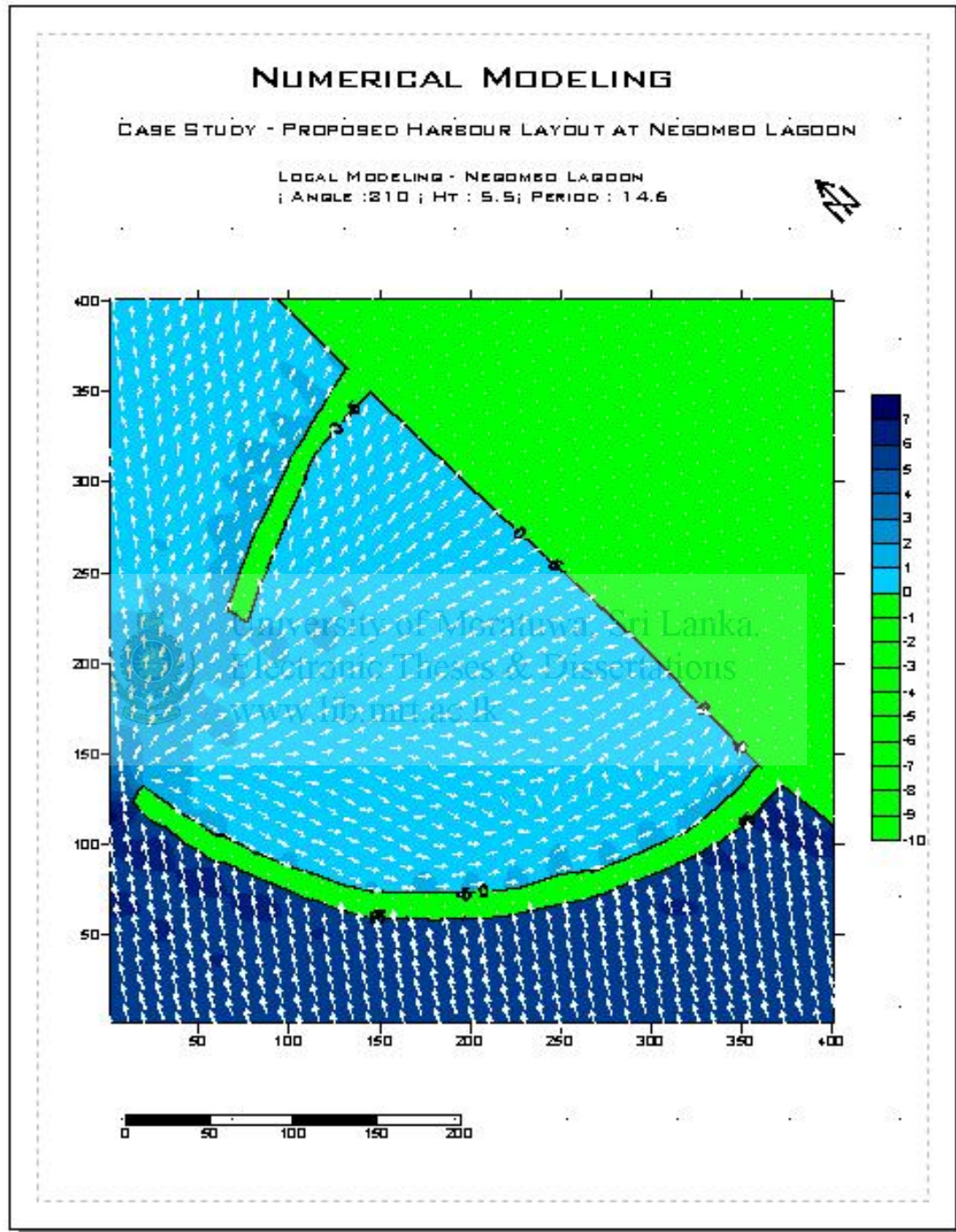


**Figure 4.8:** Local Model Critical Cases Run no 2



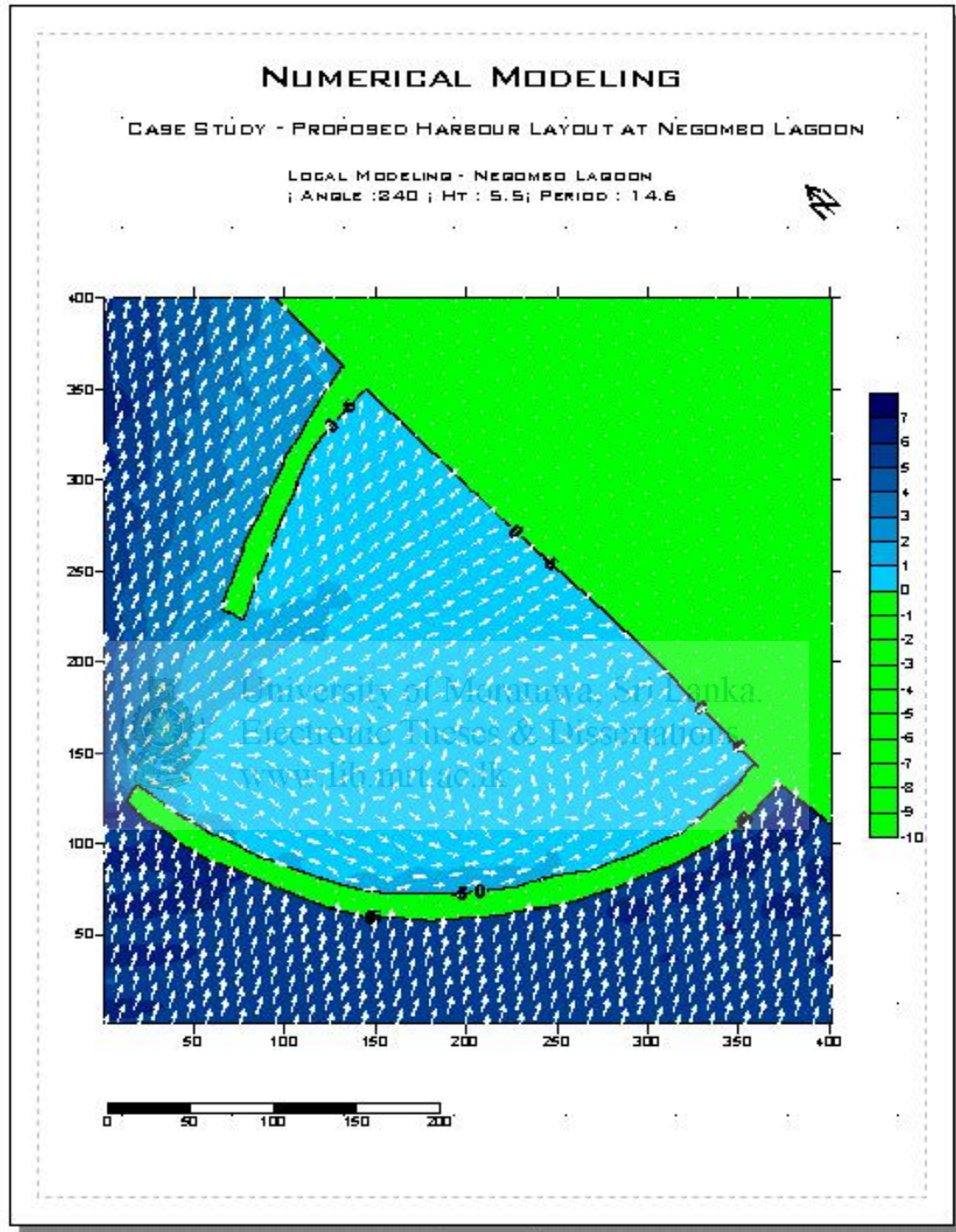


**Figure 4.9:** Local Model Critical Cases Run no 3





University of Moratuwa, Sri Lanka.  
Electronic Theses and Dissertations  
www.lib.mrt.ac.lk

## CHAPTER – 5

# APPLICATION OF MATHEMATICAL MODELING IN THE DESIGN OF PROPOSED HAMBANTHOTA FISHERY HARBOUR

## 5.0 Application of Mathematical Modeling in the Design of Proposed Hambanthota Fishery Harbour.

### 5.1 Data Review and Analysis

#### 5.1.1 Data collection

Numerous reports have been collated and reviewed during the initial stages of the project.

The following section describes the data found and reviewed.

Tide Level	Predicted Water Level (m above CD)
Mean High Water Springs (MHWS)	0.6
Mean High Water Neaps (MHWN)	0.4
Mean Sea Level (MSL)	0.4
Mean Low Water Neaps (MLWN)	0.3
Mean Low Water Springs (MLWS)	0.1

**Table 5.1**

##### 5.1.1.1 Wave Data

The near-shore wave climate at Hambantota is influenced by two distinct wave systems. Swell waves are generated in the deep sea of the Indian Ocean and have propagated out of the generating area to the Hambantota region. These waves exhibit typically long wave periods and are more or less unidirectional. Sea waves are generated by the local wind fields and have wave periods less than the swell waves. In contrast to swell waves, sea waves occur from a variety of directions.

The directional distribution of sea and swell wave conditions outside the Hambantota area were established from four different sources:

- Directional wave statistics were available from a directional wave climate study covering the south west coast of Sri Lanka carried out by the Coast Conservation

Department (CCD) under a German Technical Cooperation (GTZ) programme based on wave measurements conducted using a WAVEC type pitch and roll buoy in 70m water depth offshore of Galle for the periods February 1989 -August 1992 and May 1994 –September 1995.

- Non-directional wave measurements conducted by LHI for SLPA in approximately 20m water depth off Galle harbour, over intermittent periods during 1984 -1986 and on a continuous basis during September 1988 -August 1995.
- Directional wave measurements conducted at Kudawella by LHI in about 15m water depth using an S4DW type electromagnetic current meter from February 1996 to February 1997
- Non-directional wave measurements conducted by LHI using a Marsh McBimeycurrent meter for Nippon Tetrapod Co Ltd (NTC) in approximately 20m water depth off Kirinda over the period April 1993 to August 1994.



University of Moratuwa, Sri Lanka.  
Electronic Theses & Dissertations  
[www.lib.mrt.ac.lk](http://www.lib.mrt.ac.lk)

Wave Height (m)	Wave Direction (degrees)											
	0 - 30	30 - 60	60 - 90	90 - 120	120 - 150	150 - 180	180 - 210	210 - 240	240 - 270	270 - 300	300 - 330	330 - 360
0.00 - 0.25	0.02	0	0	0.01	0	0	0	0	0	0	0	0
0.25 - 0.50	0	0	0	0	0	0	0	0.03	0.01	0	0	0
0.50 - 0.75	0	0	0	0	0.25	1.13	0.92	0.24	0.02	0	0	0
0.75 - 1.00	0	0	0	0.05	1.78	5.16	3.91	1.05	0.22	0.02	0	0
1.00 - 1.25	0.01	0	0.01	0.20	2.68	6.73	4.74	1.34	0.68	0.08	0.02	0
1.25 - 1.50	0.01	0	0.02	0.22	1.61	2.55	5.21	2.07	1.41	0.18	0.02	0.02
1.50 - 1.75	0	0	0	0.05	0.23	0.55	4.93	2.97	1.24	0.12	0.02	0
1.75 - 2.00	0	0	0	0.01	0.03	0.20	4.64	5.23	1.70	0.02	0	0
2.00 - 2.25	0	0	0	0	0	0.26	3.94	5.51	2.40	0.06	0	0
2.25 - 2.50	0	0	0	0	0	0.25	2.73	4.45	3.15	0.17	0	0
2.50 - 2.75	0	0	0	0	0	0.02	1.07	2.69	2.05	0.13	0	0
2.75 - 3.00	0	0	0	0	0	0	0.43	1.31	0.98	0.06	0	0
3.00 - 3.25	0	0	0	0	0	0	0.17	0.43	0.47	0.09	0	0
3.25 - 3.50	0	0	0	0	0	0	0.01	0.12	0.16	0.06	0	0
3.50 - 3.75	0	0	0	0	0	0	0	0.05	0.05	0.02	0	0
3.75 - 4.00	0	0	0	0	0	0	0	0.01	0.02	0	0	0
4.00 - 4.25	0	0	0	0	0	0	0	0	0.04	0.01	0	0
4.25 - 4.50	0	0	0	0	0	0	0	0	0	0.02	0	0
4.50 - 4.75	0	0	0	0	0	0	0	0	0	0	0	0
4.75 - 5.00	0	0	0	0	0	0	0	0.02	0	0	0	0
5.00 - 5.25	0	0	0	0	0	0	0	0.02	0.01	0	0	0
5.25 - 5.50	0	0	0	0	0	0	0	0	0	0	0	0
5.50 - 5.75	0	0	0	0	0	0	0	0	0	0	0	0
5.75 - 6.00	0	0	0	0	0	0	0	0	0	0	0	0
<b>Total</b>	<b>0.03</b>		<b>0.03</b>	<b>0.54</b>	<b>6.58</b>	<b>16.85</b>	<b>32.70</b>	<b>27.53</b>	<b>14.62</b>	<b>1.03</b>	<b>0.07</b>	<b>0.02</b>

Numbers refer to 3hr wave records

**Table 5.2:** Percentage distribution of CCD-GTZ overall wave data by direction sector

Wave Height (m)	Wave Period (seconds)											
	0 - 1	1 - 2	2 - 3	3 - 4	4 - 5	5 - 6	6 - 7	7 - 8	8 - 9	9 - 10	10 - 11	11 - 12
0.00 - 0.25	0.02	0	0	0.01	0	0	0	0	0	0	0	0
0.25 - 0.50	0	0	0	0	0	0	0	0	0.02	0.02	0	0
0.50 - 0.75	0	0	0	0.12	0.63	0.92	0.67	0.16	0.06	0	0	0
0.75 - 1.00	0	0	0	0.15	2.53	4.26	2.88	1.74	0.58	0.02	0	0
1.00 - 1.25	0	0	0	0.02	2.19	6.05	4.15	2.68	1.07	0.33	0	0
1.25 - 1.50	0	0	0	0	1.27	5.44	2.78	2.15	1.20	0.28	0.17	0.02
1.50 - 1.75	0	0	0	0	0.45	4.13	3.56	1.15	0.43	0.31	0.07	0.01
1.75 - 2.00	0	0	0	0	0.07	3.51	6.35	1.43	0.25	0.14	0.04	0.02
2.00 - 2.25	0	0	0	0	0.01	1.63	7.07	2.79	0.56	0.08	0	0.02
2.25 - 2.50	0	0	0	0	0	0.61	5.42	3.81	0.86	0.02	0	0.01
2.50 - 2.75	0	0	0	0	0	0.36	2.64	2.19	0.76	0.03	0	0
2.75 - 3.00	0	0	0	0	0	0.09	1.25	0.85	0.54	0.05	0	0
3.00 - 3.25	0	0	0	0	0	0.01	0.56	0.42	0.17	0.01	0	0
3.25 - 3.50	0	0	0	0	0	0.02	0.20	0.10	0.03	0.0	0	0
3.50 - 3.75	0	0	0	0	0	0	0.09	0.02	0.01	0.01	0	0
3.75 - 4.00	0	0	0	0	0	0	0	0.03	0	0	0	0
4.00 - 4.25	0	0	0	0	0	0	0.02	0.03	0	0	0	0
4.25 - 4.50	0	0	0	0	0	0	0.01	0.01	0	0	0	0
4.50 - 4.75	0	0	0	0	0	0	0	0	0	0	0	0
4.75 - 5.00	0	0	0	0	0	0	0	0.01	0.01	0	0	0
5.00 - 5.25	0	0	0	0	0	0	0	0.01	0.02	0	0	0
5.25 - 5.50	0	0	0	0	0	0	0	0	0	0	0	0
5.50 - 5.75	0	0	0	0	0	0	0	0	0	0	0	0
5.75 - 6.00	0	0	0	0	0	0	0	0	0	0	0	0
<b>Total</b>	<b>0.02</b>	<b>0</b>	<b>0</b>	<b>0.31</b>	<b>7.15</b>	<b>27.04</b>	<b>37.66</b>	<b>19.58</b>	<b>6.56</b>	<b>1.32</b>	<b>0.27</b>	<b>0.09</b>

Number refer to 3hr wave records

**Table 5.3:** Percentage distribution of CCD-GTZ overall wave data by wave period

In addition, analysis was undertaken to investigate how the off-shore wave climate varied with season. The wave climate was broken down into four seasons in accordance with previous studies as follows:

1. The South-West monsoon (SW) – from May to September;
2. The first Inter-monsoon (IM1) – from October to November;
3. The North-East monsoon (NE) – from December to February;
4. The Second Inter-monsoon (IM2) – from March to April.

The conclusion from the analysis of the CCD-GTZ offshore wave data was:

- a) Analysis of the data set into monsoon periods has highlighted very few waves in the NW or NE direction sectors for the NE monsoon period. It has therefore been concluded that this data set does not accurately represent the NE monsoon period and hence it should not be used to derive typical wave climates at the proposed harbour for the NE monsoon period.
- b) The original data files and the precise position of the wave rider buoy were not available from CCD or LHI. Therefore it has not been possible to check the raw ASCII data files received from LHI and hence there is no way of assuring these files are correct or have not been filtered in anyway during their previous analysis.
- c) The wave climate for the SW monsoon is predominantly from the 150-300 degree sectors. There are a very small proportion of the waves, which are generated between 300 – 360 degrees but the wave height is relatively small ( $< 1.5$  m). Hence these have been ignored for all subsequent wave modeling since they are not expected to be able to propagate along the southern coast of Sri Lanka or be capable of having a significant impact on the final derived wave climates at Hambantota.



Wave Height (m)	Wave Direction (degrees)											
	0 - 30	30 - 60	60 - 90	90 - 120	120 - 150	150 - 180	180 - 210	210 - 240	240 - 270	270 - 300	300 - 330	330 - 360
0.00 – 0.25	0.03	0	0	0.02	0	0	0.02	0	0	0	0	0
0.25 – 0.50	0	0	0	0	0	0	0	0.06	0.03	0	0	0
0.50 – 0.75	0	0	0	0	0	0	0	0	0	0	0	0
0.75 – 1.00	0	0	0	0	0	0.05	0.09	0	0	0	0	0
1.00 – 1.25	0	0	0	0	0	0.39	0.94	0.39	0.26	0	0	0
1.25 – 1.50	0	0	0	0	0	0.26	2.07	1.46	1.78	0	0	0
1.50 – 1.75	0	0	0	0	0	0.26	4.29	3.62	1.77	0	0	0
1.75 – 2.00	0	0	0	0	0	0.21	6.99	8.88	2.90	0.02	0	0
2.00 – 2.25	0	0	0	0	0	0.45	6.67	10.01	4.29	0.08	0	0
2.25 – 2.50	0	0	0	0	0	0.45	4.65	8.18	5.74	0.26	0	0
2.50 – 2.75	0	0	0	0	0	0.05	1.98	4.89	3.73	0.23	0	0
2.75 – 3.00	0	0	0	0	0	0	0.95	2.94	2.17	0.14	0	0
3.00 – 3.25	0	0	0	0	0	0	0.50	1.42	1.28	0.32	0	0
3.25 – 3.50	0	0	0	0	0	0	0.08	0.35	0.48	0.29	0	0
3.50 – 3.75	0	0	0	0	0	0	0	0.12	0.14	0.05	0	0
3.75 – 4.00	0	0	0	0	0	0	0	0.03	0.06	0.05	0	0
4.00 – 4.25	0	0	0	0	0	0	0	0	0.06	0.03	0	0
4.25 – 4.50	0	0	0	0	0	0	0	0	0.02	0.05	0	0
4.50 – 4.75	0	0	0	0	0	0	0	0	0	0	0	0
4.75 – 5.00	0	0	0	0	0	0	0	0.03	0	0	0	0
5.00 – 5.25	0	0	0	0	0	0	0	0.03	0.02	0	0	0
5.25 – 5.50	0	0	0	0	0	0	0	0	0	0	0	0
5.50 – 5.75	0	0	0	0	0	0	0	0.02	0	0	0	0
5.75 – 6.00	0	0	0	0	0	0	0	0	0	0	0	0
<b>Total</b>	<b>0</b>	<b>0</b>	<b>0</b>	<b>0</b>	<b>0</b>	<b>2.11</b>	<b>29.21</b>	<b>72.44</b>	<b>24.71</b>	<b>1.48</b>	<b>0</b>	<b>0</b>

Number refer to 3hr wave records

**Table 5.4:** Percentage distribution of CCD-GTZ overall wave data by direction for SW monsoon

Wave Height (m)	Wave Direction (degrees)											
	0 - 30	30 - 60	60 - 90	90 - 120	120 - 150	150 - 180	180 - 210	210 - 240	240 - 270	270 - 300	300 - 330	330 - 360
0.00 - 0.25	0	0	0	0	0	0	0	0	0	0	0	0
0.25 - 0.50	0	0	0	0	0	0	0	0	0	0	0	0
0.50 - 0.75	0	0	0	0	0	0.16	0.6	1.20	0.11	0	0	0
0.75 - 1.00	0	0	0	0	0	2.73	4.15	4.59	0.93	0	0	0
1.00 - 1.25	0	0	0	0.16	0.77	8.47	6.23	3.99	2.30	0.16	0	0
1.25 - 1.50	0	0	0	0	0.6	4.15	11.53	5.41	2.30	0.38	0	0
1.50 - 1.75	0	0	0	0	0.05	1.26	11.86	5.68	2.08	0.60	0.11	0
1.75 - 2.00	0	0	0	0	0.05	0.38	4.32	2.95	1.15	0.05	0	0
2.00 - 2.25	0	0	0	0	0	0.05	1.75	1.04	0.98	0.05	0	0
2.25 - 2.50	0	0	0	0	0	0	1.26	0.55	0.66	0.16	0	0
2.50 - 2.75	0	0	0	0	0	0	0.05	0.55	0.66	0.05	0	0
2.75 - 3.00	0	0	0	0	0	0	0	0.11	0.22	0	0	0
3.00 - 3.25	0	0	0	0	0	0	0	0.05	0.05	0	0	0
3.25 - 3.50	0	0	0	0	0	0	0	0	0	0	0	0
3.50 - 3.75	0	0	0	0	0	0	0	0	0.05	0	0	0
3.75 - 4.00	0	0	0	0	0	0	0	0	0.11	0	0	0
4.00 - 4.25	0	0	0	0	0	0	0	0	0.05	0	0	0
4.25 - 4.50	0	0	0	0	0	0	0	0	0	0	0	0
4.50 - 4.75	0	0	0	0	0	0	0	0	0.05	0	0	0
4.75 - 5.00	0	0	0	0	0	0	0	0	0	0	0	0
5.00 - 5.25	0	0	0	0	0	0	0	0	0	0	0	0
5.25 - 5.50	0	0	0	0	0	0	0	0	0	0	0	0
5.50 - 5.75	0	0	0	0	0	0	0	0	0	0	0	0
5.75 - 6.00	0	0	0	0	0	0	0	0	0	0	0	0
<b>Total</b>	<b>0</b>	<b>0</b>	<b>0</b>	<b>0.16</b>	<b>1.48</b>	<b>17.21</b>	<b>41.75</b>	<b>26.12</b>	<b>11.69</b>	<b>1.48</b>	<b>0.11</b>	<b>0</b>

Number refer to 3hr wave records

**Table 5.5:** Percentage distribution of CCD-GTZ overall wave data by direction for NE monsoon

Wave Height (m)	Wave Direction (degrees)											
	0 - 30	30 - 60	60 - 90	90 - 120	120 - 150	150 - 180	180 - 210	210 - 240	240 - 270	270 - 300	300 - 330	330 - 360
0.00 - 0.25	0	0	0	0	0	0	0	0	0	0	0	0
0.25 - 0.50	0	0	0	0	0	0	0	0	0	0	0	0
0.50 - 0.75	0	0	0	0	1.23	5.11	3.69	0.44	0.08	0	0	0
0.75 - 1.00	0	0	0	0.24	8.49	17.05	8.60	1.47	0.36	0.08	0	0
1.00 - 1.25	0.04	0	0.04	0.87	11.62	14.04	4.48	1.31	0.79	0.28	0.12	0
1.25 - 1.50	0.04	0	0.12	1.11	6.82	4.56	1.94	0.63	0.40	0.59	0.08	0.08
1.50 - 1.75	0	0	0	0.24	1.07	0.59	0.48	0.16	0	0.12	0.04	0
1.75 - 2.00	0	0	0	0.04	0.12	0.04	0.20	0.04	0	0	0	0
2.00 - 2.25	0	0	0	0	0	0	0.04	0	0	0.04	0	0
2.25 - 2.50	0	0	0	0	0	0	0	0	0	0	0	0
2.50 - 2.75	0	0	0	0	0	0	0	0	0	0	0	0
2.75 - 3.00	0	0	0	0	0	0	0	0	0	0	0	0
3.00 - 3.25	0	0	0	0	0	0	0	0	0	0	0	0
3.25 - 3.50	0	0	0	0	0	0	0	0	0	0	0	0
3.50 - 3.75	0	0	0	0	0	0	0	0	0	0	0	0
3.75 - 4.00	0	0	0	0	0	0	0	0	0	0	0	0
4.00 - 4.25	0	0	0	0	0	0	0	0	0	0	0	0
4.25 - 4.50	0	0	0	0	0	0	0	0	0	0	0	0
4.50 - 4.75	0	0	0	0	0	0	0	0	0	0	0	0
4.75 - 5.00	0	0	0	0	0	0	0	0	0	0	0	0
5.00 - 5.25	0	0	0	0	0	0	0	0	0	0	0	0
5.25 - 5.50	0	0	0	0	0	0	0	0	0	0	0	0
5.50 - 5.75	0	0	0	0	0	0	0	0	0	0	0	0
5.75 - 6.00	0	0	0	0	0	0	0	0	0	0	0	0
<b>Total</b>	<b>0.08</b>	<b>0</b>	<b>0.16</b>	<b>2.50</b>	<b>29.34</b>	<b>41.4</b>	<b>19.43</b>	<b>4.04</b>	<b>1.63</b>	<b>1.11</b>	<b>0.24</b>	<b>0.08</b>

Numbers refer to 3hr wave records

**Table 5.6:** Percentage distribution of CCD-GTZ overall wave data by direction for IM1 monsoon

Wave Height (m)	Wave Direction (degrees)											
	0 - 30	30 - 60	60 - 90	90 - 120	120 - 150	150 - 180	180 - 210	210 - 240	240 - 270	270 - 300	300 - 330	330 - 360
0.00 – 0.25	0	0	0	0	0	0	0	0	0	0	0	0
0.25 – 0.50	0	0	0	0	0	0	0	0	0	0	0	0
0.50 – 0.75	0	0	0	0	0	0.76	0.76	0	0	0	0	0
0.75 – 1.00	0	0	0	0	0.59	9.31	11.36	0.53	0	0	0	0
1.00 – 1.25	0	0	0	0	1.64	17.63	17.28	1.99	0.35	0	0	0
1.25 – 1.50	0	0	0	0	0.82	5.68	14.47	2.64	0.53	0	0	0
1.50 – 1.75	0	0	0	0	0	0.64	0.48	1.52	0.35	0	0	0
1.75 – 2.00	0	0	0	0	0	0.18	0.20	1.17	0.35	0	0	0
2.00 – 2.25	0	0	0	0	0	0	0.04	0.23	0	0	0	0
2.25 – 2.50	0	0	0	0	0	0	0	0	0	0	0	0
2.50 – 2.75	0	0	0	0	0	0	0	0	0	0	0	0
2.75 – 3.00	0	0	0	0	0	0	0	0	0	0	0	0
3.00 – 3.25	0	0	0	0	0	0	0	0	0	0	0	0
3.25 – 3.50	0	0	0	0	0	0	0	0	0	0	0	0
3.50 – 3.75	0	0	0	0	0	0	0	0	0	0	0	0
3.75 – 4.00	0	0	0	0	0	0	0	0	0	0	0	0
4.00 – 4.25	0	0	0	0	0	0	0	0	0	0	0	0
4.25 – 4.50	0	0	0	0	0	0	0	0	0	0	0	0
4.50 – 4.75	0	0	0	0	0	0	0	0	0	0	0	0
4.75 – 5.00	0	0	0	0	0	0	0	0	0	0	0	0
5.00 – 5.25	0	0	0	0	0	0	0	0	0	0	0	0
5.25 – 5.50	0	0	0	0	0	0	0	0	0	0	0	0
5.50 – 5.75	0	0	0	0	0	0	0	0	0	0	0	0
5.75 – 6.00	0	0	0	0	0	0	0	0	0	0	0	0
<b>Total</b>	<b>0</b>	<b>0</b>	<b>0</b>	<b>0</b>	<b>3.05</b>	<b>34.21</b>	<b>19.43</b>	<b>8.08</b>	<b>1.58</b>	<b>0</b>	<b>0</b>	<b>0</b>

Numbers refer to 3hr wave records

**Table 5.7:** Percentage distribution of CCD-GTZ overall wave data by direction for IM2 monsoon

### *5.1.1.2 Preliminary Analysis of the Inshore Wave Data*

Given the importance of the inshore wave records at Galle, and Kudawella and Kirinda in the calibration of the modeling, preliminary analysis of the data was undertaken. Like the CCD-GTZ data, Lanka Hydraulic Institute was able to supply ASCII files of wave height, period and direction for all three sites. Again it was not possible to check these files or to be certain that no filtering of the raw data had taken place.

Unfortunately the Galle data set has no information about inshore wave direction. Therefore analysis of the distribution of wave height against wave direction was not possible for this data set. However, for both Kudawella and Kirinda this analysis was possible, although the directional information for Kirinda had to be determined by analyzing the measured current components. Table 5.8 and 5.9 and tables 5.10 and 5.11 show the distribution of the overall wave climate with direction for both the SW and NE monsoon period at Kudawella and Kirinda respectively. Given the CCD-GTZ wave data is not suitable for deriving the wave climate during the NE monsoon, the Kudawella and Kirinda data sets were used.

### *5.1.1.3 Beach Profiles and Sediment Sampling*

As part of the topography and bathymetry survey, beach profiles were measured at 50m centres along the coastline on either side of the proposed fishing harbour. In addition, beach sediment samples were collected and particle size distribution analysis (PSD) was undertaken. This survey work was undertaken in October/ November 2001 and the results were supplied in the form of a set of profiles and two separate reports issued by Oceanography Division, National Aquatic Resources Research and Development Agency. These reports clearly showed that the beach profiles varied considerably along the frontage of Hambantota bay. At the western end close to the proposed harbour the beach was relatively steep and there was a minimal beach crest width. Meanwhile at the eastern end of the survey region close to the Peacock hotel the beach crest width was approximately 30-50m wide and the beach relatively shallow. The beach sediment analysis (or PSD's) confirmed that generally the beach material was fine-medium sand and there was no sorting or variation in the sediment grading along the bay frontage.

Wave Height (m)	Wave Direction (degrees)											
	0 - 30	30 - 60	60 - 90	90 - 120	120 - 150	150 - 180	180 - 210	210 - 240	240 - 270	270 - 300	300 - 330	330 - 360
0.00 – 0.25	0	0	0	0	0.087	0	0	0	0	0	0	0
0.25 – 0.50	0	0	0	0	0	0	0	0	0	0	0	0
0.50 – 0.75	0	0	0	0	0	0	0	0	0	0	0	0
0.75 – 1.00	0	0	0	0	0	0.261	0	0	0	0	0	0
1.00 – 1.25	0	0	0	0	0	12.1	1.567	0	0	0	0	0
1.25 – 1.50	0	0	0	0	0	28.72	4.265	0	0	0	0	0
1.50 – 1.75	0	0	0	0	0	24.8	2.437	0	0	0	0	0
1.75 – 2.00	0	0	0	0	0	15.23	0.696	0	0	0	0	0
2.00 – 2.25	0	0	0	0	0	7.137	0.261	0	0	0	0	0
2.25 – 2.50	0	0	0	0	0	2.089	0	0	0	0	0	0
2.50 – 2.75	0	0	0	0	0	0.348	0	0	0	0	0	0
2.75 – 3.00	0	0	0	0	0	0	0	0	0	0	0	0
<b>Total</b>	<b>0</b>	<b>0</b>	<b>0</b>	<b>0</b>	<b>0.087</b>	<b>90.69</b>	<b>9.225</b>	<b>0</b>	<b>0</b>	<b>0</b>	<b>0</b>	<b>0</b>

Number refer to 3hr wave records

**Table 5.8:** Percentage distribution of Kudawella overall wave data by direction sector for the SW monsoon

Wave Height (m)	Wave Direction (degrees)											
	0 - 30	30 - 60	60 - 90	90 - 120	120 - 150	150 - 180	180 - 210	210 - 240	240 - 270	270 - 300	300 - 330	330 - 360
0.00 – 0.25	0	0	0	0	0	0	0.141	0	0	0	0	0
0.25 – 0.50	0	0	0	0	0.141	0.704	0	0	0	0	0	0
0.50 – 0.75	0	0	0	0	8.592	19.01	2.535	0	0	0	0	0
0.75 – 1.00	0	0	0	0.141	19.86	25.21	3.521	0	0	0	0	0
1.00 – 1.25	0	0	0	0.282	4.93	11.97	0.986	0	0	0	0	0
1.25 – 1.50	0	0	0	0.141	0.704	0.986	0	0	0	0	0	0
1.50 – 1.75	0	0	0	0	0	0.141	0	0	0	0	0	0
1.75 – 2.00	0	0	0	0	0	0	0	0	0	0	0	0
<b>Total</b>	<b>0</b>	<b>0</b>	<b>0</b>	<b>0.563</b>	<b>34.23</b>	<b>58.03</b>	<b>7.183</b>	<b>0</b>	<b>0</b>	<b>0</b>	<b>0</b>	<b>0</b>

Number refer to 3hr wave records

**Table 5.9:** Percentage distribution of Kudawella overall wave data by direction sector for the SW monsoon

Wave Height (m)	Wave Direction (degrees)											
	0 - 30	30 - 60	60 - 90	90 - 120	120 - 150	150 - 180	180 - 210	210 - 240	240 - 270	270 - 300	300 - 330	330 - 360
0.00 – 0.25	0	0	0	0	0	0	0	0	0	0	0	0
0.25 – 0.50	0	0	0	0	0	0	0	0	0	0	0	0
0.50 – 0.75	0	0	0	0	0	0	0	0	0	0	0	0.15
0.75 – 1.00	0	0	0	0	0	0	0.60	1.19	2.09	0.30	0	0
1.00 – 1.25	0	0	0	0	0	0.75	11.19	25.97	14.63	1.04	0	0
1.25 – 1.50	0	0	0	0.15	0	2.84	15.08	13.28	2.54	0	0	0
1.50 – 1.75	0	0	0	0	0	1.19	5.22	1.19	0.15	0	0	0
1.75 – 2.00	0	0	0	0	0	0	0	0.15	0	0	0	0.15
2.00 – 2.25	0	0	0	0	0	0	0	0	0	0	0	0
2.25 – 2.50	0	0	0	0	0	0	0	0	0	0	0	0
2.50 – 2.75	0	0	0	0	0	0	0	0	0	0	0	0
2.75 – 3.00	0	0	0	0	0.15	0	0	0	0	0	0	0
<b>Total</b>	<b>0</b>	<b>0</b>	<b>0</b>	<b>0.15</b>	<b>0.15</b>	<b>4.78</b>	<b>32.1</b>	<b>41.80</b>	<b>19.4</b>	<b>1.34</b>	<b>0</b>	<b>0.30</b>

Number refer to 3hr wave records

**Table 5.10:** Percentage distribution of overall wave data by direction sector for the SW monsoon at Kirinda

Wave Height (m)	Wave Direction (degrees)											
	0 - 30	30 - 60	60 - 90	90 - 120	120 - 150	150 - 180	180 - 210	210 - 240	240 - 270	270 - 300	300 - 330	330 - 360
0.00 – 0.25	0	0	0	0	0	0	0.141	0	0	0	0	0
0.25 – 0.50	0	0	0	0	0.141	0.704	0	0	0	0	0	0
0.50 – 0.75	0	0	0	0	8.592	19.01	2.535	0	0	0	0	0
0.75 – 1.00	0	0	0	0.141	19.86	25.21	3.521	0	0	0	0	0
1.00 – 1.25	0	0	0	0.282	4.93	11.97	0.986	0	0	0	0	0
1.25 – 1.50	0	0	0	0.141	0.704	0.986	0	0	0	0	0	0
1.50 – 1.75	0	0	0	0	0	0.141	0	0	0	0	0	0
1.75 – 2.00	0	0	0	0	0	0	0	0	0	0	0	0
<b>Total</b>	<b>0</b>	<b>0</b>	<b>0</b>	<b>0.563</b>	<b>34.23</b>	<b>58.03</b>	<b>7.183</b>	<b>0</b>	<b>0</b>	<b>0</b>	<b>0</b>	<b>0</b>

Number refer to 3hr wave records

**Table 5.11:** Percentage distribution of overall wave data by direction sector for the NE monsoon at Kirinda

## 5.2 Wave Modelling

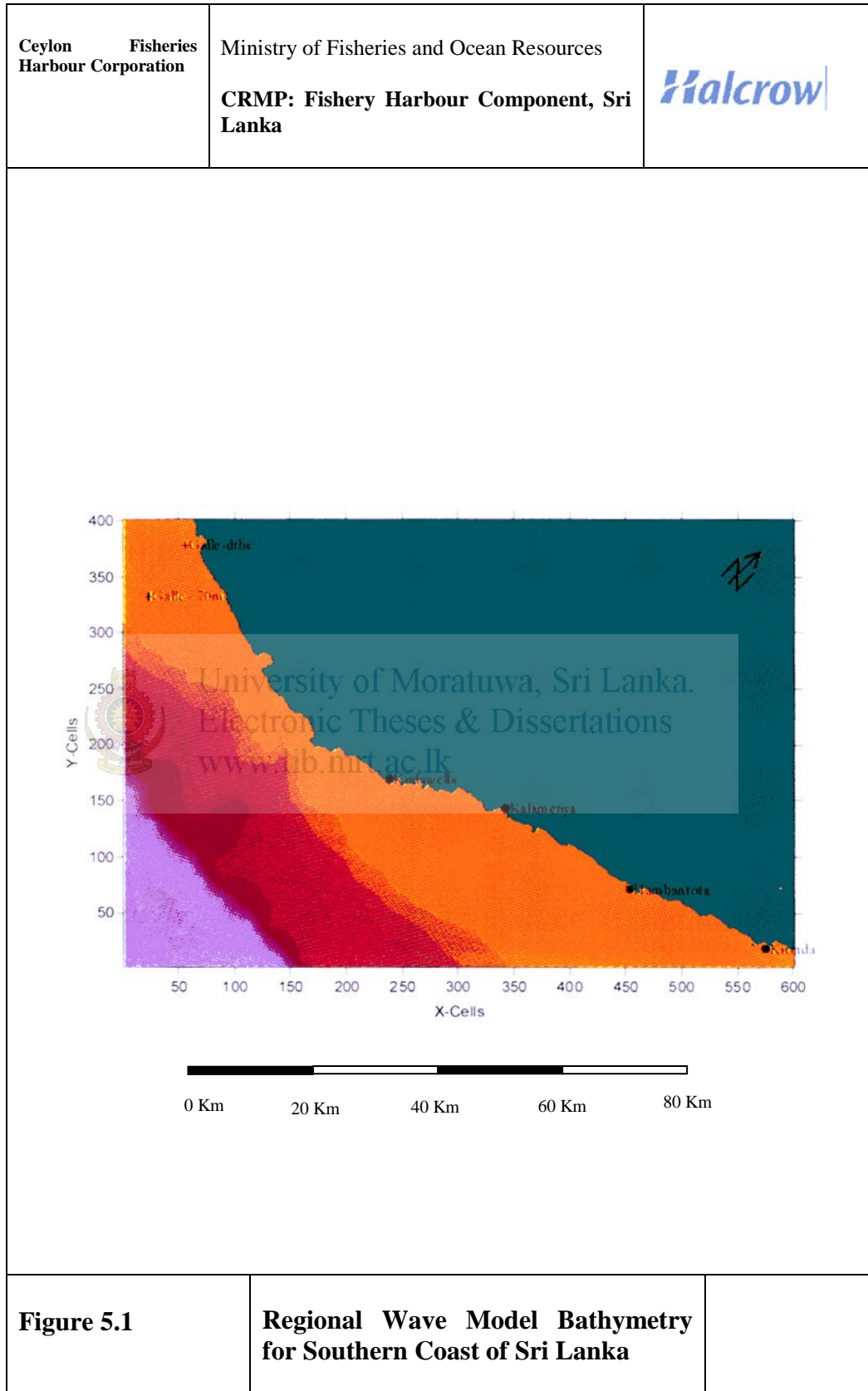
### 5.2.1 Model Basis

Recent advances in computer technology mean that mathematical modelling provides an alternative to physical scale modelling in tackling complex hydrodynamic problems. Mathematical models are particularly suited to design studies where a number of alternative layouts can be investigated without incurring large configuration costs.

The regional wave model MWAV\_REG is based on an evolution of the mild slope equation for water waves, which is described in more detail in Li (1994). It has been used in a wide range of different wave modelling applications and incorporates the effects of wave refraction, diffraction, breaking and bottom friction on a monochromatic wave field. Like MWAV\_REG the local wave model MWAV\_LOC is also based on an evolution equation of the mild slope equation for water waves (Li, 1994), but in addition also includes the effects of wave reflection off quay walls and other structures.







In order to derive the wave matrix for transforming the offshore wave data to inshore a total of 165 runs were undertaken. These runs consisted of 5 wave periods, 11 directions and 3 water levels as summarized in Table 5.12 below.

Parameter	Values modelled	Number of runs
Wave Height (m)	Unity (1.0)	1 No.
Wave Period (s)	3.0,6.0,9.0,12.0,15.0	5 No.
Wave Directions (degrees)	150, 165, 180, 195, 210, 225, 240, 255, 270, 285, 300	11 No.
Water Level (m)	-1.0,0.0,1.0	3 No.
	Total	165 No.

**Table 5.12:** Summary of MWAVE\_REG model runs undertaken

Halcrow's wave data transformation model MWAV\_TRN, was then used to transform each offshore wave record to a point in the shallower (20m depth) water nearer to the study site, and typical of the depth at the boundary of the local wave model. This inshore point is referred to as H1. This process results in a time series that represents a nearshore transformation of the offshore time series data. This model and processes has been successfully used for many similar projects around the world.

Having generated a time series inshore at point H1, the offshore wave data (Galle CCD-GTZ) time series was also transformed to three other sites within the model domain in order to calibrate and verify the wave model. The sites chosen were Galle, Kudawella and Kirinda. By comparing the predicted time series to actual measurements it was possible to adjust the inshore wave climate time series derived at Hambantota.

Once the nearshore wave time series has been calibrated, analyses of the extreme wave heights were undertaken for each nearshore direction sector. The nearshore wave heights were analyzed according to frequency distribution. The results of this analysis are presented in Table 5.13, which shows that the dominant wave direction is from 210 – 240.

Table 5.13 also shows that the waves are predominantly from directions 150 to 240, and so the waves used in the wave analysis were those from the sectors 150 to 240.

Wave Height (m)	Wave Direction (degrees)											
	0 - 30	30 - 60	60 - 90	90 - 120	120 - 150	150 - 180	180 - 210	210 - 240	240 - 270	270 - 300	300 - 330	330 - 360
0.00 - 0.25	0	0	0	0	0	0	0	0	0	0	0	0
0.25 - 0.50	0	0	0	0	0	0	0	0	0	0	0	0
0.50 - 0.75	0	0	0	0	0	0	0	0.04	0	0	0	0
0.75 - 1.00	0	0	0	0	0	0	0.14	0.04	0	0	0	0
1.00 - 1.25	0	0	0	0	0	0	0.51	0.1	0	0	0	0
1.25 - 1.50	0	0	0	0	0	0.03	1.74	0.5	0	0	0	0
1.50 - 1.75	0	0	0	0	0	0.26	4.31	1.17	0	0	0	0
1.75 - 2.00	0	0	0	0	0	0.45	6.94	2.46	0	0	0	0
2.00 - 2.25	0	0	0	0	0	0.4	7.5	5.59	0	0	0	0
2.25 - 2.50	0	0	0	0	0	0.9	6.09	6.2	0	0	0	0
2.50 - 2.75	0	0	0	0	0	3.73	5.65	5.21	0	0	0	0
2.75 - 3.00	0	0	0	0	0	8.21	5.05	3.96	0	0	0	0
3.00 - 3.25	0	0	0	0	0	5.61	4.07	4.23	0	0	0	0
3.25 - 3.50	0	0	0	0	0	0.97	0.95	3.63	0	0	0	0
3.50 - 3.75	0	0	0	0	0	0	0.4	2.03	0	0	0	0
3.75 - 4.00	0	0	0	0	0	0.25	0.59	0.09	0	0	0	0
<b>Total</b>	<b>0</b>	<b>0</b>	<b>0</b>	<b>0</b>	<b>0</b>	<b>20.80</b>	<b>43.95</b>	<b>33.25</b>	<b>0</b>	<b>0</b>	<b>0</b>	<b>0</b>

Number refer to 3hr wave records

**Table 5.13:** Percentage distribution of nearshore wave data at H1 by direction sector

In order to derive extreme wave conditions for the dominant wave directions, wave data from the 3 sectors covering 150 to 240 were used to determine best-fit Weibull and Gumbell distributions using Halcrow's model MWAV\_FIT. Frequently the Weibull distribution provides best fits to extreme wave height data, but for this study the results reveal that the Gumbell fits were more reliable. The predicted results from the Gumbell distribution for 1 in 1, 1 in 20 and 1 in 50 year extreme significant wave conditions are shown in Table 5.14. The wave records are at three hourly intervals, and all records within a particular direction sector were used. The percentage of the wave data in the

particular direction sector over whole wave records (all directions) was an input parameter of the MWAVE\_FIT model.

Wave Direction (degrees)	1 in 1 year		1 in 20 year		1 in 50 year	
	Hs	Tz (s)	Hs	Tz (s)	Hs	Tz (s)
150° - 180°	2.306	8.6	3.037	9.9	3.261	10.2
180° - 210°	4.925	12.6	6.546	14.5	7.043	15.0
210° - 240°	4.255	11.7	5.691	13.5	6.131	14.0

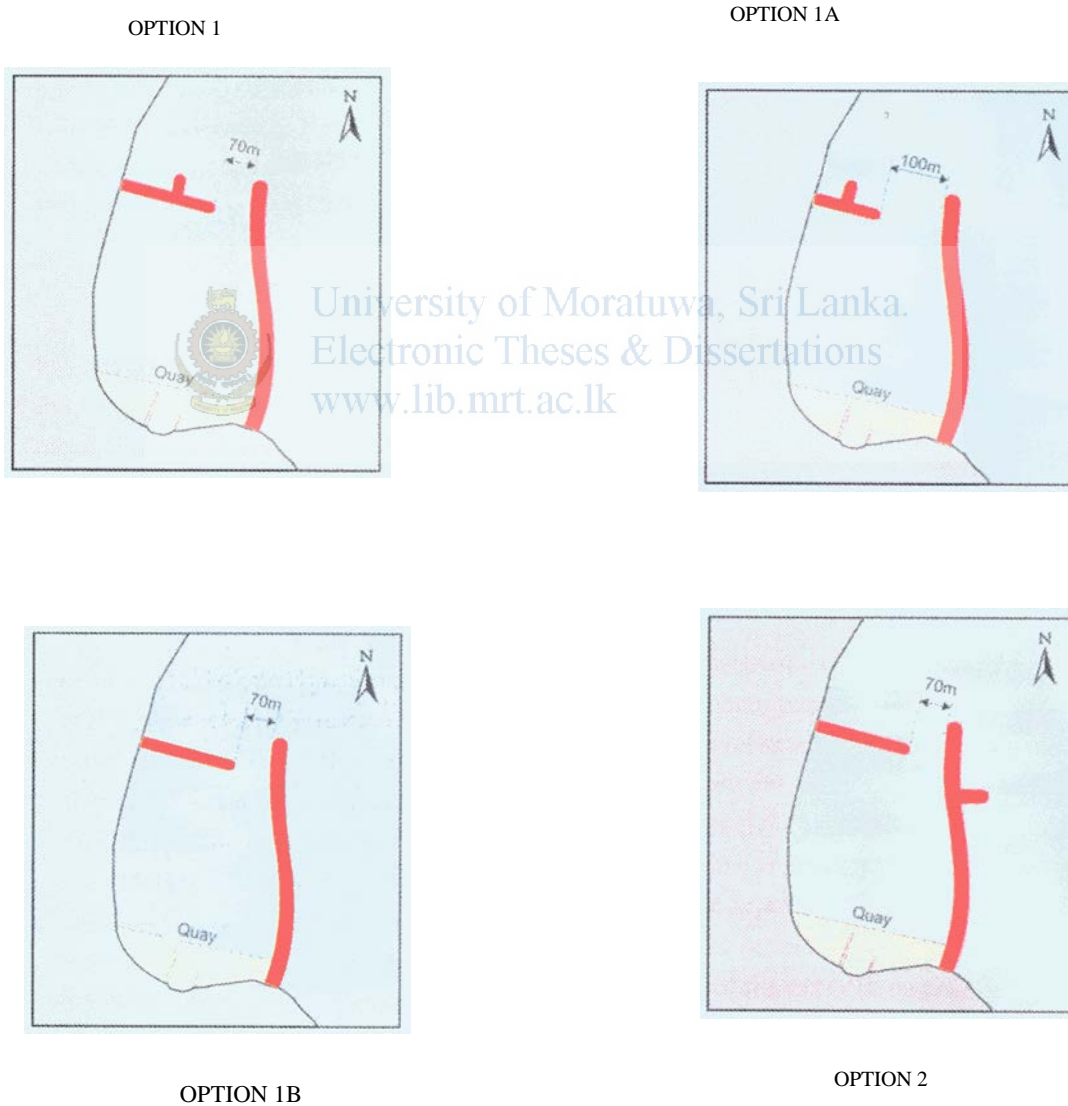
**Table 5.14:** *Extreme Wave Heights predicted for nearshore point H1*

The results in Table 5.14 along with other derived wave extremes were used to estimate the design conditions at the boundary of the local wave model.

## 5.2.2 Local Wave Modelling

Local wave modelling consisted of two phases. The first phase was the harbour layout optimization and the second phase was the wave penetration (or harbour disturbance) modelling. The following section briefly discusses the modelling work undertaken.

### 5.2.2.1 Harbour Layout Optimization



PROPOSED FISHING HARBOUR, HAMBANTOTA

**Figure 5.2:** *Layout Options*

In order to minimize runtimes, the regional wave model MWAV\_REG was used to optimize the harbour layouts. The model domain consisted of 309 cells by 308 cells with a mesh size of 10m and covered the Hambantota bay area only. The model was used to optimize four harbour layouts/permutations and these are shown in Figure 5.2. The boundary wave conditions used for the modelling were the 1 in 1, 5, 10, 20 and 50 year wave extremes for various directions. This resulted in a total of 95 model runs being undertaken for each permutation and these consisted of 60 wave scenarios for the SW monsoon period and 35 for the NE monsoon period.

The harbour optimization modelling has revealed that the recommended layout is Option 2. The entrance width has been increased from 70m to 100m to improve tidal flushing and reduce harbour resonance. The stub has been retained on the northern breakwater to minimize sediment movement from the beach area into the harbour entrance.

In addition, the wave model results were also used to supply the design wave conditions for the breakwater structures.



University of Moratuwa, Sri Lanka.  
Electronic Theses & Dissertations  
www.lib.mrt.ac.lk

#### *5.2.2.2 Wave Penetration Modelling*

The wave model used to study wave penetration into the proposed fishing harbour is MWAV\_LOC. The model was developed from an evolution equation solution to the mild slope equation for water waves (Li, 1994). The evolution equation is a time dependant parabolic equation and its solutions will approach the results of the elliptical mild-slope equation at time increases. A perturbation method was used to derive the evolution equation. The equation takes into account the combined effects of refraction, diffraction, wave reflections and wave breaking. The mild slope equation is derived from the exact linearised governing equations of irrotational flow in the three dimensional domain under the assumption that the bottom varies very slowly over one wavelength. It reduces to the Helmholtz diffraction solution for constant water depth on the one hand and to the long wave equation for shallow water on the other hand. The accuracy of the equation is still satisfactory for a bottom slope of the order of unity.

The calculation results from the regional wave model MWAV\_REG were used as the boundary conditions for the wave penetration model MWAV\_LOC. Like the local MWAV\_REG modelling discussed above, a total of 95 MWAV\_LOC model runs were undertaken. The grid spacing for the wave penetration model was 5 metres so that waves propagating into the harbour can be calculated accurately with a fine grid size.

A typical model result is shown in Figure 5.3 for a 1 in 50 year wave extreme from the NE monsoon direction. This model result clearly demonstrates that the wave heights within the proposed harbour are significantly reduced when compared to the wave heights outside the harbour. The worst wave directions are for the NE monsoon period when waves approach the harbour entrance from 90 -120 degrees. The local wave modelling study reveals that there is no significant wave penetration ( $H_s > 0.3\text{m}$ ) for the proposed harbour and hence no downtime calculations have been determined.



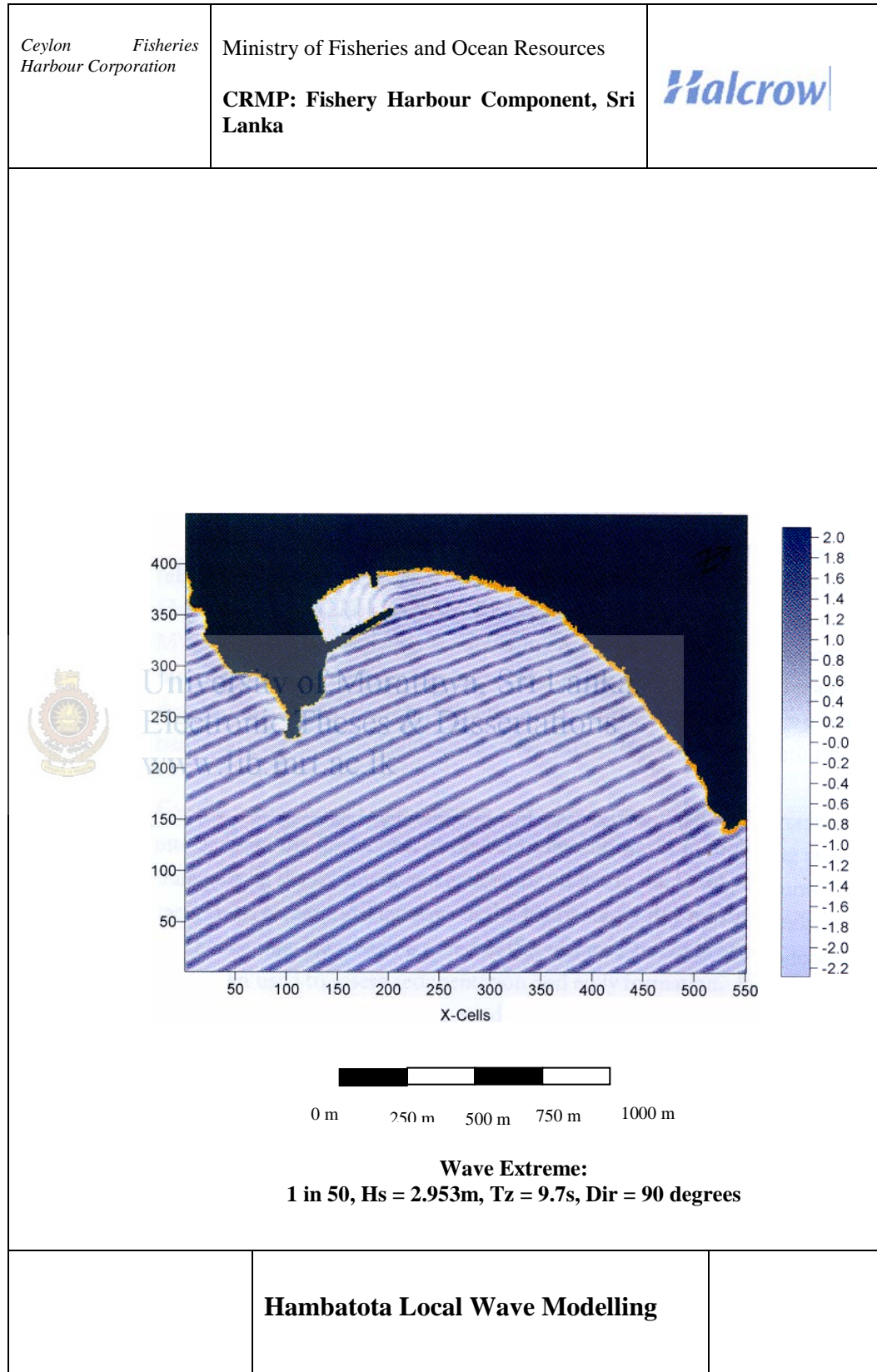


**Figure 5.3:** Typical wave penetration model result



### 5.2.3 Wave- Induced Current Modelling

In addition to tidal flow, currents can be generated by the action of waves. In the vicinity of structures wave-induced currents can have a significant effect on local sediment movements. Wave breaking also induces currents in shallow water. In order to avoid excessive scour or deposition the influence of wave-induced currents must be considered. The model MWAV\_WIC provides an efficient and up to date means of determining the patterns of wave- induced currents in the vicinity of complex bathymetry and surface piercing structures. The numerical model MWAV\_WIC solves a linear elliptical partial differential equation for wave- induced currents. It is based on the linearised depth-integrated flow equation for two horizontal dimensions. It includes the wave radiation stresses and a linear bed shear stress formula. A stream function representation of the velocity field results in an elliptical equation, which is solved using the method of successive over relaxation. The model takes as input wave heights and directions computed by Halcrow's wave models MWAV\_REG or MWAV\_LOC Results from MWAV\_WIC are produced as current speeds and directions at each point in the model grid. The results can provide valuable data for harbour and breakwater design, design of offshore structures or reefs, investigating the effect of shoals and banks on nearshore morphological development or beach stability study.

For the modelling of sedimentation and eddy formation, it is important to take into account the interaction of tidal currents and waves in mobilizing and transporting the sediment and generating eddies in the lee of structures. As mentioned earlier, tidal currents in the Hambantota Bay region are relatively weak and hence they have been ignored in this instance and only wave-induced currents have been used to assess sedimentation and eddy formation. Halcrow's grid based wave model MWAV\_REG was used to define the wave conditions across the whole model domain for the sedimentation and eddy formation modelling studies and were used as input data for the wave- induced current model MWAV\_WIC. An example of a typical wave-induced current pattern is shown in Figure 5.4

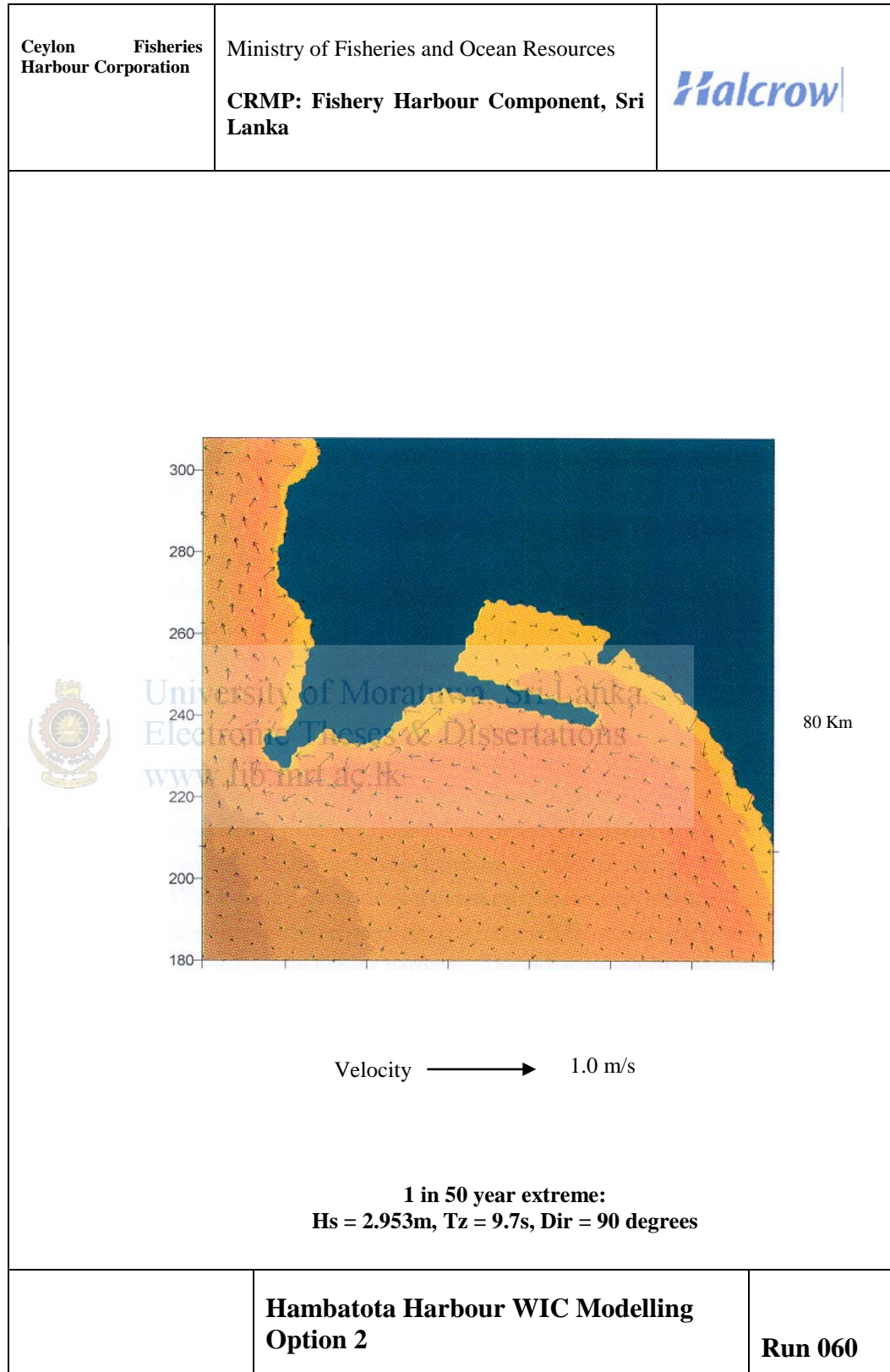


**Figure 5.4:** Typical wave-induced current pattern

## **5.3 Modelling of Sediment Movements**

### **5.3.1 General**

Sediment transport and beach evolution within Hambantota Bay has been investigated using two mathematical models. Both these models have been developed in house at Halcrow and have been tried and tested over several years, and yet incorporate the latest developments in the field. Where possible the models are normally calibrated against available field data. However, it should be noted that sediment transport is notoriously difficult to model; at best, models can only be expected to reproduce trends in real data and order of magnitude estimates of sediment movements.

### **5.3.2 Alongshore Drift**

The beach evolution in response to the proposed fishing harbour has been modelled with Halcrow's Beach Plan Shape Model (BPSM). BPSM is a fully evolutionary one line beach model that updates the beach plan position after calculating the alongshore drift rate for every wave record in a time series.

For this study BPSM has been driven using 6 years of time series wave data and the transformation coefficients derived from the additional regional wave modelling which was undertaken for the Hambantota Bay only. Wave transformation results are therefore available at 10m resolution and hence, the BPSM model has also been based on the same regular 10m grid. The BPSM grid extends between a point approximately 2000m east of the proposed fishing harbour, to the fishing harbour. The origin of the BPSM grid is approximately at 241110E, 103145N, and the grid is orientated with an offshore normal at a bearing of 180 degrees.

As mentioned earlier, it is normal to calibrate and verify BPSM by comparing the modelled alongshore drift rate on the open coast to actual measurements of alongshore drift rate obtained from analysis of regular beach surveys or aerial photographs.

Unfortunately, due to lack of beach profile data (1 year only) and due to sporadic data collection along the Sri Lanka coastline, it was not possible in this instance to calibrate the BPSM model.

Therefore the BPSM model has been used as tool to indicate potential changes in coastline response by comparing the effect of constructing a fishing harbour in the western corner of Hambantota bay. The results show that in general the drift rate for a SW monsoon period is in an easterly direction. The potential movement of sediment in anyone year may vary considerably by up to:  $50,000$  to  $150,000$  m<sup>3</sup>/year, but general the net movement is relatively small at around  $5,000$  - $15,000$  m<sup>3</sup>/year. Figure 5.5 shows the predicted coastline with and without the proposed fishing harbour over the next 25 years and clearly shows the impact of the proposed fishing harbour on the general bay shape is negligible.

Wave data for the NE monsoon period is available from two sources (Kirinda and Kudawella). However, both these wave records are measured close inshore and are affected by the headlands. In addition, these time series are short in time frame at just over a year in length. Given all these factors it was not technically viable to use either of these data sets for assessing the potential alongshore movement of sediment during the NE monsoon period at Hambantota. However, from numerous site visits and by speaking to local fishermen, it appears that the beach has a tendency to accrete in the corner close to the proposed fishing harbour. This may lead to an increase in beach crest width by up to 50m. Based on this information, it is anticipated that the general drift in the bay is relatively constant between monsoon periods and that some build up against the harbour breakwater will occur during the NE Monsoon period, although precise estimates are not possible. For this reason, a stub has been provided on the northern breakwater to prevent sediment moving along the breakwater into the harbour entrance. Furthermore, it is also expected that this accretion along the breakwater will not cause a significant problem since, under a SW monsoon it is anticipated that the beach will erode close to the fishing harbour. However, this situation will need to be carefully monitored and if necessary

preventative measures like sediment bypassing or recycling may need to be undertaken to prevent siltation of the harbour entrance.

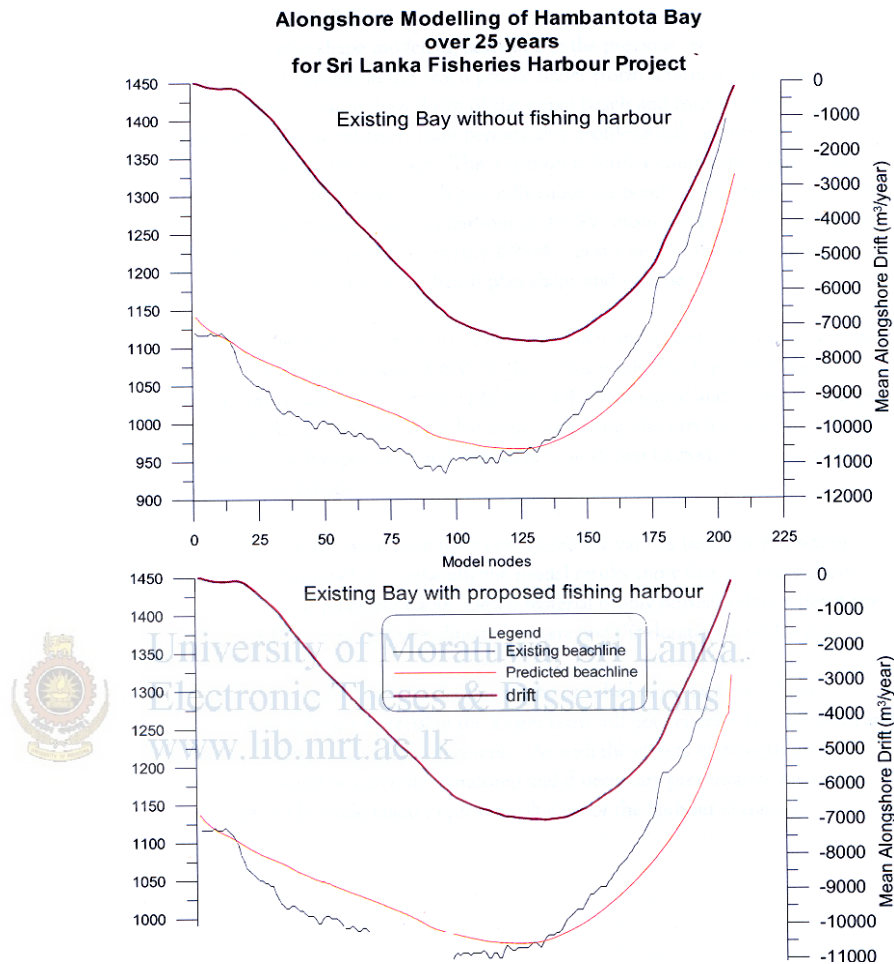


**Figure 5.5:** Typical alongshore model result

### 5.3.3 Cross-shore Modelling

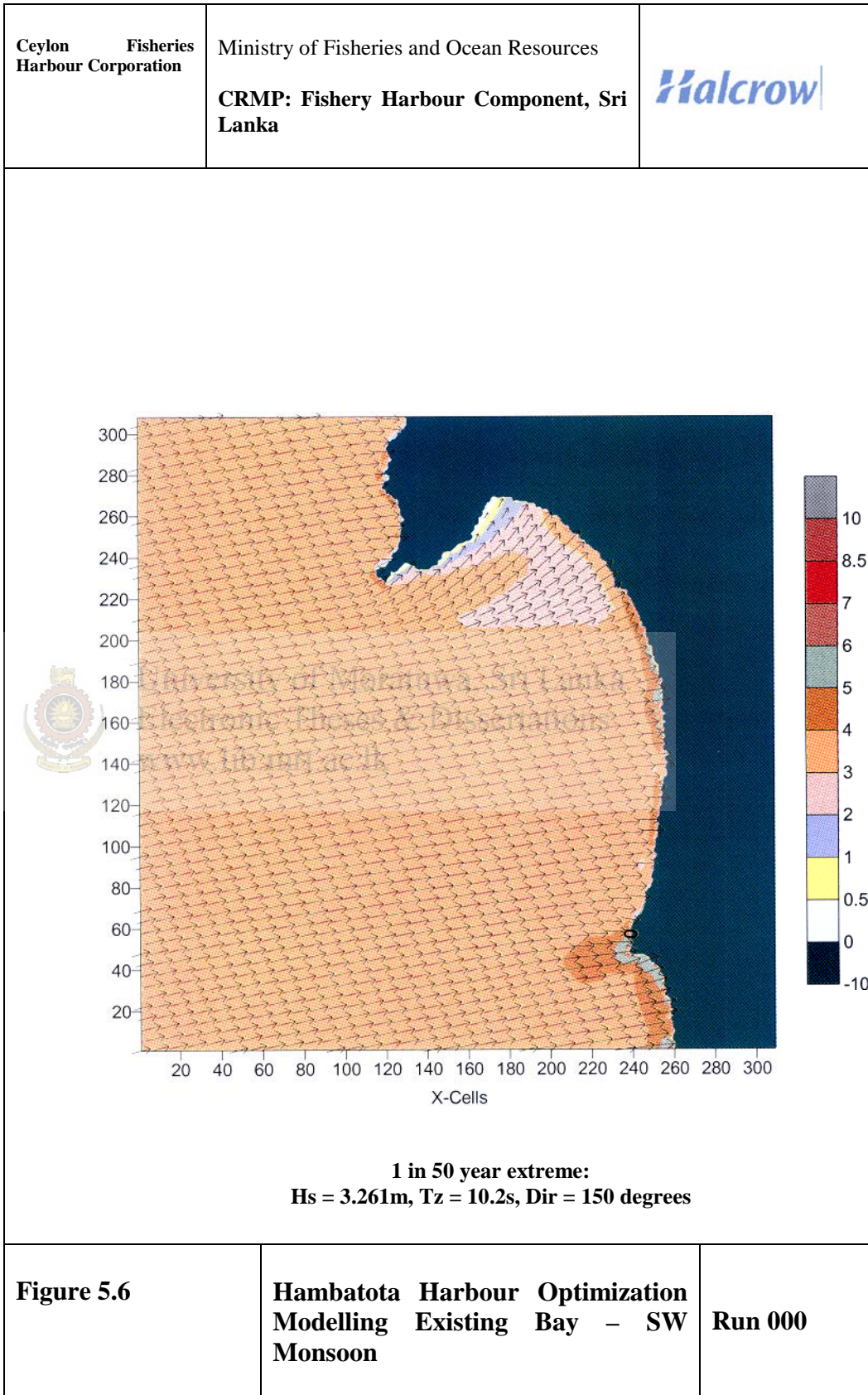
The beach plan shape modelling described in the previous section does not take into account changes in the beach profile under storm action. It is normal for storm waves to cause draw down of the upper beach and formation of a bar offshore. During relatively calm periods, this profile usually adjusts, with rebuilding of the upper beach. This

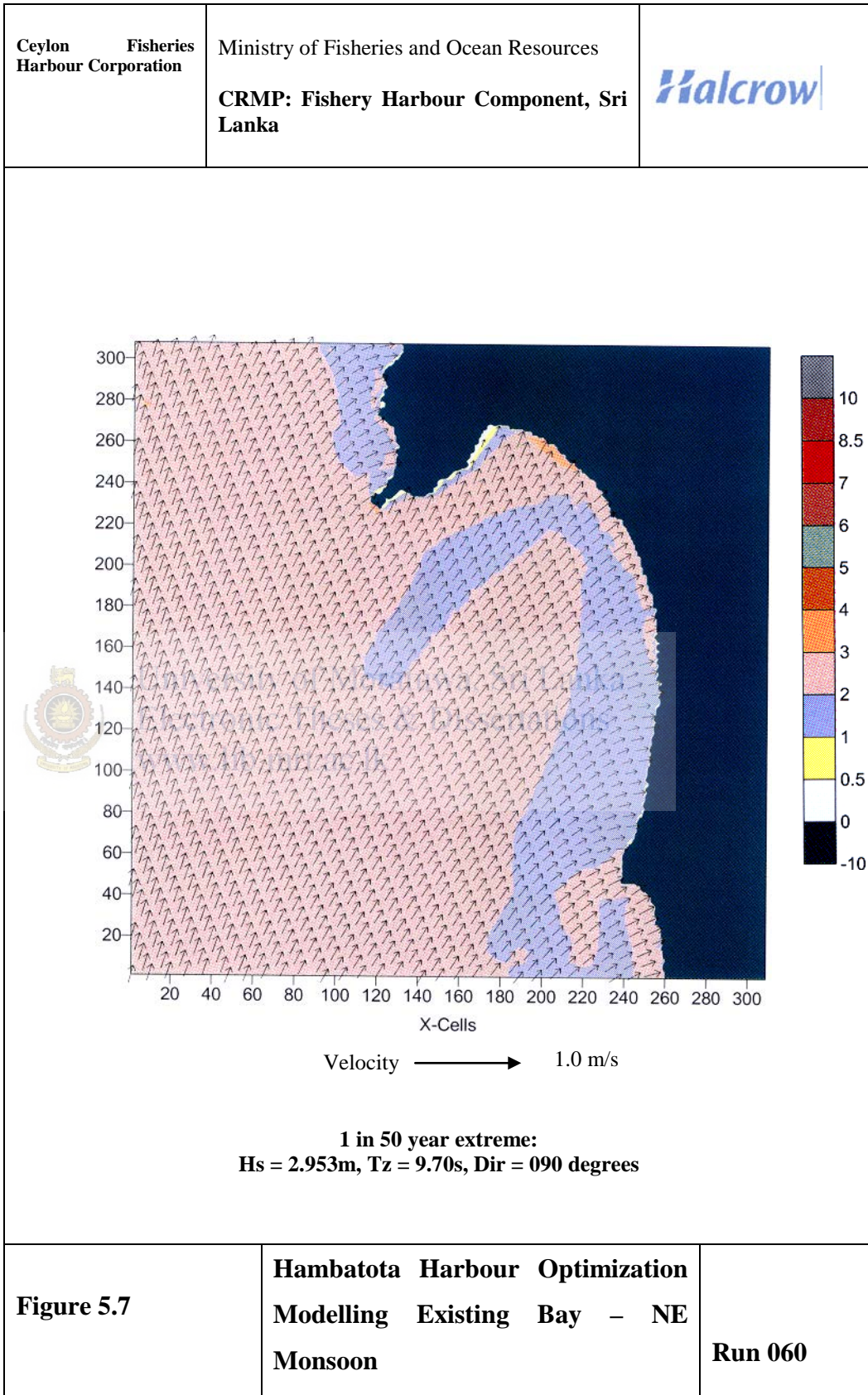
situation is further complicated in Sri Lanka by the monsoon periods, which generally cause the beach to be drawn down in the region of the proposed fishing harbour under SW monsoon periods and built up during the NE monsoon. Therefore BPSM is best suited to the assessment of longer term gross changes in beach plan shape and volume.

Beach profile modelling of storm events has been undertaken with Halcrow's two-dimensional profile model COSMOS\_2D. This model has been developed in a collaborative agreement between Halcrow, HR Wallingford and Imperial College, London. Recent reviews in the literature comparing the various cross-shore models in use by specialists and engineers have shown COSMOS\_2D to be the best all round model.

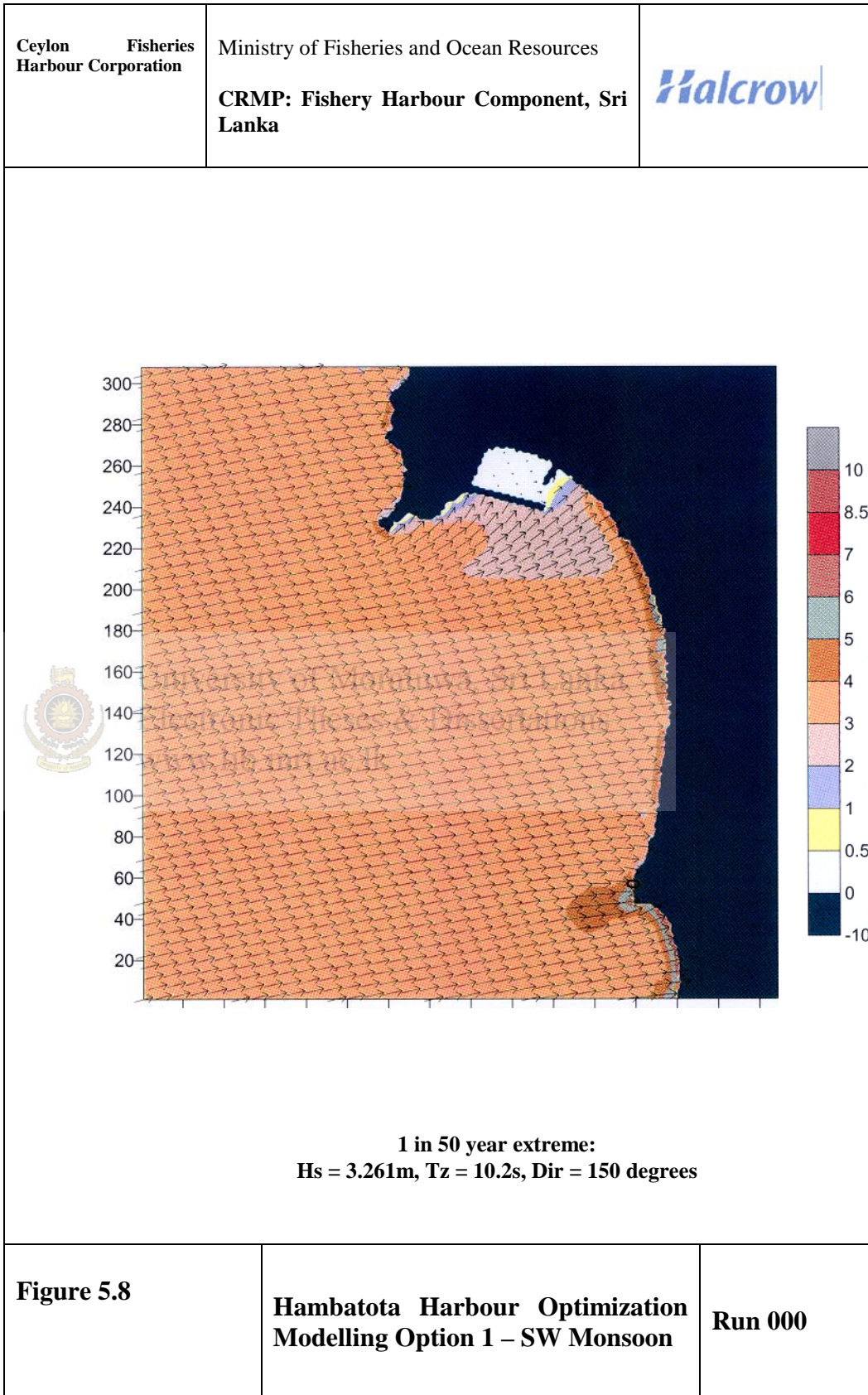
Several model scenarios have been considered for various beach cross sections along Hambantota bay. Generally the model results show that the cross-shore beach profile is relatively stable. Beach material is only normally drawn down the beach profile when the wave climate is severe and the duration is prolonged.

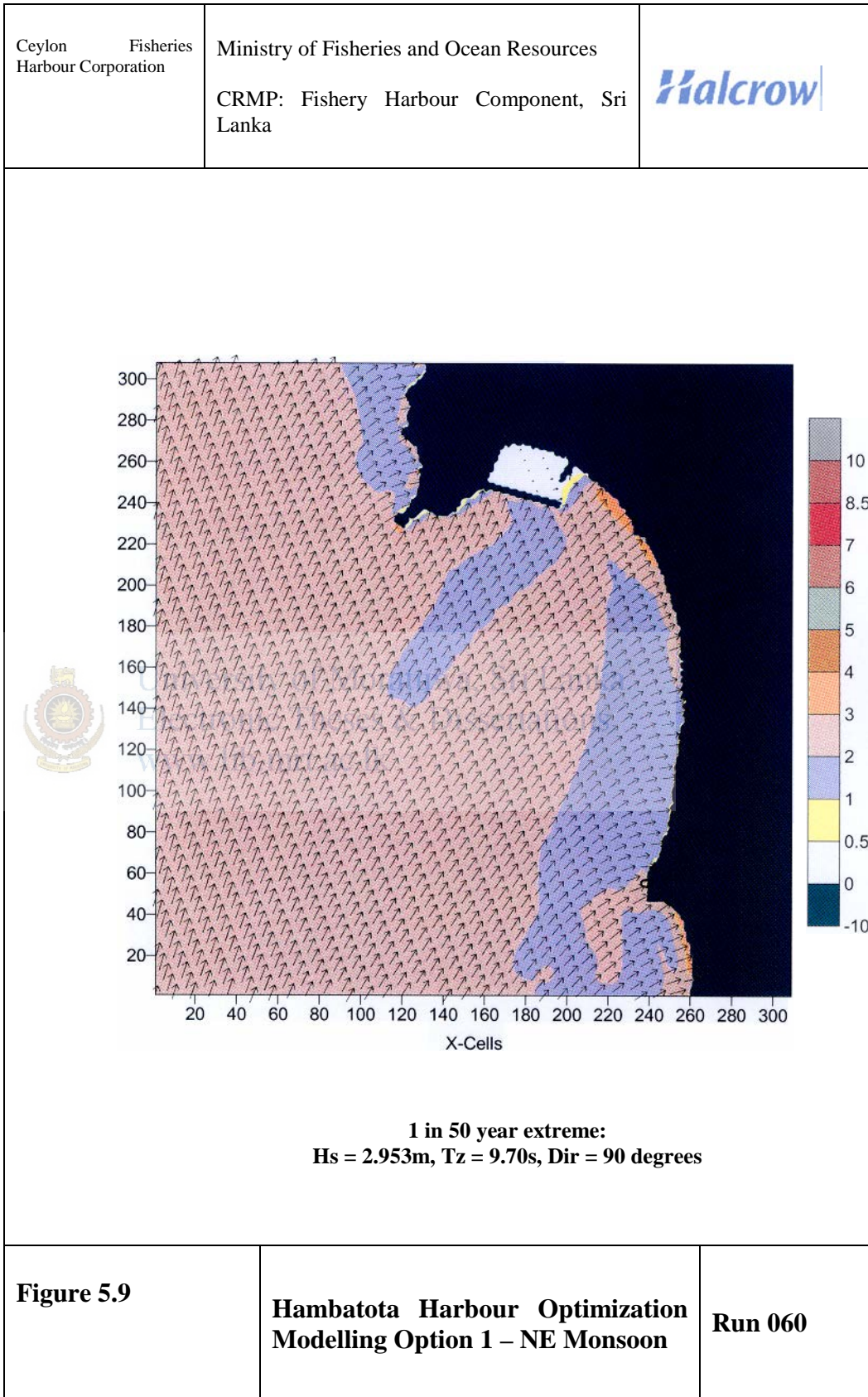
Based on the cross-shore model results, the conclusion is that cross-shore movement of beach material in the longer term will not generally be a problem and that any short-term effects will reverse. As with the effects of alongshore drift, situation should be carefully monitored and if necessary preventative measures may need to be undertaken to prevent siltation of the harbour entrance.

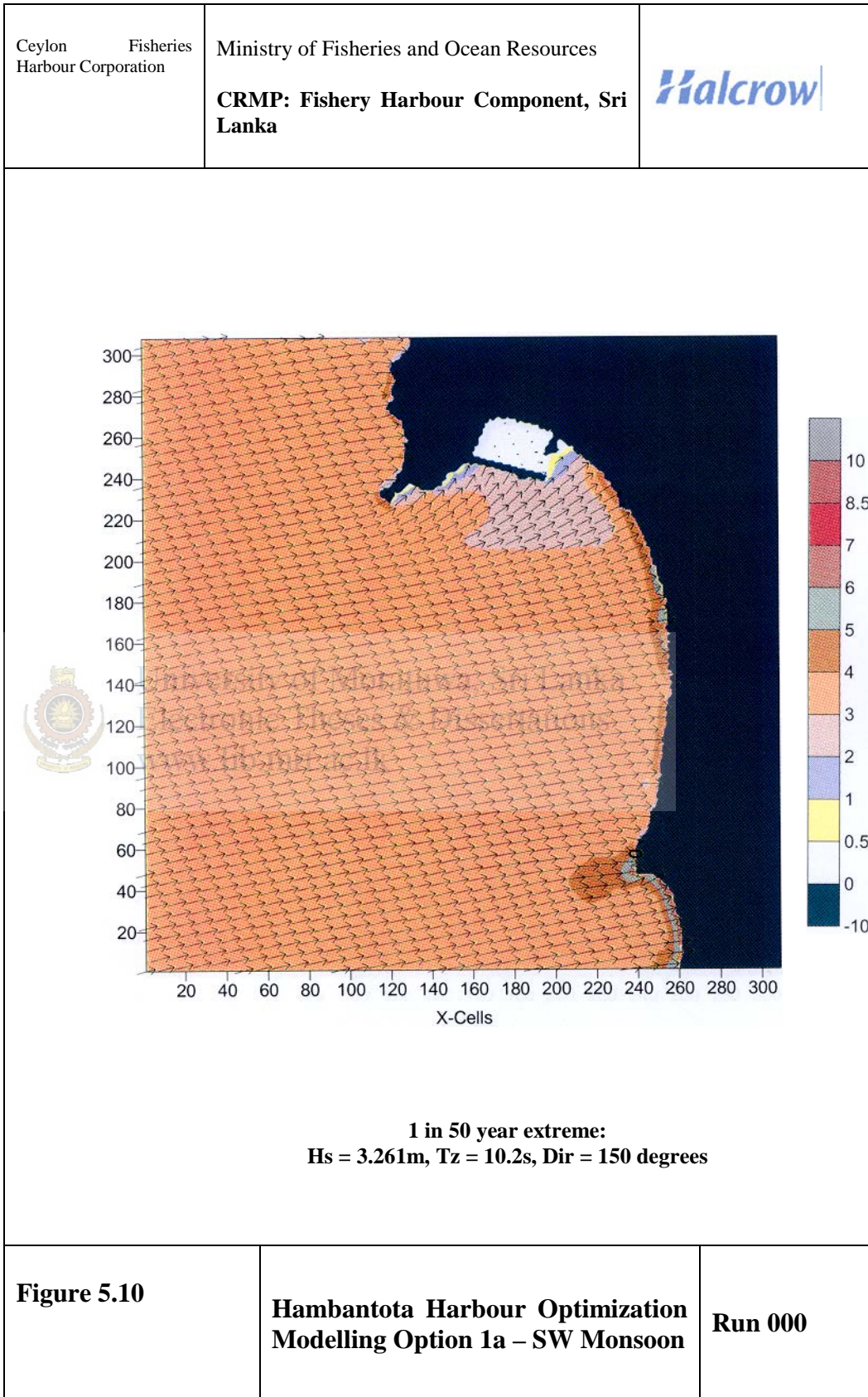












## CHAPTER – 6



University of Moratuwa, Sri Lanka.  
Electronic Theses & Dissertations  
[www.lib.mrt.ac.lk](http://www.lib.mrt.ac.lk)

# CONCLUSIONS AND RECOMMENDATIONS

## 6.0 Conclusions

### 6.1 Design of Sediment Transport Model

From the identified flowchart of development the following tasks were completed as the preliminary stage of *SandPro* – the Sediment Transport Model.

- Identification of theories and numerical solutions for the whole process
- Validity of theories behind the period for which the entire process is implemented
- Reliability of theories and the degree of suitability for the real-world implementation of *SandPro*
- Overall design for data flow between elements
- Sub-divisions of the whole process
- Detailed design of each process
- Design and Analysis of each modularized process
- Walkthrough the design

The development process of the model is identified as an on-going research which should be guided through the next stages which are mentioned as follows:

- Nature of development (Isolated program or as a part of another application platform)
- Coding and Testing (Development)
- Development as *identified*
- Develop *SandPro* as a part of *ArcView* GIS engine
  - Develop Dynamic Link Libraries for each modularized process
  - Develop avenue modules for internal data processing
    - Input data
    - Surface interpolation and create bathymetry
    - Defining Structures and other coastal elements alongshore
  - Create customized GUI through *ArcView* GIS and Call Win 32 dlls for external operations

- Test the development with number of testing data
  - Determine how realistic the results are
  - Fine-tune the design
  - Sensitivity Analysis and determine global system variables
  - Revise the development
  - Modify the GUI to make the program consider about System dependant variables
- Once the development proves to be reliable and suitable in its results, incorporate all functionality and carry out an isolated design

With the completion of the above model it would possess the following features and would always be one of the most sophisticated models for the processing of Alongshore Sediment Flow.

Features of the Model:

- The shoreline boundary can be very irregular in shape;
- The model will consist of continuous set of runs for a period that is required to observe;
- With each run the Bathymetry is updated (Bathymetry update interval has to be fed in);
- Since the algorithm is efficient the bathymetry update interval can be very low;
- The model is of dynamic nature, (with each run the model could accept a new wave climate from wave series)
- With GIS, and GUI enhancement the model would show the bathymetry and sand accumulation in 2D/3D graphic forms;

## 6.2 Proposed Fishery Harbour at Hambantota Bay

- a) The regional wave model MWAV\_REG and wave data transformation model MWAV\_TRN have been used to generate the nearshore wave climate near to Hambantota for the SW monsoon period. Offshore wave condition was obtained from Galle CCD-GTZ and inshore measurement points at Galle DTBS and Kudawella/Kirinda.
- b) To derive nearshore wave climate for the NE monsoon period the measured wave climate at Kudawella and Kirinda have been compared and the worst case has been assumed to be applicable for Hambantota bay.
- c) The nearshore wave heights were analyzed according to frequency distribution. The results of the analysis show that the dominant wave direction is from 150–210 degrees for the SW monsoon and 90–120 degrees for the NE monsoon period. The nearshore extreme wave conditions were obtained from extreme value analysis model MWAVE\_FIT and they are used as boundary conditions for the local wave modelling.
- d) Local wave modelling has been undertaken using models. Firstly MWAV\_REG was used to optimize the proposed harbour layout and determine wave design parameters on the external faces of the breakwaters and secondly MWAV\_LOC was used to investigate wave penetration.
- e) The local wave modelling results using MWAV\_LOC demonstrate that the wave height inside the new harbour is significantly reduced compared to the wave height outside the harbour. The worst direction is 90 degrees, which occurs under the NE monsoon period. The local wave modelling study also reveals that there is no significant wave penetration problem for the proposed fishing harbour (i.e.  $H < 0.3$ )
- f) The nearshore wave data was also used as boundary conditions for the wave induced current model MWAV\_WIC, which provides wave and current results for the assessment of sedimentation and eddy formation. This work has concluded that, although an eddy will form close to the harbour entrance, its magnitude will be relatively weak. This eddy will possibly promote sediment movement and it is

likely that a small amount of siltation will accumulate in the harbour entrance area. Periodic maintenance dredging will be required to minimize the impact of this bar formation.

- g) Alongshore and cross-shore modelling of the existing bay was undertaken to investigate the likely consequence on beach evolution. The results of the modelling have shown that generally the fishing harbour will have a minimal effect on alongshore and cross-shore beach movement although the bay is highly mobile and susceptible to rapid change in severity of the wave climate. Periodic maintenance dredging might be required to minimize the impact of this beach accumulation at the harbour entrance.



University of Moratuwa, Sri Lanka.  
Electronic Theses & Dissertations  
[www.lib.mrt.ac.lk](http://www.lib.mrt.ac.lk)



### 6.3 Proposed Fishery Harbour at Negombo

- a) The regional wave model MWAV\_REG and wave data transformation model MWAV\_TRN have been used to generate the nearshore wave climate near to Hambantota for the SW monsoon period. Offshore wave condition was obtained from Galle CCD-GTZ.
- b) It was assumed that NE wave climate affected by NE monsoon would not be critical as much as the wave climate induced by SW monsoon.
- c) The nearshore wave heights were analyzed according to frequency distribution. The results of the analysis show that the dominant wave direction is from 180–270 degrees for the SW monsoon. The nearshore extreme wave conditions were obtained from extreme value analysis model MWAVE\_FIT and they are used as boundary conditions for the local wave modelling.
- d) Local wave modelling has been undertaken using models. Firstly MWAV\_LOC was used to optimize the proposed harbour layout with alterations to the original breakwater layout, and determine wave design parameters on the external faces of the breakwaters and secondly it was used to investigate wave penetration.
- e) The local wave modelling results using MWAV\_LOC demonstrate that the wave height inside the new harbour is significantly reduced compared to the wave height outside the harbour. The worst direction is 270 degrees, which occurs under the SW monsoon period. The local wave modelling study reveals that there are areas with significant wave penetration problem for the proposed fishery harbour with modified layout of breakwaters. However with further alterations such as elongation of the longer breakwater further, to cover the critical wave direction of 270 or proposing another offshore breakwater further away from current breakwater layout towards west direction could eliminate and reduce the wave heights at nearshore area.

## **BIBLIOGRAPHY**



University of Moratuwa, Sri Lanka.  
Electronic Theses & Dissertations  
[www.lib.mrt.ac.lk](http://www.lib.mrt.ac.lk)

## **1.0 IHO S44 Standards for Hydrographic Surveys and the Variety of Requirements for Bathymetric Data**

### **1.1 Intended uses for bathymetric data**

The traditional mandate of hydrography has been to survey, chart and supply all spatial information required to assist in safe navigation, and safety of life at sea, primarily for those commercial shipping vessels which fall under the conditions of the Safety of Life at Sea (SOLAS) convention administered by the International Maritime Organization (IMO).

However, driven by technological change, hydrographic needs and capabilities are becoming more broadly concerned with the management of spatial information concerning all marine features, processes and properties in four dimensions (space and time) including the acquisition, analysis and visualization of this spatial information (Kenny, 2000; Hecht, 2001; Monahan *et al*, 2001). Bathymetry is that aspect of hydrography that is concerned with delineating the marine floor, including features of both natural origin and those due to human activity. Bathymetric mapping has four broadly defined intended uses: to improve knowledge and understanding; to establish sovereignty and security; economic purposes (including offshore resource management and shipping) and environmental management.

Hydrographic information, in particular bathymetric information, is used to make informed decisions of several types: for example vessel navigation decisions; resource management decisions; resource development decisions; marine infrastructure decisions; marine construction decisions; coastal development decisions; tactical and strategic military decisions and environmental management decisions. The confidence with which such decisions can be made depends on the confidence that can be placed on the hydrographic (and other) information available to assist in making informed decisions. It is consequently critical that users be informed of the uncertainty associated with the data and with products constructed from it. For suppliers of bathymetry to provide information about uncertainty, they must first assess it. They are aided in this assessment by

mathematical tools and an international standard, S44 of the International Hydrographic Organization (IHO, 1998).

## 1.2 Assessment of uncertainty in bathymetric data

The uncertainty associated with bathymetric measurements includes (a) uncertainty in the location of a measured bathymetric data point; (b) uncertainty in the depth associated with a bathymetric data point and (c) uncertainty in the backscatter strength associated with a bathymetric measurement.

Bathymetric uncertainty management involves both the design of a bathymetric system and the evaluation of results and products derived from bathymetric data. Measurements are always uncertain, to a greater or lesser degree. Uncertainties are of three fundamentally different types: *accidental*, *systematic* and *random*. Each type must be dealt with differently. A common characteristic shared by all three, however, is that the reliability with which we can determine uncertainty is completely dependant upon the degree to which the bathymetric data is redundant (repeated measurements of the same seabed feature, or even footprint, which can be directly compared to ascertain consistency).

'Data cleaning' describes methods used to deal with 'accidental' uncertainties, (also called mistakes, blunders, or outliers). Comparison of a suspected outlier with its geographical nearest neighboring data points (taking hydrographic judgment into account) is the most powerful data-cleaning tool. A rule of thumb which has emerged for cleaning high-density bathymetric data is that real features are distinguished from points created accidentally according to whether multiple consistent data points (multiple 'hits') in close proximity are observed or not.

'Artifact' describes the effect of a systematic uncertainty. 'Artifact detection' and, where possible, 'artifact removal' describe further steps in the data-cleaning process. Artifacts are most often manifested as identifiable artificial features in a data series, with a strong correlation in time or space with some other data series. Effective artifact detection requires dense data, and powerful visualization tools.

Whatever remains after (perhaps incomplete) data cleaning and artifact removal, are considered as random uncertainties, or noise, in the data. Sometimes it is appropriate and possible to reduce the noise level by use of suitable filtering and smoothing of the data, but this can be dangerous, re-introducing systematic uncertainties, due to the filtering process itself.

In any case, in the best case some remaining 'random' uncertainties will be left. Otherwise there will still be residual systematic uncertainties that cannot be removed. In extremely unfortunate cases, there may still be blunders or outliers which cannot be removed with certainty, because it is impossible to decide whether these data points represent real features, or are accidents of measurement.

To meet the requirements for informed decision-making, it must be possible to describe these remaining uncertainties in some standard way. One uncertainty descriptor is 'precision' which describes data consistency. Good precision indicates that outliers have been successfully removed, and random uncertainties are small - but large systematic effects may still exist. Another uncertainty descriptor is 'accuracy', which in a perfect world indicates the agreement of data with the 'truth' (whatever that may be). Good accuracy indicates that the systematic effects have been reduced or eliminated, although occasional outliers may still exist, and the random uncertainties may be large or small.

Both these uncertainty descriptors are based on statistical principles and standards. The 'mean' and the 'standard deviation' are the two most common statistical descriptors of measurement uncertainties. The mean describes the central tendency of a series of measurements. The standard deviation describes the dispersion of a series of measurements. If the mean value (or perhaps a 'true value' if such is known) is subtracted from every measurement, a series of 'residuals' or deviations from the mean will result. If the square root of the sum of the squares of these residuals is calculated, the standard deviation for that measurement series is obtained.

When discussing measurements that have a number of 'dimensions' or time-correlated quantities (as is most certainly the case for a modern bathymetric survey), then these concepts are extended into several dimensions by considering a 'mean vector' and a 'covariance matrix'.

Data-sets containing many measurements tend to have a special statistical character, known as a Gaussian distribution (the familiar 'bell-shaped curve'), provided all accidental and systematic uncertainties have been removed, so that the uncertainties are purely random. This Gaussian character is an approximate model of reality, and becomes a better model the larger the number of values which are being considered (something called the Central Limit Theorem), and the more rigorous or successful the data cleaning process. An important descriptor of uncertainty, when the data density permits, is the probability that the data residuals (the random component of uncertainty) obey the Gaussian distribution.

But what does all this have to do with the confidence which can be placed in the information or measurements? Another statistical principle that can be predicted, under specific statistical conditions, is how often the measurement uncertainties (or more specifically the measurement residuals) are likely to exceed a certain value. The value (or values) in question is referred to as the 'confidence region', and the likelihood that the measurements lie inside this confidence region is referred to as the 'confidence level'.

The international standard for confidence level is 95% – in other words 19 times out of 20. 95% is the confidence level associated with weather predictions. 95% is the confidence level associated with election outcome predictions or public polling results. And 95% has become the standard for expressing the confidence level for results derived from hydrographic measurements. If data has a Gaussian distribution, the 95% confidence region is related to the standard deviation (in one dimension) or the covariance matrix (in several dimensions) by a simple scale factor.

In summary, key quality factors in bathymetric survey design are 'coverage', 'resolution' and 'redundancy'. The key quality factor in bathymetric data assessment is 'uncertainty' - what are the uncertainties in the resulting bathymetric, positioning and sonar backscatter information, and how do these uncertainties compare with the informed decision-making requirements for the intended uses? Bathymetric uncertainty management requires redundancy and consists of two or three steps - data cleaning for both outliers and artifact removal, perhaps followed by a noise reduction process, and finally an assessment of the 95% confidence region associated with the remaining residual discrepancies.

Having applied the tools discussed in the previous section, it is possible to arrive at numerical values for uncertainty of the bathymetry data, either grouped by adjacent areas, or individually. One way to assess these numbers (decide if they are fit for their intended purpose) is to compare them against a standard.

A standard can be used as a planning document before data are collected and as an evaluation document after the data are in. The *a priori* approach tries to assess the uncertainty with which each piece of data could or should be collected, before a survey is conducted. This is implemented through an uncertainty prediction estimation process or model. These predicted uncertainties are compared with those required to meet the appropriate standard, and the survey redesigned if they fall short. The *a posteriori* approach attempts to determine what uncertainties actually exist in the collected data, using the data cleaning and assessment tools referred to earlier in this paper. The results of these post-survey checks are then compared with the appropriate standard, to determine whether the survey results are actually 'fit for their intended purpose'. Sometimes it is claimed that a survey 'met' the standard, but if no post survey check was carried out to verify this claim, it is not supported by evidence. Claiming that surveys were planned to meet the standard is not enough. Planning and realization are not always the same thing.

In the following sections some of the standards that are available for this assessment are considered. For simplicity, just one of the many standard parameters required for assessing hydrographic data will be addressed: the uncertainty in determination of depth.

### **1.3 S44 - IHO standards for hydrographic surveys**

The International Hydrographic Organization (IHO) has issued standards for hydrographic surveys (S44) since 1957, and most recently in 1998 (IHO, 1998). These are the standards used by most producers of hydrographic data. Their stated purpose is:

*To specify minimum standards for hydrographic surveys in order that hydrographic data collected according to these standards is sufficiently accurate and that the spatial uncertainty of data is adequately quantified to be safely used by mariners (commercial, military or recreational) as primary users of this information.*

S44 identifies itself as a 'performance standard' and thus contains no instructions on how to evaluate whether a survey meets the standard. Nor does it specifically require the inclusion of redundancy, the most powerful tool for evaluating the uncertainty of any set of measurements. These are left to each agency to implement:

*Equipment and procedures used to achieve the standards laid down in this publication are left to the discretion of the agency responsible for the survey quality.*

Producing a standard like S44 is no easy task. Usual practice is for several member states of the IHO to nominate specialists who not only have a profound knowledge of the theory underlying the subject but are also aware of upcoming improvements in the technology that may impact on the standard during its lifetime. The group must also have a strong sense of the pragmatic: there is no value in producing a standard that cannot be achieved or can only be achieved at costs not sustainable by some member states. Finally, the members must possess a thick skin, since their work can never please everyone.

The work of producing the standard is ongoing, in a periodic manner, with the published intention of issuing a new edition every five years. An examination of the changes between succeeding editions gives a strong indication the perceived progress in hydrographic technology and evolution in users' needs. For instance, the current (4th) edition:

*...departs from previous editions by specifying different accuracy requirements for different areas according to their importance for the safety of navigation. The most stringent requirements entail higher accuracies than previously specified, but for areas of less critical nature for navigation the requirements have been relaxed.*

Improvements in positioning technology that allow vessels to determine their locations at a level of uncertainty smaller than that required by the previous standard, together with the development of high density bathymetric mapping tools (such as multibeam sonar echo sounders and LIDAR), are reasons behind this demand for higher accuracies in certain areas. Future editions will likewise adapt the standard to evolving technology and users requirements.

S44 4th Edition classifies surveys into four different types (four 'intended uses'):

*Special Order - for specific critical areas with minimum under keel clearance and where bottom characteristics are potentially hazardous to vessels (generally less than*



40m), such as harbours, berthing areas, and associated critical channels with minimum under keel clearances.

*Order 1 – for harbours, harbour approach channels, recommended tracks, inland navigation channels, and coastal areas of high commercial traffic density (less than 100m), such as harbours, harbour approach channels, recommended tracks and some coastal areas with depths up to 100 m.*

*Order 2 – for areas with depths less than 200m not covered by Special Order and Order 1.*

*Order 3 – for areas not covered by Special Order, and Orders 1 and 2 and in water depths in excess of 200m*

For each of these it specifies Horizontal Accuracy, Depth Accuracy, 100% Bottom Search, System Detection Capability and Maximum Line Spacing.

S44 4th Edition divides depth uncertainties into two contributing types: fixed and variable. It makes no mention of the primary classification of random, systematic and accidental, within these fixed and variable types. Fixed errors dominate the uncertainty budget in shallow water. Variable (depth-dependent) errors are characterized as a fixed percentage of water depth and thus grow larger with deepening water. The two types are combined in the Root-Sum-of-Squares (RSS) sense to give the 95% uncertainty  $s$ . That

$$s = [a^2 + (bd)^2]^{1/2}$$

Where  $a$  = sum of all depth-independent errors,  $b$  = sum of all depth-dependent errors, expressed as a fraction of water depth, and  $d$  = depth of water column in metres.

S44 4th Edition draws a distinction between the sampling of the seabed bathymetry represented by the measured depths, and the complete bathymetric model which is presented (in some form) to the end user for informed decision making. Unless the sampling density is dense enough to delineate all seabed features, this model will be based, either implicitly or explicitly, on some form of interpolation between the sampled depths. Consequently the uncertainty associated with a bathymetric model will include uncertainties introduced by the interpolation process, and will be larger than the depth measurement (sampling) uncertainty.

Order	S44 Special	S44 1	S44 2	S44 3
Depth uncertainty for reduced depths (95% Confidence Level)	a = 0.25m b = 0.75%	a = 0.5m b = 1.3%	a = 1.0m b = 2.3%	a = 1.0m b = 2.3%
Bathymetric model uncertainty (95% Confidence Level)	a = 0.25m b = 0.75%	a = 1m b = 2.6%	a = 2m b = 5%	a = 5m b = 5%

**Table 1.1:** *Summary of Minimum Standards for Depth Uncertainties from S44 4th Edition (IHO, 1998)*

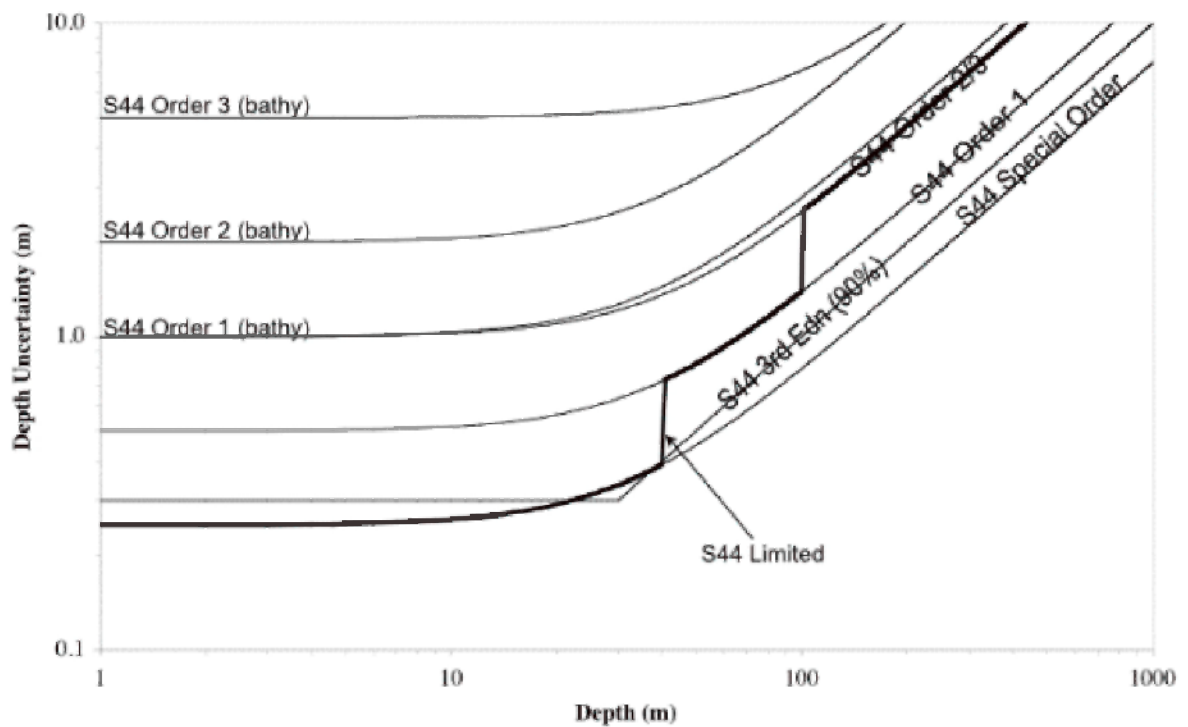
In the case of the Special Order, this algorithm is somewhat more demanding than the single depth uncertainty specification from S44 3rd Edition (IHO, 1987), which was

*30cm to the depth of 30m, and 1% of depth thereafter.*

The S44 3rd Edition specification was at the 90% confidence level, and did NOT include uncertainties in water level reduction, which are included in the 4th edition specifications.

For Orders 1 to 3, this algorithm results in higher permitted uncertainties than did the single 3rd Edition specification.

There are two ways in which the S44 4th Edition depth uncertainty standards can be interpreted. In the first interpretation, the word 'minimum' standards is taken as the operative word, and the unlimited extension of each of the four S44 orders to deeper depths is permitted, even though not mandatory. In the second, more limited, interpretation, each Order is assigned a maximum depth to which it should be applied (Special Order to 40m, Order 1 to 100m, Order 2 to 200m, and Order 3 in deeper water).



University of Moratuwa, Sri Lanka.  
Electronic Theses & Dissertations  
www.lib.mrt.ac.lk

**Figure 1.1:** Log-log plot of S44 3rd and 4th Editions.

*In subsequent Figures, the S44 Special Order plot is used as a reference.*

#### 1.4 Beyond S44 - other intended uses, other standards

S44 4th Edition broke a lot of new ground. It addresses the use of high density bathymetric methods, such as multibeam, sweep and LIDAR. It emphasizes the need to determine and record ('attribute') depth and position uncertainties. It distinguishes between depth measurement uncertainty and bathymetric model uncertainty.

Previous S44 editions were based on the scale of a specified chart, and the draughting skill of experienced marine cartographers. S44 4th Edition is based on uncertainty budgets and (at least nominally) on intended uses. However, despite this nominal objective, the intended use for which S44 4th Edition was created is still almost exclusively nautical charting.

Some of those seeking depth uncertainty standards for other intended uses of bathymetric information have referred to S44 4th Edition, as is (e.g. United Nations, 1999). Others have extended, modified and replaced the standards embodied in S44 4th Edition.

This paper will consider four examples of standards that go beyond S44 4th Edition:

- The Exclusive Order introduced by the Swedish Maritime Administration (SMA).
- The US Army Corps of Engineers shallow water standards.
- Standards proposed by Land Information New Zealand for deep water multibeam echosounder surveys.
- Standards proposed by the International Marine Contractors Association for offshore construction.

## 1.5 Swedish implementation of S44

IHO S44 are *minimum* standards. At least one hydrographic office, the Swedish Maritime Administration, has defined standards which are based on S44 4th Edition, but which are more demanding than those minimum standards (SMA, 2000).

On 1 May 2000, these new standards came into effect for Swedish surveys, and are being considered for adoption by other Baltic hydrographic offices.

- SMA extended S44 4th Edition in four ways:
- A new Exclusive Order specification was added, intended for the most demanding applications.
- 100% seafloor coverage is required in all cases by SMA, whereas for S44 4th Edition 100% coverage is specified only for Special Order and, if there is a grounding hazard, for other Orders as well.
- Depth uncertainty in the standards refer to both acoustic sounding measurements (topographical reproduction) as well as determinations of the minimum depth by means of mechanical sensors (sweeping bars).
- The SMA depth uncertainty standards include the entire error budget from the surveying uncertainties up to the final result - storage in the digital depth database. In this way, the SMA depth uncertainty standards are conceptually closer to the S44 4th Edition bathymetric model uncertainties, than to the depth measurement uncertainties. However

the SMA standards are much tighter than the S44 4th Edition standards, since the numerical values are derived from the S44 4th Edition depth measurement uncertainties.

The SMA established two 'intended uses' - 'fairway areas' and 'other'. Fairway areas are defined as:

*existing, proposed or planned, fairways, traffic separations, deepwater routes, ports and areas of anchorage or waiting.*

Fairway area surveys require an initial acoustic sounding survey. This is followed by a mechanical bar sweep, when the acoustic soundings indicate that the fairway depths are either:

- less than 150% of the minimum existing, proposed or planned underkeel clearance safety margin, including squat, or
- the underkeel clearance safety margin is less than 1m.

Order	SMA Exclusive	SMA Special	SMA 1st	SMA 2nd	SMA 3rd
Depth uncertainty for bathymetric models (95% Confidence Level)	a = 0.15m b = 0.40%	a = 0.25m b = 0.75%	a = 0.5m b = 1.3%	a = 1.0m b = 2.3%	a = 1.0m b = 2.3%
Depth range to apply order for fairway areas		0 - 20m	20 - 50m	50 - 100m	100m +
Depth range to apply order for other areas			0 - 6m	6 - 100m	100m +
Maximum depth to apply order	50m	50m	100m	100m	unlimited

**Table 1.2:** *The Swedish implementation of S-44*

## 1.6 USACE Hydrographic Manual 2001

The United States Army Corps of Engineers has published a Hydrographic Manual, containing background information, field procedures, and survey standards for Corps hydrographic projects since 1991. This document defines two categories of hydrographic surveys (intended uses):

- Navigation and dredging support surveys, including project condition surveys of navigation channels, dredging contract plans and specifications surveys, dredging measurement, payment, clearance, and acceptance surveys, and river charting surveys.

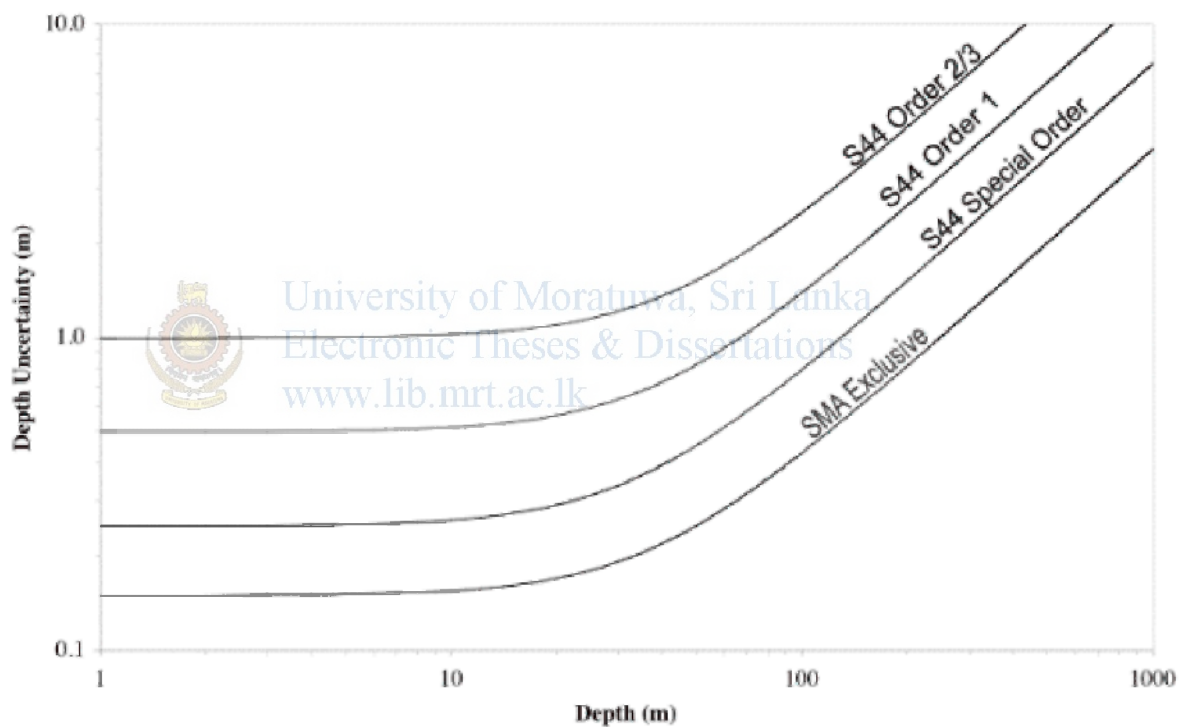


**Figure 1.2:** Log-log plot of SMA implementation of S-44

- General surveys and studies, including general reconnaissance or planning surveys/studies, flood control project surveys, reservoir sedimentation surveys, flood plain boundary surveys, hydrological and hydraulic surveys, coastal engineering surveys,

beach surveys, environmental investigations, geotechnical investigations, and disposal area surveys.

Based on the following principle:

- survey instrumentation requirements, accuracy standards, and quality control procedures vary as a function of bottom type in a navigation channel; as does the required accuracy of dredge measurement and payment.

USACE navigation and dredging support surveys are further divided into three categories:

- Hard bottom material and/or new work. Navigation projects where low under-keel clearances are anticipated over potentially hazardous bottom conditions, hazardous cargo is transported, or where bottom sediment could adversely impact naval vessels transiting a project only a small number of Corps projects fall under this category.
- Soft bottom material and/or maintenance dredging. Navigation projects containing soft sand/silt bottoms not judged to be hazardous to vessel hulls; or projects with soft, featureless, and relatively continuous channel bottoms where gaps in coverage between survey lines are unlikely to yield potential hazards/strikes. The vast majority of the Corps deep- and shallow-draft navigation projects . . . fall within this category.
- Underwater investigation surveys. Precise investigation surveys of/around locks, dams, power plants, abutments, piers, jetties, bulkheads, and other structures.

The USACE depth uncertainty standards include all uncertainty components that make up a reduced elevation: uncertainties in datum, in tide/stage modelling-extrapolation-interpretation, in dynamic-latency/roll/pitch/heave, in acoustic measurement, sound speed, refraction, and beam forming, and bathymetric mis-modelling through uncertainty in horizontal positioning (depth georeferencing uncertainty). The Manual notes that mechanical and acoustic depth measurement uncertainty increases with increasing depth, that multibeam system uncertainties increase with increasing beam angle, and that tide/stage and water level surface model uncertainties will generally be smaller for shallow (<5m) projects than for deeper (>12m) projects. The USACE depth uncertainty standards are depth –dependent, but do not follow the S44 4th Edition a/b coefficient model for depth independent and depth dependent uncertainty components.

Method	Depth	Nav & dredging hard bottom	Nav & dredging soft bottom	Other
Mechanical	< 4.5m	a = 0.075m	a = 0.075m	a = 0.15m
Acoustic	< 4.5m	a = 0.15m	a = 0.15m	a = 0.30m
Acoustic	4.5m to 12m	a = 0.30m	a = 0.30m	a = 0.60m
Acoustic	> 12m	a = 0.30m	a = 0.60m	a = 0.60m

**Table 1.3:** USACE depth uncertainty standards (2001 draft version)

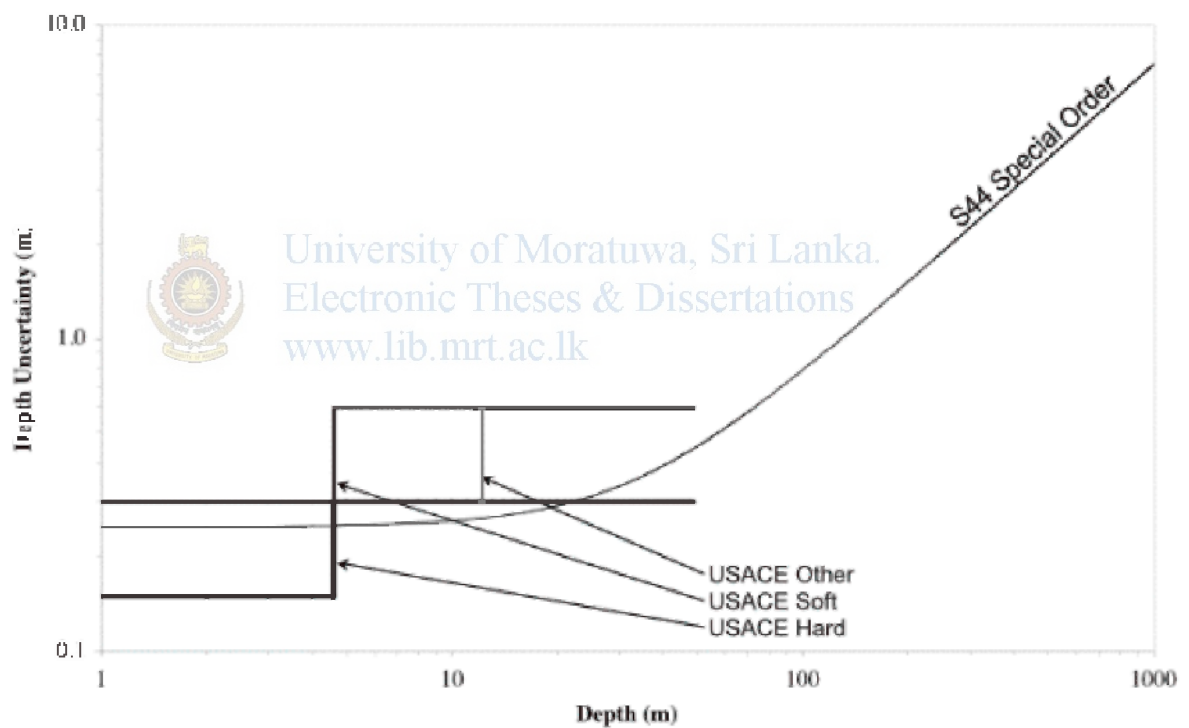


**Figure 1.3:** Log-log plot of USACE standards, and S44 4th Edition Special Order



## 1.6 The LINZ standard, specifically addressing MBES performance

In response to a request from Land Information New Zealand (LINZ), John Hughes Clarke, of the University of New Brunswick, prepared a set of 'Provisional Swath Sonar Survey Specifications' (Hughes Clarke, 1999) for surveys involving the use of multibeam sonar echosounders (MBES). The rationale for this project was as follows:

The [IHO S44 4th Edition] standards unfortunately contain significant ambiguity and are drafted for the sole purpose of data collection for nautical charting (a mandate much narrower than that of LINZ). One example of this broader mandate is that, as of July 1997, LINZ has taken the responsibility for New Zealand's Continental Shelf Delimitation Project. This involves the 'measurement and analysis of seabed information according to internationally agreed criteria developed by the United Nations Commission on the Law of the Sea (UNCLOS)'. Unfortunately these criteria do not include any specifications for the acquisition or delivery of data that might be acquired by MBES.

The LINZ report explains that uncertainties associated with MBES depth measurements, expressed as a percentage of water depth (coefficient 'b' in S44 4th Edition) are actually *smaller* in deep water than in shallow water. Depth-independent factors such as tide and heave, and one of the major depth-dependent factors, unstable sound velocity profiles, all have larger magnitudes in shallow (inshore) water than in deep (offshore) water. Consequently the depth uncertainties resulting from imperfect measurement/recovery of these factors, are also far more significant in shallow than in deep water. The report points out that uncertainties as small as 0.2% of water depth have been reported for deep water MBES depths. To demand only 2.3%, as specified in S44 4th Edition Order 3, ignores the capability of MBES, and is less appropriate than S44 3rd Edition, which required 1% for both shallow and deep water depth measurements.

The LINZ report also explains that MBES bottom detection, roll, and refraction uncertainties are all larger for outer beams than for inner (near nadir) beams. Bottom detection uncertainties for the inner beams of a typical MBES are in the range of 40% to 60% of the S44 4th Edition Special Order depth measurement specifications. On the other hand, bottom detection uncertainties alone will exceed the entire Special Order uncertainty limit (from all sources) for outer beams (say those with a grazing angle of less

than 30°). Therefore, a MBES survey designed to meet a particular depth uncertainty standard for all beams (out to a certain outer-beam cutoff), will likely outperform that uncertainty standard significantly for the inner beam (near nadir) data.

This MBES beam-angle dependence is not addressed in S44 4th Edition. The LINZ report addresses this dependence head-on by proposing MBES depth uncertainty specifications based on the differences between inner-beam and outer-beam uncertainty performance. Rather than requiring that all depths from a MBES survey meet the same uncertainty standard, inner-beam standards are required to meet something closely related to S44 4th edition Special Order, while the outer-beam standards are more relaxed. In addition, the permitted balance between inner-beam and outer-beam coverage is allowed to relax as the survey specifications move from LINZ Special Order to LINZ Order 3.

The expected performance of a MBES is divided into several sectors, from the inner-beam sector to the outermost-beam sector. The number of sectors is allowed to increase from one to four, and the specified coverage within each sector is partitioned more generously in favour of the outer-beam sectors, as the survey order descends from Special to Order 3. Since this approach could be quite complex to design, realize and assess in practice, a simpler approach is also proposed, which is based on the performance of the worst (outer beam) sector. In each case, everything is tied to the S44 4th Edition Special Order specification, and the lower order S44 specifications are ignored. Four uncertainty levels are specified: 1.0, 1.5, 2.0 and 2.5 times the S44 4th Edition Special Order depth uncertainty specification, that is

For 1.0 x SO, a = 0.25 m, b = 0.75% of depth

For 1.5 x SO, a = 0.375 m, b = 1.125% of depth

For 2.0 x SO, a = 0.5 m, b = 1.5% of depth

For 2.5 x SO, a = 0.625 m, b = 1.875% of depth.

Order	LINZ Special	LINZ 1st	LINZ 2nd	LINZ 3rd
Depth uncertainty, by sector, for reduced depths (95% Confidence Level)	100%1.0 x SO	50%1.0 x SO 50%1.5 x SO	33%1.0 x SO 33%1.5 x SO 33%2.0 x SO	25%1.0 x SO 25%1.5 x SO 25%2.0 x SO
Depth uncertainty for worst-case sector (outer-beams) reduced depths (95% Confidence Level)	1.0 x SO	1.5 x SO	2.0 x SO	2.5 x SO

**Table 1.4:** *Proposed LINZ Depth uncertainty specifications*

## 1.7 IMCA offshore construction standards

The International Marine Contractors Association (IMCA) have adapted the S44 and LINZ standards to standards for informed decision making in offshore construction activities (IMCA, 2000). The intended uses associated with each of the four IMCA depth measurement uncertainty orders are:

- IMCA First Order - site surveys for offshore engineering, requiring high quality seafloor definition: Template or jacket installations; Detailed route engineering surveys; Route surveys in confined areas; Surveys in ports and harbours; Dredging and inshore engineering surveys
- IMCA Second Order – site surveys for offshore engineering, less stringent than First Order: Route reconnaissance surveys; Geo-Hazard and clearance surveys; Coastal engineering surveys; Deepwater geophysical and engineering surveys (conducted by remote vehicle)
- IMCA Third Order – general bathymetric surveys: Continental shelf cable route surveys; Continental shelf charting surveys; Export pipeline route surveys
- IMCA Fourth Order – Reconnaissance surveys: Deepwater cable route surveys; Deepwater charting surveys; Surveys for Exclusive Economic Zone assessments and delineation

Order	IMCA 1st	IMCA 2nd	IMCA 3rd	IMCA 4th
Depth Accuracy for Reduced Depths (95% Confidence Level)	1 x IHO SO a = 0.25 m b = 0.0075	1.5 x IHO SO a = 0.375 m b = 0.01125	2 x IHO SO a = 0.5 m b = 0.015	2.5 x IHO SO a = 0.625 m b = 0.01875
Maximum depth to apply order	200m	500m	750m	No maximum

**Table 1.5:** Proposed IMCA Depth Measurement Uncertainty Standards

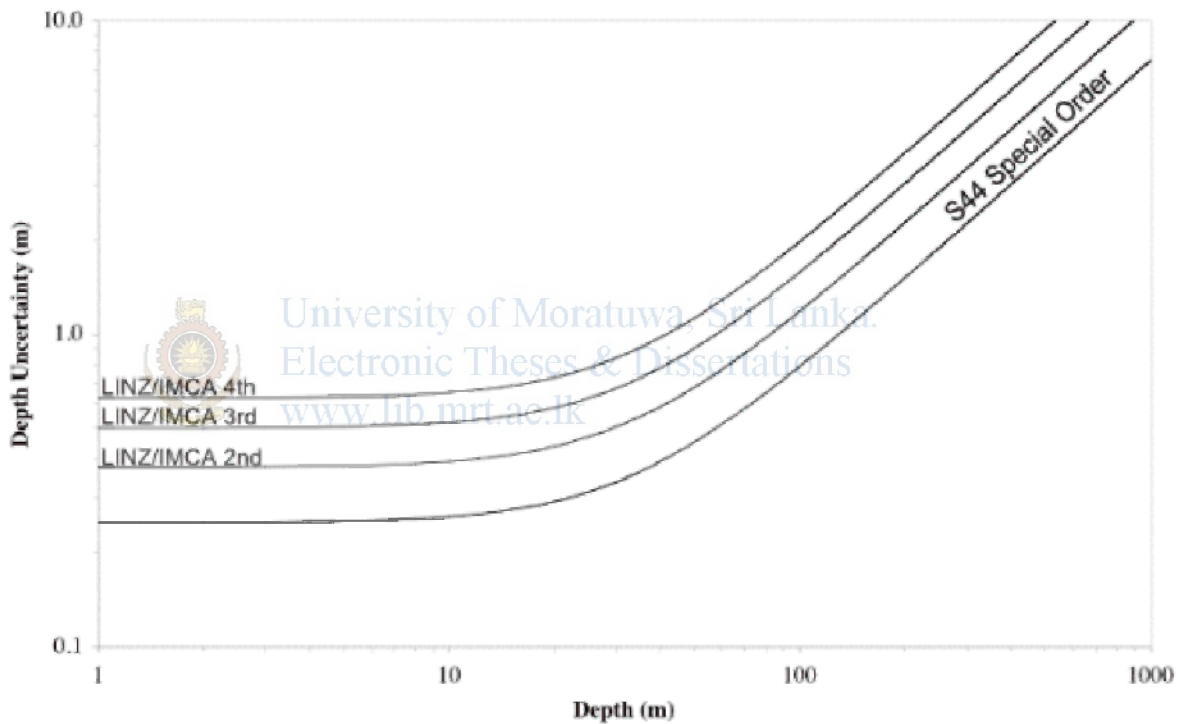


**Figure 1.4:** Log-log plot of Proposed LINZ worst-case sector / IMCA depth uncertainty, and S44 4th Edition Special Order

## 1.8 What's next for S44?

The IHO formally intends to reconsider S44 on a five year schedule, to account for technological and procedural improvements as they occur. Hence work on S44 5th Edition is expected to start soon. This review concludes with speculation on the issues to be dealt with by the S44 working group tasked with preparing S44 5th Edition.

Perhaps the most important issue is whether S44 5th Edition should aspire to address all intended uses for hydrographic data, as was hinted at in S44 4th Edition. As this paper has tried to demonstrate, there are many non-nautical-charting uses for hydrographic data, for which the depth uncertainty standards are quite different (often more demanding) than the standards provided by S44 4th Edition. This brief review is by no means an exhaustive survey of these other intended uses for bathymetric data.

An argument in favour of S44 5th Edition addressing all intended uses for hydrographic data, is that many Hydrographic Offices aspire to be suppliers of data/information/products to a broader clientele. It has even been argued that the survival of some HOs may depend upon cultivating a broader user base (Monahan et al, 2001). It would be appropriate for the IHO to establish data standards within S44 5th Edition which would facilitate these aspirations.

On the other hand, this approach to a new edition of S44 would require broader representation on the working group. The working group would benefit from inclusion of members involved in specifying the uncertainty requirements for several of the diverse intended uses for hydrographic data, as listed in S44 4th Edition:

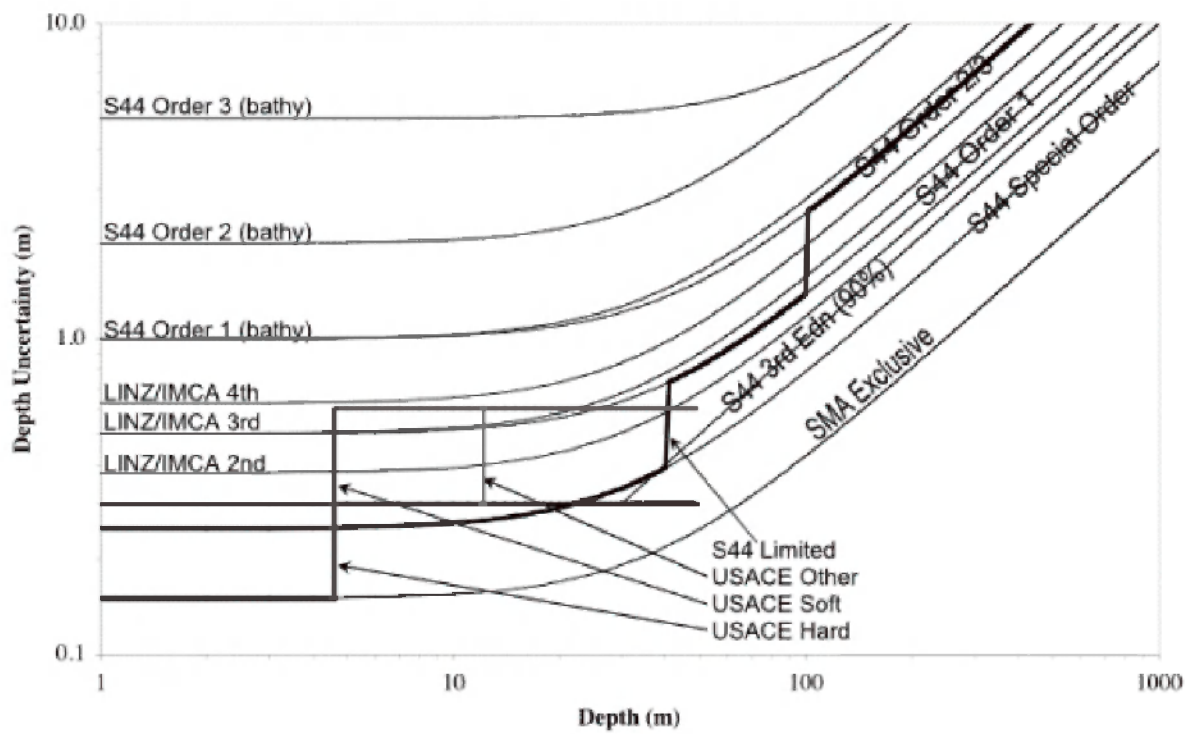
*Coastal zone management, environmental monitoring, resource development (hydrocarbon and mineral exploitation), legal and jurisdictional issues, ocean and meteorological modelling, engineering and construction planning.*

Here are a few ideas for consideration, when work on S44 5th Edition begins:

- Consider moving S44 from a performance standard, to a document that provides guidance on how to apply the performance standard, both *a priori* for planning purposes, and *a posteriori* to determine end use (informed decision making) uncertainty.
- Recognize, as the SMA seems to have done, that the 'bathymetric model' introduced in S44 4th Edition is what both navigational and non-navigational clients want and use for

informed decision making. Place more emphasis on specifying, on methods for assessing and on methods for informing end users, of the uncertainty associated with this model, and products based upon it (in contrast to depth measurement uncertainty).

- Consider separating navigational intended uses into use for (a) certified commercial navigation, (b) uncertified commercial navigation, (c) recreational boating and (d) military operations, with uncertainty management standards specific to each category. Specify the quantity and spatial distribution of redundant measurements, as well as methods of analyzing them.
- Clarify the issue of the maximum depth to which the depth uncertainty associated with a particular order of survey should be applied. Consider removing all limits (essentially stressing that S44 represents *minimum* standards).
- Consider simplifying the relationship between the various orders of survey, by tying the depth uncertainty definitions for Orders 1, 2 and 3 to multiples of the Special Order uncertainty, as has been done in the proposed LINZ and IMCA standards.
- Reconsider depth of water column as the sole independent quality variable. For work from submerged submarines, ROVs and AUVs, depth under the sensor would be a more appropriate quality variable than depth of the water column. Accurate high resolution bathymetry is often required in deep water for marine construction surveys. Bottom slope and roughness, area ensonified and multibeam beam angle should be considered as additional quality variables.
- Consider providing guidelines for managing all three types of uncertainties (accidental, systematic and random) rather than providing a performance standard based on random uncertainties alone.



University of Moratuwa, Sri Lanka.  
Electronic Theses & Dissertations  
[www.lib.mrt.ac.lk](http://www.lib.mrt.ac.lk)

**Figure 1.5:** Compilation of all depth uncertainty standards from Figures 1 to 4.

**REFERENCES**

**Models in Hydraulic Engineering: physical principles and Design Applications**, Pavel Novak, and J Cabelka, Pitman Advanced Publishing Program, Boston – London – Melbourne, 1981

**Long-term Tide and Wave-Induced Sedimentation at a Lagoon Entrance**. S.P. Samarawickrama, PhD Thesis, Department of Civil Engineering, Imperial College of Science, Technology and Medicine, London, August 1999

**Environmental Impact Assessment of Development Proposals for A Fishery Harbour in Negombo**, W. Salinda Perera, R. H. Dias, K.P.D. De Silva, Final Year Project, Department Civil Engineering, University of Moratuwa, Sri Lanka, 2001.

**Final report on NERC grant GR3/11899 'A new approach to modeling internal waves in the ocean'** D.G. Dritschel, Mathematical Institute, University of St. Andrews, O.Bijhler, Courant Institute, New York University, U.S.A. A. Viudez, Institute de Ciencies del Mar, Barcelona, Spain

Li Bin, 1994 “**An evolution equation for water waves**”, Coastal Engineering, Volume 23, pp 227 -242

CCD-GTZ Coast Conservation Project, 1994 “**Directional wave climate study south-west coast of Sri Lanka – report on the wave measurements off Galle**”.

LHI, 1989 “**Final report on wave condition at Kirinda** (May 1988 – February 1989)”

Japan International Cooperation Agency, 1989 “**Draft final report for the study on sand drift in the south-eastern coast of Sri Lanka**”



---

LHI, 1997 “**Coastal Engineering Investigations for Kudawella Fishery Anchorage Development – final report**”

LHI, 1999 “**Galle port development, numerical and physical modelling of wave and tidal conditions inside Galle harbour, part 1: wave studies**”.

NARA, 2001 “**Bathymetry survey for the proposed fishing harbour at Hambanthota**”, Scale 1:5000, MISC 003/01.

NARA, 2001 “**Bathymetry survey of the harbour area at Hambantota**”, Scale 1:1000, MISC 008/02.

NARA, 2001 “**Beach profiles of Hambantota bay**”, MISC 000/01.

NARA, 2001 “**Sediment sampling and PSD analysis within the harbour area at Hambantota**”, MISC 000/01



University of Moratuwa, Sri Lanka.  
Electronic Theses & Dissertations  
www.lib.mrt.ac.lk

Arjuna Consulting Co Ltd, 1997 “**Arjuna’s Atlas of Sri Lanka**”

**Colombo Wave Measurements – 1989**

**Colombo Wave Measurements – 1989**

**Colombo Wave Measurements – 1991**

**Colombo Wave Measurements – 1993**

**Colombo Wave Measurements – 1993**

**Colombo Wave Measurements – 1993**

**Colombo Wave Measurement Program – 1994**

**Offshore Directional Wave Measurements and Wave Measurements in the Harbour Basin – 1990**

**Investigation for Chilaw Anchorage – 1998**

**Dikkowita Fishery Harbour Feasibility Report – 1996**

**CEB Coal-Fired Thermal Development Project - Assessment of Wave Climate – 1998**

**Directional Wave and Current Measurements at Kudawella – 1997**

**Directional Wave Measurements at Colombo – 2002**

**Report on Wave and Current Measurements – 1987**



University of Moratuwa, Sri Lanka.  
Electronic Theses & Dissertations  
[www.lib.mrt.ac.lk](http://www.lib.mrt.ac.lk)

**Report on Wave and Current Measurements – 1987**

**The Port of Colombo, 1940-1995, Volume II, Dharmasena K, 1998**



## **APPENDIX**

University of Moratuwa, Sri Lanka.  
Electronic Theses & Dissertations  
[www.lib.mrt.ac.lk](http://www.lib.mrt.ac.lk)

## 1.0 Development Tools and Resources Required for Development

- ⇒ ArcView GIS Ver 3.2 with
  - Spatial Analyst Extension
  - 3D Analyst for better enhancement at User-End
- ⇒ Surfer Ver 7.0 or Above
- ⇒ Microsoft Visual Studio as Integrated Development Environment with C++ functionality with Win 32 API through Microsoft Foundation Classes
- ⇒ Complete Reference of (For the initial Development)
  - Visual C++ MFC Classes
  - Avenue for ArcView GIS Engine
  - Avenue for Spatial Analyst

## 2.0 Sample Program Listing: Using C++

### Listing 2.1

```

int Celerity_Generation(int T)
{
double I,J,C,G,K,Ks;
int i,j;
char WBuff[80];
char DValue[20];

FILE *fc;
FILE *fl;
FILE *fKs;

fc = fopen("d:\\temp\\cpor12.asc", "w");
fl = fopen("d:\\temp\\lpor12.asc", "w");
fKs = fopen("d:\\temp\\Ksport2.asc", "w");

if((fc != NULL) && (fl != NULL) && (fKs != NULL))
{
strcpy(WBuff, "ncols 500\n");
fprintf(WBuff, fc);
strcpy(WBuff, "nrows 500\n");
fprintf(WBuff, fc);
}

```

```

strcpy(WBuff,"xlcorner 0.n");
fputs(WBuff,fc);
strcpy(WBuff,"ylcorner 0.n");
fputs(WBuff,fc);
strcpy(WBuff,"cellsize 0.38.n");
fputs(WBuff,fc);
strcpy(WBuff,"NODATA value -9999.n");
fputs(WBuff,fc);

```

```

strcpy(WBuff,"ncols 500.n");
fputs(WBuff,fl);
strcpy(WBuff,"nrows 500.n");
fputs(WBuff,fl);
strcpy(WBuff,"xlcorner 0.n");
fputs(WBuff,fl);
strcpy(WBuff,"ylcorner 0.n");
fputs(WBuff,fl);
strcpy(WBuff,"cellsize 0.38.n");
fputs(WBuff,fl);
strcpy(WBuff,"NODATA value -9999.n");
fputs(WBuff,fl);

```

```

strcpy(WBuff,"ncols 500.n");
fputs(WBuff,jKs);
strcpy(WBuff,"nrows 500.n");
fputs(WBuff,jKs);
strcpy(WBuff,"xlcorner 0.n");
fputs(WBuff,jKs);
strcpy(WBuff,"ylcorner 0.n");
fputs(WBuff,jKs);
strcpy(WBuff,"cellsize 0.38.n");
fputs(WBuff,jKs);
strcpy(WBuff,"NODATA value -9999.n");
fputs(WBuff,jKs);

```

```

for(i=0;i < 500;i++)
{
    for(j=0;j < 500;j++)
    {
        D = Zzone[i][j];
        if(D > 0.0)
        {
            if( (L/9.81/pow(T,2)) > 0.08)
                C = (9.81 * pow(T,2) / 2 / pi) / T;
            else if( ((L/9.81/pow(T,2)) > 0.0025) && ((L/9.81/pow(T,2)) < 0.08) )
            {
                //cont = "Entered transition zone" << endl;
                for(l = (9.81 * pow(T,2) / 2 / pi); fabs(l - (9.81 * pow(T,2) / 2 / pi * tanh(2 * pi * L / l))) > 0.00001; l = 9.81 * pow(T,2) / 2 / pi * tanh(2 * pi * L / l));
                C = l / T;
            }
            else if( (L/9.81/pow(T,2)) < 0.0025)

```

```

        {
            C = pow(9.81 * D, 0.5);
        }
        else C = -9999;
    }
    else
        C = -9999;
    //cout<<C<<endl;
    strcpy(WBuff, gcvt(C, 6, DValue));
    c[i][j] = C;
    fputs(WBuff, fc);
    strcpy(WBuff, " ");
    fputs(WBuff, fc);
    if(C != -9999.0)
        L = C * T;
    else
        L = -9999;
    strcpy(WBuff, gcvt(L, 6, DValue));
    fputs(WBuff, fl);
    strcpy(WBuff, " ");
    fputs(WBuff, fl);
    if(C != -9999.0)
    {
        K = 2 * pi / L;
        G = 1 - (2 * K * D / sinh(2 * K * D));
        Ks = 1 / pow(tanh(K * D) * (1 + G), 0.5);
    }
    else Ks = -9999;
    strcpy(WBuff, gcvt(Ks, 6, DValue));
    fputs(WBuff, fKs);
    strcpy(WBuff, " ");
    fputs(WBuff, fKs);
}
strcpy(WBuff, "\n");
fputs(WBuff, fc);
strcpy(WBuff, "\n");
fputs(WBuff, fl);
strcpy(WBuff, "\n");
fputs(WBuff, fKs);
cout<<endl<<" Row completed"<<endl;
}

fcloseall();
return 1;
}
else return 0;
}

```



**Listing 2.2**

```

int alpha_Generation(double AlphaInit)
{
double D,L,PrevC,PrevAlpha,alpha,G,K,Kr;
int i,j;
char WBuff[80];
char DValue[20];
FILE *fAlpha,*fKr;

fAlpha=fopen("d:\\temp\\aport2.asc","w");
fKr=fopen("d:\\temp\\krport2.asc","w");

if(fAlpha!=NULL)
{
strcpy(WBuff,"ncols 500\n");
fprintf(WBuff,fAlpha);
strcpy(WBuff,"rows 500\n");
fprintf(WBuff,fAlpha);
strcpy(WBuff,"xllcorner 0\n");
fprintf(WBuff,fAlpha);
strcpy(WBuff,"ylldcorner 0\n");
fprintf(WBuff,fAlpha);
strcpy(WBuff,"cellsize 0.38\n");
University of Moratuwa, Sri Lanka.
Electronic Theses & Dissertations
www.lib.mrt.ac.lk
fprintf(WBuff,fAlpha);
strcpy(WBuff,"NO_DATA_value -9999\n");
fprintf(WBuff,fAlpha);
strcpy(WBuff,"ncols 500\n");
fprintf(WBuff,fKr);
strcpy(WBuff,"rows 500\n");
fprintf(WBuff,fKr);
strcpy(WBuff,"xllcorner 0\n");
fprintf(WBuff,fKr);
strcpy(WBuff,"ylldcorner 0\n");
fprintf(WBuff,fKr);
strcpy(WBuff,"cellsize 0.38\n");
fprintf(WBuff,fKr);
strcpy(WBuff,"NO_DATA_value -9999\n");
fprintf(WBuff,fKr);

for(j=0;j<500;j++)
{
PrevAlpha=AlphaInit;
PrevC=c[0][j];
for(i=0;i<500;i++)
{
D=Zzone[i][j];
if((D>0.0)&&(PrevC!=-9999.0))
{

```

```

        alpha = asin(c[i][j] / PrevC * sin(PrevAlpha));
        Kr = pow(cos(PrevAlpha) / cos(alpha), 0.5);
        PrevAlpha = alpha;
        PrevC = c[i][j];
    }
else
{
    alpha = -9999;
    Kr = -9999;
}
Alpha[i][j] = alpha;
kr[i][j] = Kr;
}
}
for(i=0; i<500; i++)
{
    for(j=0; j<500; j++)
    {
        strcpy(WBuff, gcvt(Alpha[i][j], 6, DValue));
        strcpy(WBuff, gcvt(kr[i][j], 6, DValue));
        fputs(WBuff, falpha);
        fputs(WBuff, fKr);
        strcpy(WBuff, " ");
        fputs(WBuff, falpha);
        fputs(WBuff, fKr);
        strcpy(WBuff, "\n");
        fputs(WBuff, falpha);
        fputs(WBuff, fKr);
        cout<<endl<< " column completed" << endl;
    }
}
fcloseall();
return 1;
}
else return 0;
}

```





**Listing 2.3**

```

char *Fgetc(char *SdeS,int No_Ch,FILE *FR)
{
char ch;
int No_Char = 0;
ch = fgetc(FR);
while((ch!=EOF)&&(ch!='\n')&&(No_Char<No_Ch))
{
*(SdeS + No_Char) = ch;
ch = fgetc(FR);
No_Char ++;
}
*(SdeS + No_Char) = '\0';

if(ch==EOF)
Ret = NULL;
else if(ch == '\n')
Ret = SdeS;
return Ret;
}

char *StrChopCol(char *S)
{
static int StartPos = 0;
static int times = 0;
static int i = 0;
static char *Word;

for( *(S + StartPos) == '\n'; StartPos ++ );
for( i = 0; *(S + StartPos + i) != '\n' && *(S + StartPos + i) != '\0'; i ++ );
times ++;
Word = (char *) malloc(i + 1);
if(Word != NULL)
{
strcpy(Word, S + StartPos);
StartPos = StartPos + i;
*(Word + i) = '\0';
}
if( times == nCols)
{
StartPos = 0;
times = 0;
i = 0;
}
return Word;
}

```



**Listing 2.4**

```

int File_Ch_Count(char *File_Name)
{
    FILE *fr;
    char ch;
    int No_Char_Line;
    int max=0;
    fr = fopen(File_Name,"r");
    if(fr == NULL)
    {
        cout<<"File Opening Error.."<<endl;
        return -1;
    }
    ch = fgetc(fr);
    while(ch!=EOF)
    {
        No_Char_Line = 0;
        while((ch!='\n') && (ch!=EOF))
        {
            No_Char_Line ++;
            ch = fgetc(fr);
        }
        if(ch == '\n') ch = fgetc(fr);
        if(No_Char_Line > max) max = No_Char_Line;
    }
    fclose(fr);
    return max;
}

```

**Listing 2.5**

```

int Data_Extractor(void)
{
    int nRows,xCorner,yCorner;
    int No_Rows = 0;
    float CellSize;
    int No_Char_Line;
    char *Mem_Line;
    char *Ret_fgets;
    char dest[80];
    char *ChoppedV;
    char Finter;
    FILE *fr;

```

```

No_Char_Line = File_Ch_Count("d:\\temp\\xport2.asc");
Mem_Line = (char *)malloc(No_Char_Line + 5);

    if(Mem_Line == NULL)
        return -1;
else
    {
        cout<<"Memory Success"<<endl;
        fr = fopen("d:\\temp\\xport2.asc","r");
        if(fr == NULL)
            {
                cout<<"File Opening Error.."<<endl;
                return -1;
            }

Ret_Fgets = Fgets(Mem_Line,No_Char_Line + 2,fr);
nCols = atoi(strcpy(dest,Mem_Line + 6));
cout<<nCols<<endl;
Ret_Fgets = Fgets(Mem_Line,No_Char_Line + 2,fr);
nRows = atoi(strcpy(dest,Mem_Line + 6));
cout<<nRows<<endl;

Ret_Fgets = Fgets(Mem_Line,No_Char_Line + 2,fr);
xCorner = atoi(strcpy(dest,Mem_Line + 10));
cout<<xCorner<<endl;
Ret_Fgets = Fgets(Mem_Line,No_Char_Line + 2,fr);
yCorner = atoi(strcpy(dest,Mem_Line + 10));
cout<<yCorner<<endl;
Ret_Fgets = Fgets(Mem_Line,No_Char_Line + 2,fr);
CellSize = atof(strcpy(dest,Mem_Line + 9));
cout<<CellSize<<endl;
*Mem_Line = '\0';
Ret_Fgets = Fgets(Mem_Line,No_Char_Line + 2,fr);
*Mem_Line = '\0';

Ret_Fgets = Fgets(Mem_Line,No_Char_Line + 2,fr);
while(Ret_Fgets != NULL)
    {
        for(i = 0;i<nCols;i++)
            {
                ChoppedV = StrChopCol(Mem_Line);
                if(ChoppedV!=NULL)
                    {
                        Zzone[No_Rows][i] = atof(ChoppedV);
                    }
                else
                    {
                        cout<<"Memory Error.."<<endl;
                        return -1;
                    }
            }
    }

```

```
    free(ChoppedV);
    }
    //No Rows = 0;
    *Mem_Line = '0';
    Ret_Fgets = Fgets(Mem_Line, No_Char_Line + 2, fr);
    No Rows + 1;
    //
    //No Rows = No Rows % nRows;
}

free(Mem_Line);
cout<<"File Display Finished"<<endl;
}

    Celerity Generation(8);
    alpha Generation(45 * pi / 180);

return 0;
}
```

